

AD-A070 886

STEVENS INST OF TECH HOBOKEN N J DAVIDSON LAB

F/G 13/10

ADDED MASS AND DAMPING OF THE HEAVING SURFACE EFFECT SHIP IN UN--ETC(U)

DEC 78 C H KIM, S TSAKONAS

N00014-77-C-0061

UNCLASSIFIED

SIT-DL-78-9-2040

NL

1 OF 2

AD A070686



ADA 070886

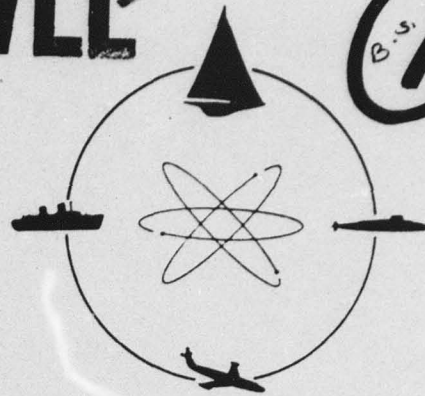


STEVENS INSTITUTE
OF TECHNOLOGY

CASTLE POINT STATION
HOBOKEN, NEW JERSEY 07030

LEVEL II

R-2040



DAVIDSON LABORATORY

Report SIT-DL-78-9-2040
December 1978

ADDED MASS AND DAMPING
OF THE HEAVING SURFACE EFFECT SHIP
IN UNIFORM TRANSLATION

by

C.H. Kim and S. Tsakonas



APPROVED FOR PUBLIC RELEASE
DISTRIBUTION UNLIMITED

Prepared
for

David Taylor Naval Ship Research
and Development Center (1505)
Bethesda, MD 20084
General Hydromechanics Research Program
under
Contract N00014-77-C-0061

Office of Naval Research
800 N. Quincy Street
Arlington, VA 22217

06 26 013

UNCLASSIFIED

SECURITY CLASSIFICATION OF THIS PAGE (When Data Entered)

REPORT DOCUMENTATION PAGE		READ INSTRUCTIONS BEFORE COMPLETING FORM
1. REPORT NUMBER 14 SIT-DL-78-9-2040 ✓	2. GOVT ACCESSION NO.	3. RECIPIENT'S CATALOG NUMBER
4. TITLE (and Subtitle) 6 ADDED MASS AND DAMPING OF THE HEAVING SURFACE EFFECT SHIP IN UNIFORM TRANSLATION.	5. TYPE OF REPORT & PERIOD COVERED FINAL - Dec. 1976 - Feb. 1978	
7. AUTHOR(s) 10 C.H. Kim and S. Tsakonas	6. PERFORMING ORG. REPORT NUMBER SIT-DL-78-9-2040	
9. PERFORMING ORGANIZATION NAME AND ADDRESS Davidson Laboratory Stevens Institute of Technology Hoboken, NJ 07030	8. CONTRACT OR GRANT NUMBER(s) 15 N00014-77-C-0061	
11. CONTROLLING OFFICE NAME AND ADDRESS David W. Taylor Naval Ship R&D Center Bethesda, MD 20084 (Code 1505)	10. PROGRAM ELEMENT, PROJECT, TASK AREA & WORK UNIT NUMBERS SR 023 01 01 61153N 19077	
14. MONITORING AGENCY NAME & ADDRESS (if different from Controlling Office) Office of Naval Research 800 N. Quincy Street Arlington, VA 22217	12. REPORT DATE 11 December 1978	
12 104 p.	13. NUMBER OF PAGES 102 pp.	
16. DISTRIBUTION STATEMENT (of this Report) APPROVED FOR PUBLIC RELEASE; DISTRIBUTION UNLIMITED. 16 SR 023 01 17 SR 023 01 01	15. SECURITY CLASS. (of this report) Unclassified	
17. DISTRIBUTION STATEMENT (of the abstract entered in Block 20, if different from Report) 9 Final rept. Dec 76 - Feb 78.	15a. DECLASSIFICATION/DOWNGRADING SCHEDULE	
18. SUPPLEMENTARY NOTES Sponsored by the Naval Sea Systems Command, General Hydromechanics Research Program administered by David W. Taylor Naval Ship Research and Development Center, Code 1505, Bethesda, MD 20084		
19. KEY WORDS (Continue on reverse side if necessary and identify by block number) Surface Effect Ship - Water Waves - Aero-hydrodynamic Forces - Bubble Pressure Added Mass - Damping Factor - Heave Response.		
20. ABSTRACT (Continue on reverse side if necessary and identify by block number) The analysis presents a practical method for evaluating the added mass and damping coefficients of a heaving surface effect ship in uniform translation. The theoretical added mass and damping coefficients and the heave response show fair agreement with the corresponding experimental values. Comparisons of the coupled aero-hydrodynamic and uncoupled analytical results with the experimental data prove that the uncoupled theory, dominant (Cont'd)		

89 06 26 078

For
elt

UNCLASSIFIED

SECURITY CLASSIFICATION OF THIS PAGE (When Data Entered)

20. Abstract (Continued)

→ for a long time, that neglects the free surface effects is an oversimplified procedure.

The analysis also provides means of estimating the wave elevation of the free surface, escape area at the stern and the volume which are induced by a heaving surface-effect ship in uniform translation in otherwise calm water. Computational procedures have been programmed in FORTRAN IV language and adapted to the PDP-10 high-speed digital computer. ↙

UNCLASSIFIED

SECURITY CLASSIFICATION OF THIS PAGE (When Data Entered)

STEVENS INSTITUTE OF TECHNOLOGY

DAVIDSON LABORATORY
CASTLE POINT STATION
HOBOKEN, NEW JERSEY

Report SIT-DL-78-9-2040

December 1978

ADDED MASS AND DAMPING
OF THE HEAVING SURFACE EFFECT SHIP IN UNIFORM TRANSLATION

by

C.H. Kim and S. Tsakonas

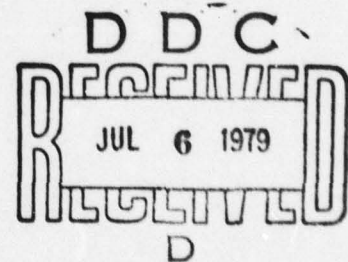
This Research Was Sponsored By The
David Taylor Naval Ship Research and Development Center
General Hydromechanics Research Program

Under

Contract N00014-77-C-0061

DL Project 4480/015

APPROVED FOR PUBLIC RELEASE;
DISTRIBUTION UNLIMITED



Approved:

John P. Breslin
Director

Accession For	
NTIS GRA&I	<input checked="" type="checkbox"/>
DDC TAB	
Unannounced Justification	
By _____	
Distribution/ _____	
Availability Codes	
Dist	Avail and/or special
A	

102 pp.

ABSTRACT

The analysis presents a practical method for evaluating the added mass and damping coefficients of a heaving surface effect ship in uniform translation.

The theoretical added mass and damping coefficients and the heave response show fair agreement with the corresponding experimental values.

Comparisons of the coupled aero-hydrodynamic and uncoupled analytical results with the experimental data prove that the uncoupled theory, dominant for a long time, that neglects the free surface effects is an oversimplified procedure.

The analysis also provides means of estimating the wave elevation of the free surface, escape area at the stern and the volume which are induced by a heaving surface-effect ship in uniform translation in otherwise calm water. Computational procedures have been programmed in FORTRAN IV language and adapted to the PDP-10 high-speed digital computer.

KEYWORDS

Surface Effect Ship
Water Waves
Aero-hydrodynamic Forces
Bubble Pressure
Added Mass
Damping Factor
Heave Response

TABLE OF CONTENTS

ABSTRACT	iv
NOMENCLATURE	vi
INTRODUCTION	1
THE VELOCITY POTENTIAL	4
STEADY STATE SOLUTION	9
SURFACE ELEVATION	14
ESCAPE AREA AND VOLUME	21
RELATIONSHIP BETWEEN BUBBLE PRESSURE AND HEAVE	25
ADDED MASS AND DAMPING COEFFICIENTS	31
SCALE EFFECT ON THE BUBBLE PRESSURE	34
NUMERICAL CALCULATIONS AND DISCUSSION	35
SUMMARY AND CONCLUSIONS	39
REFERENCES	41
ACKNOWLEDGMENTS	42
TABLE: Principal Characteristics of XR-5 SES Model	43
FIGURES (18)	
APPENDICES A, B, C, D and E	

NOMENCLATURE

A	escape area or area of nozzle throat
A_0	escape area at the equilibrium
A_c	cushion area
A_s	variation of the seal opening area
a	half length of the pressure patch or wave amplitude
b	half width of the pressure patch
C_a	non-dimensional added mass coefficient
C_d	non-dimensional damping coefficient
F_n	Froude number
g	gravitational acceleration
h	cushion height
i	$\sqrt{-1}$, or the suffix indicating the imaginary component
j	integer
K	nozzle flow coefficient or constant
k_j	wave number
L	nominal ship length
l	integer
M''	added mass
m	integer
N	damping factor
n	integer
P	pressure
p_a	atmospheric pressure
p_b	bubble pressure
p_0	ambient pressure

Q	discharge
Q_0	discharge at equilibrium
r	distance or the suffix indicating the real component
s_m	distance
t	time
U	ship speed
V	the wave-induced volume
v	non-dimensional coefficient of the wave-induced volume
w	suffix indicating the water
x, y, z	coordinates
z	heave displacement
α	non-dimensional coefficient of the escape area
γ	ratio of specific heats
ϵ	a parameter
ϕ	the velocity potential
λ	scale ratio
Π	pressure
σ	circular frequency
τ	frequency, $\sigma U/g$
ρ, ρ_w	density of water
ρ_a	density of air
ζ	wave elevation

INTRODUCTION

The analysis is directed at the problem of finding the effect of the presence of the water wave upon the bubble (or cushion) pressure in the plenum of a surface-effect ship as it is forced in simple harmonic heaving motion while translating at constant speed over otherwise calm water.

The surface-effect ship undergoing the above-mentioned motion is a multi-parameter system influenced by the coupled aero- and hydrodynamic actions of water and air in the plenum which is under a continuous supply of air through a system of fans and leakage through the peripheral gap.

The analysis when linearized yields the aero-hydrodynamic forces due to the forced heaving motion and thus provides the corresponding added mass and damping force coefficients in waves which is vital information for the evaluation of particular design characteristics of a ship at the desired speed and sea state.

The theory has been developed by referring to the works by Kaplan and Davis,¹ Doctors,² and Breslin and Hires.³ The relevant experimental literature referenced here are the investigations due to Van Den Brug and Van Staveren,⁴ Magnuson and Wolff,⁵ Fein and Murray,⁶ Moran, Fein and Ricci,⁷ and Fridsma.^{8,9}

Kaplan and Davis¹ assume that the free surface behaves as a rigid boundary at constant pressure whereas Doctors and Breslin, et al, assume that the deformation of water surface participates in the generation of the bubble pressure in conjunction with the actions of seals and fans, etc. The second cardinal assumption in the latter works^{2,3} is that the deformation of the wave surface under the oscillatory rectangular pressure patch in uniform translation be used to display the way in which the motion of the water surface participates in the determination of the pressure variations in the plenum air.

Doctors deals with the three-dimensional rectangular pressure patch whereas Breslin and Hires idealize the problem to two-dimensional flow conditions.

*Superior numbers in text matter refer to similarly numbered references listed at the end of this report.

The analysis has been developed independently from that of Doctors,² although along the same lines, leading to expressions for the evaluation of the wave elevation, escape area and volume, quite different from those reported in Reference 2. In addition, a numerical approach has been developed valid for the entire range of frequency of practical interest, from very low to considerably high, in contrast to Doctors' numerical results which are restricted to the very low frequency regime.

In the dynamic analysis of the airflow phenomena, pressure and volume changes are assumed as by others¹⁻³ to occur sufficiently rapidly so that the adiabatic law governs the basic thermodynamic variations in the air cushion. The cushion pressure is assumed to be spatially uniform which is approximately valid according to Moran¹⁰ and Tsakonas et al.¹¹ Since this work is intended to be applied to the high length-beam-ratio sidewalled surface effect ships,⁵⁻⁷ it assumes also that the leakage of air takes place only at stern seal. The seal response dynamics are beyond the scope of the present investigation. It assumes a semi-rigid planing seal which has been the subject of the experimental study of the XR-5 SES Model.⁵

Following the calculation of the waves due to an oscillatory rectangular pressure patch in uniform translation, the bubble pressure is determined. The linearized equation of bubble pressure in plenum chamber and that of the heaving displacement are both derived by applying the perturbation method through the time derivative of the adiabatic law. The asymptotic behavior of the bubble pressures as the frequency $\rightarrow 0$ and ∞ is analyzed and discussed with and without water wave effects.

The motion-induced aero-hydrodynamic forces are calculated from the bubble pressure distribution on the cushion area as a function of Froude number and of reduced frequency. From its real and imaginary components, the added mass and damping coefficients are determined respectively. The asymptotic behavior of the added mass and damping as the frequency $\rightarrow 0$ and ∞ are evaluated and discussed both with and without water wave effects.

The scale effect, essential information for the extrapolation of the model measurements to the full-scale condition, is also the subject of the present analysis. The scale effect determined in the previous study¹² indicates a great dissimilitude in general. The scale effect ratio of the

pressure of the ship to the model as calculated here shows that the dissimilitude is small at low frequency but quite large at higher frequencies.

The present analysis does not include the sidewall hydrodynamic effects since experiments on the XR-5 SES^{6,7} have shown slight effect of the sidewalls on added mass and damping.

A series of numerical computations has been done to determine the water waves, bubble pressure, heave added mass and damping coefficients, scale effect on bubble pressure, and the heave responses of the XR-5 SES model running in head waves.

The waves, escape area and volume which are induced by the oscillating pressure at uniform speed in otherwise calm water have been calculated for the model used by Doctors.² A computational procedure has been developed and established for any frequency and speed without limitation. The bubble pressure, added mass and damping coefficients have been computed for the XR-5 SES model, with and without incorporating the water elevation. A remarkable difference has been found between the two groups.

Experimental values⁶ of the heave added mass and damping coefficients have been compared with the theoretical results. To study the validity of the theoretical added mass and damping coefficients, the heave response of the model has been calculated on the assumption that the pitch is restrained, using the theoretical added mass and damping factors with the experimentally⁶ determined static stiffness and heave-exciting forces.

The analytical developments at limiting cases (i.e., high and low frequencies) have been derived and discussed in detail as well as the results of the comparison of predictions with measurements. The comparisons of the results of both the coupled aero-hydrodynamic analysis and the uncoupled analysis with the results of experiments have shown strongly that omission of the water waves in calculating the bubble pressure and the hydrodynamic forces is not a valid assumption.

This research was sponsored by the David Taylor Naval Ship Research and Development Center, General Hydromechanics Research Program, under Contract N00014-77-C-0061, Davidson Laboratory Project 4480/015.

THE VELOCITY POTENTIAL

The hydrodynamic boundary value problem for a pressure patch oscillating with constant amplitude and moving on the surface of a deep, incompressible, ideal fluid can be determined through the velocity potential method.

The right-handed Cartesian coordinate system is set up on the calm water surface with its vertical z -axis pointing upwards. See Figure 1a.

This problem is formulated as an unsteady boundary value problem^{13,14} in the framework of the linearized conditions.

The pulsating pressure distribution of a rectangular shape on the calm water surface, which is a simple harmonic in time, is expressed as

$$p(x,y,0;t) = \begin{cases} \Pi(x,y)e^{i\sigma t} & |x| \leq a, |y| \leq b \\ 0 & |x| > a, |y| > b \end{cases}, t > 0 \quad (1)$$

The deformation of water due to the above pressure distribution is assumed to be small and is represented by the velocity potential $\varphi(x,y,z;t)$ which is harmonic in space below the free surface; satisfying the d.e.,

$$\varphi_{xx} + \varphi_{yy} + \varphi_{zz} = 0, \quad z < 0, \quad t > 0 \quad (2)$$

On the free surface the velocity potential φ and the surface elevation $\zeta = \zeta(x,y;t)$ satisfy the linearized kinematical and dynamical boundary conditions,

$$-\zeta_t + U\zeta_x + \varphi_z = 0, \quad z=0, \quad t > 0 \quad (3)$$

and

$$\frac{p}{\rho} + g\zeta + \varphi_t - U\varphi_x = 0, \quad z=0, \quad t > 0 \quad (4)$$

Eliminating ζ from Eqs.(3) and (4), we have the linearized free surface condition

$$\varphi_{tt} + U^2\varphi_{xx} - 2U\varphi_{xt} + g\varphi_z = \frac{1}{\rho}(Up_x - p_t), \quad z=0, \quad t > 0 \quad (5)$$

In addition to the above, φ and φ_t satisfy the condition of being

initially at rest on the surface

$$\varphi(x, y, 0; 0) = \varphi_t(x, y, 0; 0) = 0 \quad (6)$$

where $\varphi_t=0$ is valid under the assumption $p(x, y, 0; 0)=0$ [Eq.(1)]¹⁵, and on the bottom

$$\varphi_z = 0, \quad z = -\infty, \quad t > 0 \quad (7)$$

In the far field we suppose that φ and its first and second derivatives tend to zero for any given time; in fact, they tend to zero in such a way that Fourier transforms exist.

Now we seek the form of φ which satisfies the above conditions by employing Fourier transform technique. Define the double Fourier transforms

$$\bar{\varphi}(w, u, z; t) = \frac{1}{2\pi} \int_{-\infty}^{\infty} \int_{-\infty}^{\infty} \varphi(x, y, z; t) e^{-i(wx+uy)} dx dy \quad (8)$$

and inversion

$$\varphi(x, y, z; t) = \frac{1}{2\pi} \int_{-\infty}^{\infty} \int_{-\infty}^{\infty} \bar{\varphi}(w, u, z; t) e^{i(wx+uy)} dw du \quad (9)$$

Here w and u are the longitudinal and transverse wave numbers and are related to the circular wave number k and the wave angle θ by

$$\begin{aligned} w &= k \cos \theta \\ u &= k \sin \theta \end{aligned} \quad (10)$$

The Fourier transform (8) applied to Eq.(2) yields

$$\bar{\varphi}_{zz} - k^2 \bar{\varphi} = 0 \quad (11)$$

The general solution of the above differential equation is

$$\bar{\varphi} = A(w, u; t) e^{|k|z} + B(w, u; t) e^{-|k|z} \quad (12)$$

where A and B are arbitrary constants. By making use of the Fourier transform of the bottom condition (7), we obtain $B=0$. Hence the above is reduced to

$$\bar{\varphi} = A(w, u; t) e^{|k|z} \quad (13)$$

To determine A , take the Fourier transform of the linearized free surface condition (5),

$$\bar{\varphi}_{tt} - U^2 w^2 \bar{\varphi} - i2Uw\bar{\varphi}_t + g\bar{\varphi}_z = i(Uw-\sigma) \frac{\bar{\Pi}}{\rho} e^{i\sigma t} \quad (14)$$

where

$$\begin{aligned} \bar{\Pi}(w,u) &= \frac{1}{2\pi} \int_{-\infty}^{\infty} \int_{-\infty}^{\infty} \Pi(x,y) e^{-i(wx+uy)} dx dy \\ &= \frac{1}{2\pi} \int_{-b}^b d\eta \int_{-a}^a \Pi(\xi,\eta) e^{-i(w\xi+u\eta)} d\xi \end{aligned} \quad (15)$$

Substituting $\bar{\varphi}$ from Eq.(13) in (14) yields

$$A_{tt} - U^2 w^2 A - i2UwA_t + g|k|A = i(Uw-\sigma) \frac{\bar{\Pi}}{\rho} e^{i\sigma t} \quad (16)$$

which by means of the Laplace transform and utilizing the initial condition

$$A(w,u;0) = A_t(w,u;0) = 0$$

yields the following solution in the transform plane

$$L(A) = \frac{(Uw-\sigma)\bar{\Pi}}{2\rho\sqrt{g|k|}} \left(\frac{1}{q-q_1} - \frac{1}{q-q_2} \right) L(e^{i\sigma t})$$

with

$$q_1 = i(Uw + \sqrt{g|k|})$$

$$q_2 = i(Uw - \sqrt{g|k|})$$

Inversion of the above is given by the convolution integral,

$$A = \sum_{l=\pm 1} \frac{l\bar{\Pi}(Uw-\sigma)}{2\rho\sqrt{g|k|}} \int_0^t e^{i\sigma\tau} e^{i(l\sqrt{g|k|} + Uw)(t-\tau)} d\tau \quad (17)$$

Equation (17) after integration is substituted in (13) and we have

$$\bar{\varphi} = e^{i\sigma t} \sum_{l=\pm 1} \frac{i l \bar{\Pi}(Uw-\sigma)}{2\rho\sqrt{g|k|}} e^{i|k|z} \frac{[1 - e^{i(Uw+l\sqrt{g|k|}-\sigma)t}]}{Uw + l\sqrt{g|k|} - \sigma} \quad (18)$$

The inverse transform of (18) is given by

$$\varphi = e^{i\sigma t} \frac{i}{8\pi^2 \rho} \int_{-b}^b d\eta \int_{-a}^a d\xi \Pi(\xi, \eta) \int_{-\infty}^{\infty} \int_{-\infty}^{\infty} \frac{1}{\sqrt{g|k|}} e^{i|k|z + i(wx_0 + uy_0)} (uw - \sigma) \\ \left(\frac{1 - e^{i(Uw + \sqrt{g|k|} - \sigma)t}}{Uw + \sqrt{g|k|} - \sigma} - \frac{1 - e^{i(Uw - \sqrt{g|k|} - \sigma)t}}{Uw - \sqrt{g|k|} - \sigma} \right) dwdu \quad (19)$$

where $x_0 = x - \xi$

$$y_0 = y - \eta \quad (20)$$

Now the variables (w, u) are transformed into (k, θ) by the relation (10). Replacing the elementary area $dwdu$ with

$$dwdu = kd\theta dk \quad (10')$$

for the intervals $0 \leq k \leq \infty$, $-\pi \leq \theta \leq \pi$, we have

$$\varphi = e^{i\sigma t} \frac{i}{8\pi^2 \rho} \int_{-b}^b d\eta \int_{-a}^a d\xi \Pi(\xi, \eta) \int_{-\pi}^{\pi} d\theta \int_0^{\infty} dk \sqrt{\frac{k}{g}} (Uk \cos \theta - \sigma) e^{kz + ik(x_0 \cos \theta + y_0 \sin \theta)} \\ \left(\frac{1 - e^{i(Uk \cos \theta + \sqrt{gk} - \sigma)t}}{Uk \cos \theta + \sqrt{gk} - \sigma} - \frac{1 - e^{i(Uk \cos \theta - \sqrt{gk} - \sigma)t}}{Uk \cos \theta - \sqrt{gk} - \sigma} \right) \quad (21)$$

To fold up the integration interval $(-\pi, \pi)$ to $(0, \frac{\pi}{2})$, the integral $\int_{-\pi}^{\pi}$ is subdivided into four quadrants,

$$\int_{-\pi}^{\pi} = \int_{-\pi}^{-\pi/2} + \int_{-\pi/2}^0 + \int_0^{\pi/2} + \int_{\pi/2}^{\pi}$$

and each integral is transformed into $\int_0^{\pi/2}$. For instance, $\int_{-\pi}^{-\pi/2} \rightarrow \int_0^{\pi/2}$ is

achieved by setting $\theta = \gamma - \pi$, where γ is a new variable. It follows that $\cos \theta = -\cos \gamma$, $\sin \theta = -\sin \gamma$.

By replacing γ with θ and applying a similar procedure to $\int_{-\pi/2}^0$ and $\int_{\pi/2}^{\pi}$, we have the following folded form,

$$\varphi = e^{i\sigma t} \frac{i}{8\pi^2 \rho} \int_{-b}^b d\eta \int_{-a}^a d\xi \Pi(\xi, \eta) \int_0^{\pi/2} d\theta \int_0^{\infty} dk \sqrt{\frac{k}{g}} e^{kz}$$

$$\left\{ (Uk \cos \theta - \sigma) (e^{ikr_1} + e^{ikr_2}) \left(\frac{1 - e^{i\omega_1 t}}{\omega_1} - \frac{1 - e^{i\omega_2 t}}{\omega_2} \right) \right.$$

$$\left. + (Uk \cos \theta + \sigma) (e^{-ikr_1} + e^{-ikr_2}) \left(-\frac{1 - e^{-i\omega_3 t}}{\omega_3} + \frac{1 - e^{-i\omega_4 t}}{\omega_4} \right) \right\} \quad (22)$$

where

$$r_1 = (x - \xi) \cos \theta + (y - \eta) \sin \theta$$

$$r_2 = (x - \xi) \cos \theta - (y - \eta) \sin \theta \quad (23)$$

and

$$\left. \begin{array}{l} \omega_1 \\ \omega_2 \end{array} \right\} = Uk \cos \theta \pm \sqrt{gk} - \sigma$$

$$\left. \begin{array}{l} \omega_3 \\ \omega_4 \end{array} \right\} = Uk \cos \theta \pm \sqrt{gk} + \sigma \quad (24)$$

STEADY STATE SOLUTION

In Eq.(22), φ is the solution of unsteady conditions which have been stated at the outset. The next step is to derive the steady state solution from Eq.(22) by eliminating the time-dependent terms. This is achieved in the following manner: 1) determine the wave numbers k_i from $\omega_i=0$, and 2) take the proper indenting paths in the neighborhood of k_i in the k -plane in order to have the exponentials vanish in time as $t \rightarrow \infty$. The integration paths determined as such are therefore not arbitrary but strictly bound to derivation of the steady solution and to the roots k_i .

Solving for the zeros of ω_i in Eq.(24), namely k_i , we have

$$\left. \begin{array}{l} k_1 \\ k_2 \end{array} \right\} = \frac{\left(\mp 1 + \sqrt{1 + \frac{4U\sigma \cos \theta}{g}} \right)^2}{\frac{4U^2 \cos^2 \theta}{g}} \quad (25a)$$

$$\left. \begin{array}{l} k_3 \\ k_4 \end{array} \right\} = \frac{\left(1 \mp \sqrt{1 - \frac{4U\sigma \cos \theta}{g}} \right)^2}{\frac{4U^2 \cos^2 \theta}{g}} \quad (26a)$$

or

$$\left. \begin{array}{l} k_1 \\ k_2 \end{array} \right\} = \frac{1}{2} k_0 \sec^2 \theta \left[1 + 2\tau \cos \theta \mp \sqrt{1 + 4\tau \cos \theta} \right] \quad (25b)$$

$$\left. \begin{array}{l} k_3 \\ k_4 \end{array} \right\} = \frac{1}{2} k_0 \sec^2 \theta \left[1 - 2\tau \cos \theta \mp \sqrt{1 - 4\tau \cos \theta} \right] \quad (26b)$$

with

$$k_0 = \frac{g}{U^2}, \quad \tau = \frac{U\sigma}{g} \quad (26c)$$

It is seen from (25a) that k_1 and k_2 are positive real and $k_1 \leq k_2$ for interval $0 \leq \theta \leq \frac{\pi}{2}$. It is seen from (26a) that k_3 and k_4 are positive real and $k_3 \leq k_4$ if

$$1 - \frac{4U\sigma \cos \theta}{g} \geq 0$$

and k_3 and k_4 are complex with $\text{Im}k_3 < 0$ and $\text{Im}k_4 > 0$ (i.e., $k_4 =$ complex conjugate of k_3) if

$$1 - \frac{4U\sigma\cos\theta}{g} < 0$$

In other words k_3 and k_4 are positive real in

$$\theta_c \leq \theta \leq \frac{\pi}{2} \quad (27)$$

and complex in the interval

$$0 \leq \theta < \theta_c \quad (28)$$

where

$$\theta_c = \cos^{-1} \left(\frac{g}{4U\sigma} \right) \quad (29)$$

Now we consider the integrals with respect to k in the k -plane.

Since Taylor expansions of k and \sqrt{gk} in the neighborhood of k_i , up to the first order, are

$$k \approx k_i + (k - k_i) + O(k^2)$$

$$\sqrt{gk} \approx \sqrt{gk_i} + (k - k_i) \frac{\sqrt{g}}{2\sqrt{k_i}} \quad (i=1,2,3,4) \quad (30)$$

we obtain the following expressions in the neighborhood of k_i :

$$i(Uk\cos\theta + \sqrt{gk} - \sigma) \approx \begin{cases} i(Uk_1\cos\theta + \sqrt{gk_1} - \sigma) + i(k - k_1) \left(U\cos\theta + \frac{\sqrt{g}}{2\sqrt{k_1}} \right) \\ i(Uk_2\cos\theta + \sqrt{gk_2} - \sigma) + i(k - k_2) \left(U\cos\theta + \frac{\sqrt{g}}{2\sqrt{k_2}} \right) \end{cases}$$

$$i(Uk\cos\theta - \sqrt{gk} - \sigma) \approx \begin{cases} i(Uk_1\cos\theta - \sqrt{gk_1} - \sigma) + i(k - k_1) \left(U\cos\theta - \frac{\sqrt{g}}{2\sqrt{k_1}} \right) \\ i(Uk_2\cos\theta - \sqrt{gk_2} - \sigma) + i(k - k_2) \left(U\cos\theta - \frac{\sqrt{g}}{2\sqrt{k_2}} \right) \end{cases} \quad (31)$$

$$i(Uk\cos\theta + \sqrt{gk} + \sigma) \approx \begin{cases} i(Uk_3\cos\theta + \sqrt{gk_3} + \sigma) + i(k-k_3)\left(U\cos\theta + \frac{\sqrt{g}}{2\sqrt{k_3}}\right) \\ i(Uk_4\cos\theta + \sqrt{gk_4} + \sigma) + i(k-k_4)\left(U\cos\theta + \frac{\sqrt{g}}{2\sqrt{k_4}}\right) \end{cases}$$

$$i(Uk\cos\theta - \sqrt{gk} + \sigma) \approx \begin{cases} i(Uk_3\cos\theta - \sqrt{gk_3} + \sigma) + i(k-k_3)\left(U\cos\theta - \frac{\sqrt{g}}{2\sqrt{k_3}}\right) \\ i(Uk_4\cos\theta - \sqrt{gk_4} + \sigma) + i(k-k_4)\left(U\cos\theta - \frac{\sqrt{g}}{2\sqrt{k_4}}\right) \end{cases} \quad (32)$$

From Eqs. (25a) and (26a), we have the positive real root k_i for the interval $0 \leq \theta \leq \frac{\pi}{2}$

$$\sqrt{k_1} = \frac{\sqrt{g} \left(-1 + \sqrt{1 + \frac{4U\sigma\cos\theta}{g}} \right)}{2U\cos\theta}$$

$$\sqrt{k_2} = \frac{\sqrt{g} \left(1 + \sqrt{1 + \frac{4U\sigma\cos\theta}{g}} \right)}{2U\cos\theta} \quad (33)$$

and for the interval $\theta_c \leq \theta \leq \frac{\pi}{2}$

$$\sqrt{k_3} = \frac{\sqrt{g} \left(1 - \sqrt{1 - \frac{4U\sigma\cos\theta}{g}} \right)}{2U\cos\theta}$$

$$\sqrt{k_4} = \frac{\sqrt{g} \left(1 + \sqrt{1 - \frac{4U\sigma\cos\theta}{g}} \right)}{2U\cos\theta} \quad (34)$$

Employing Eqs. (33) and (34), we have

$$i(Uk\cos\theta + \sqrt{gk} - \sigma) \sim \begin{cases} i(k-k_1) \frac{\sqrt{g} \sqrt{1 + \frac{4U\sigma\cos\theta}{g}}}{2\sqrt{k_1}} \\ +i2\sqrt{gk_2} \end{cases}$$

$$i(Uk\cos\theta - \sqrt{gk} - \sigma) \sim \begin{cases} -i2\sqrt{gk_1} \\ i(k-k_2) \frac{\sqrt{g} \sqrt{1 + \frac{4U\sigma\cos\theta}{g}}}{2\sqrt{k_2}} \end{cases} \quad (35)$$

$$i(Uk\cos\theta + \sqrt{gk} + \sigma) \sim \begin{cases} i2\sqrt{gk_3} \\ i2\sqrt{gk_4} \end{cases}$$

$$i(Uk\cos\theta - \sqrt{gk} + \sigma) \sim \begin{cases} -i(k-k_3) \frac{\sqrt{g} \sqrt{1 - \frac{4U\sigma\cos\theta}{g}}}{2\sqrt{k_3}} \\ +i(k-k_4) \frac{\sqrt{g} \sqrt{1 - \frac{4U\sigma\cos\theta}{g}}}{2\sqrt{k_4}} \end{cases} \quad (36)$$

Equation (35) shows that for the interval $0 \leq \theta \leq \frac{\pi}{2}$ the path of integration of the terms containing $e^{i\omega_1 t}$ and $e^{i\omega_2 t}$ in Eq.(22) in the complex k -plane should be deformed above the real axis in the neighborhood of both k_1 and k_2 in order to have the exponentials in t vanish as $t \rightarrow \infty$. Let this deformed path be denoted by L_1 . (See Fig.1b.) Equation (36) shows that for the interval $\theta_c \leq \theta < \frac{\pi}{2}$, the path of integration containing the factors $e^{-i\omega_3 t}$ and $e^{-i\omega_4 t}$ in Eq.(22) in the complex k -plane should be deformed above the real axis in the neighborhood of k_3 and below the real axis in the neighborhood of k_4 in order to have the exponentials in t vanish as $t \rightarrow \infty$. Let this path be denoted by L_2 . Equation (24) shows that for the complex wave numbers k_3 and k_4 in the interval $0 \leq \theta < \theta_c$, the integration

path requires no deformation in order to have the exponentials in t vanish as $t \rightarrow \infty$; for the path along the real axis the exponentials vanish as $t \rightarrow \infty$. Let this be denoted by L_3 . (See Figure 1b.)

From Eqs. (24), (25a) and (26a), we have the following relations,

$$\begin{aligned} -\frac{1}{2} \sqrt{k/g} U^2 \cos^2 \theta \left(\frac{1}{\omega_1} - \frac{1}{\omega_2} \right) &= \frac{1}{k_1 - k_2} \left(\frac{k_1}{k - k_1} - \frac{k_2}{k - k_2} \right) \\ -\frac{1}{2} \sqrt{k/g} U^2 \cos^2 \theta \left(\frac{1}{\omega_3} - \frac{1}{\omega_4} \right) &= \frac{1}{k_3 - k_4} \left(\frac{k_3}{k - k_3} - \frac{k_4}{k - k_4} \right) \end{aligned} \quad (37)$$

Then substituting the above relations in Eq. (22) and omitting the time factor $e^{i\sigma t}$ we have,

$$\begin{aligned} \varphi &= \frac{i}{4\pi^2 \rho U^2} \int_{-b}^b d\eta \int_{-a}^a d\xi \Pi(\xi, \eta) \\ &\left\{ - \int_0^{\pi/2} d\theta \sec^2 \theta \int_{L_1}^{\infty} dk F_1(\theta, k) \right. \\ &\left. + \int_{\theta_c}^{\pi/2} d\theta \sec^2 \theta \int_{L_2}^{\infty} dk F_2(\theta, k) + \int_0^{\theta_c} d\theta \sec^2 \theta \int_{L_3}^{\infty} dk F_2(\theta, k) \right\} \end{aligned} \quad (38)$$

where

$$\begin{aligned} F_1(\theta, k) &= (Uk \cos \theta - \sigma) \left(e^{k(z+ir_1)} + e^{k(z+ir_2)} \right) \frac{1}{k_1 - k_2} \left(\frac{k_1}{k - k_1} - \frac{k_2}{k - k_2} \right) \\ F_2(\theta, k) &= (Uk \cos \theta + \sigma) \left(e^{k(z-ir_1)} + e^{k(z-ir_2)} \right) \frac{1}{k_3 - k_4} \left(\frac{k_3}{k - k_3} - \frac{k_4}{k - k_4} \right) \end{aligned} \quad (39)$$

The above φ is the ultimate form of the velocity potential for the steady state oscillation.

SURFACE ELEVATION

The surface elevation at a point on the calm water surface, $z=0$, is evaluated by assuming uniform pressure distribution $\Pi = \Pi(\xi, \eta)$ of a rectangular shape, omitting the time factor $e^{i\sigma t}$,

$$\zeta = -\frac{\Pi}{\rho g} + \frac{U}{g} \varphi_x - \frac{i\sigma}{g} \varphi, \quad z=0 \quad (40)$$

where the first term is the static elevation while the remainder represents the elevation due to the dynamic effect.

Let the velocity potential φ in Eq.(38) be written in the following form, omitting the factor $e^{i\sigma t} \frac{\Pi}{4\pi^2 \rho U^2}$,

$$\begin{aligned} \varphi = & - \int_0^{\pi/2} d\theta \sec^2 \theta \left(\frac{k_1}{k_1 - k_2} \varphi_{1,1}(\theta) - \frac{k_2}{k_1 - k_2} \varphi_{1,2}(\theta) \right) \\ & + \int_{\theta_c}^{\pi/2} d\theta \sec^2 \theta \left(\frac{k_3}{k_3 - k_4} \varphi_{2,1}(\theta) - \frac{k_4}{k_3 - k_4} \varphi_{2,2}(\theta) \right) \\ & + \int_0^{\theta_c} d\theta \sec^2 \theta \left(\frac{k_3}{k_3 - k_4} \varphi_{3,1}(\theta) - \frac{k_4}{k_3 - k_4} \varphi_{3,2}(\theta) \right) \end{aligned} \quad (41)$$

with

$$\begin{aligned} \varphi_{1,1}(\theta) &= \int_{-b}^b d\eta \int_{-a}^a d\xi \int_0^{\infty} dk (Uk \cos \theta - \sigma) \frac{e^{k(z+ir_1)} e^{k(z+ir_2)}}{k - k_1} \\ \varphi_{1,2}(\theta) &= \int_{-b}^b d\eta \int_{-a}^a d\xi \int_0^{\infty} dk (Uk \cos \theta - \sigma) \frac{e^{k(z+ir_1)} e^{k(z+ir_2)}}{k - k_2} \\ \varphi_{2,1}(\theta) &= \int_{-b}^b d\eta \int_{-a}^a d\xi \int_0^{\infty} dk (Uk \cos \theta + \sigma) \frac{e^{k(z-ir_1)} e^{k(z-ir_2)}}{k - k_3} \\ \varphi_{2,2}(\theta) &= \int_{-b}^b d\eta \int_{-a}^a d\xi \int_0^{\infty} dk (Uk \cos \theta + \sigma) \frac{e^{k(z-ir_1)} e^{k(z-ir_2)}}{k - k_4} \end{aligned} \quad (42)$$

[Cont'd]

$$\begin{aligned} \varphi_{3,1}(\theta) &= \int_{-b}^b d\eta \int_{-a}^a d\xi \int_0^{\infty} dk (Uk \cos \theta + \sigma) \frac{e^{k(z-ir_1)} + e^{k(z-ir_2)}}{k-k_3} \\ \varphi_{3,2}(\theta) &= \int_{-b}^b d\eta \int_{-a}^a d\xi \int_0^{\infty} dk (Uk \cos \theta + \sigma) \frac{e^{k(z-ir_1)} + e^{k(z-ir_2)}}{k-k_4} \end{aligned} \quad (42)$$

where

$$r_1 = (x-\xi) \cos \theta + (y-\eta) \sin \theta$$

$$r_2 = (x-\xi) \cos \theta - (y-\eta) \sin \theta$$

The first subscript in φ_{ij} denotes the path of integration as identified in Figure 2 and the second denotes the singular point along the given line from left to right. To evaluate the integrals systematically, rearrange the above in the following form:

$$\begin{aligned} I_{1,1}(x,y,z;\theta,k_1) &= \int_{-b}^b d\eta \int_{-a}^a d\xi \int_0^{\infty} dk (Uk \cos \theta - \sigma) \frac{e^{k(z+ir_1)}}{k-k_1} \\ I'_{1,1}(x,y,z;\theta,k_1) &= \int_{-b}^b d\eta \int_{-a}^a d\xi \int_0^{\infty} dk (Uk \cos \theta - \sigma) \frac{e^{k(z+ir_2)}}{k-k_1} \\ J_{1,1}(x,y,z;\theta,k_1) &= \frac{\partial}{\partial x} I_{1,1} \\ J'_{1,1}(x,y,z;\theta,k_1) &= \frac{\partial}{\partial x} I'_{1,1} \end{aligned} \quad (43a)$$

$$\begin{aligned} I_{1,2}(x,y,z;\theta,k_2) &= \int_{-b}^b d\eta \int_{-a}^a d\xi \int_0^{\infty} dk (Uk \cos \theta - \sigma) \frac{e^{k(z+ir_1)}}{k-k_2} \\ I'_{1,2}(x,y,z;\theta,k_2) &= \int_{-b}^b d\eta \int_{-a}^a d\xi \int_0^{\infty} dk (Uk \cos \theta - \sigma) \frac{e^{k(z+ir_2)}}{k-k_2} \\ J_{1,2}(x,y,z;\theta,k_2) &= \frac{\partial}{\partial x} I_{1,2} \\ J'_{1,2}(x,y,z;\theta,k_2) &= \frac{\partial}{\partial x} I'_{1,2} \end{aligned} \quad (43b)$$

$$I_{2,1}(x,y,z;\theta,k_3) = \int_{-b}^b d\eta \int_{-a}^a d\xi \int_0^{\infty} dk (Uk \cos \theta + \sigma) \frac{e^{k(z-ir_1)}}{k-k_3}$$

$$I'_{2,1}(x,y,z;\theta,k_3) = \int_{-b}^b d\eta \int_{-a}^a d\xi \int_0^{\infty} dk (Uk \cos \theta + \sigma) \frac{e^{k(z-ir_2)}}{k-k_3}$$

$$J_{2,1}(x,y,z;\theta,k_3) = \frac{\partial}{\partial x} I_{2,1}$$

$$J'_{2,1}(x,y,z;\theta,k_3) = \frac{\partial}{\partial x} I'_{2,1}$$

(43c)

$$I_{2,2}(x,y,z;\theta,k_4) = \int_{-b}^b d\eta \int_{-a}^a d\xi \int_0^{\infty} dk (Uk \cos \theta + \sigma) \frac{e^{k(z-ir_1)}}{k-k_4}$$

$$I'_{2,2}(x,y,z;\theta,k_4) = \int_{-b}^b d\eta \int_{-a}^a d\xi \int_0^{\infty} dk (Uk \cos \theta + \sigma) \frac{e^{k(z-ir_2)}}{k-k_4}$$

$$J_{2,2}(x,y,z;\theta,k_4) = \frac{\partial}{\partial x} I_{2,2}$$

$$J'_{2,2}(x,y,z;\theta,k_4) = \frac{\partial}{\partial x} I'_{2,2}$$

(43d)

$$I_{3,1}(x,y,z;\theta,k_3) = \int_{-b}^b d\eta \int_{-a}^a d\xi \int_0^{\infty} dk (Uk \cos \theta + \sigma) \frac{e^{k(z-ir_1)}}{k-k_3}$$

$$I'_{3,1}(x,y,z;\theta,k_3) = \int_{-b}^b d\eta \int_{-a}^a d\xi \int_0^{\infty} dk (Uk \cos \theta + \sigma) \frac{e^{k(z-ir_2)}}{k-k_3}$$

$$J_{3,1}(x,y,z;\theta,k_3) = \frac{\partial}{\partial x} I_{3,1}$$

$$J'_{3,1}(x,y,z;\theta,k_3) = \frac{\partial}{\partial x} I'_{3,1}$$

(43e)

$$I_{3,2}(x,y,z;\theta,k_4) = \int_{-b}^b d\eta \int_{-a}^a d\xi \int_0^\infty dk (Uk \cos \theta + \sigma) \frac{e^{k(z-ir_1)}}{k-k_4}$$

$$I'_{3,2}(x,y,z;\theta,k_4) = \int_{-b}^b d\eta \int_{-a}^a d\xi \int_0^\infty dk (Uk \cos \theta + \sigma) \frac{e^{k(z-ir_2)}}{k-k_4}$$

$$J_{3,2}(x,y,z;\theta,k_4) = \frac{\partial}{\partial x} I_{3,2}$$

$$J'_{3,2}(x,y,z;\theta,k_4) = \frac{\partial}{\partial x} I'_{3,2} \quad (43f)$$

The integrations in Equations (43a) through (43f) are given in Appendices A-C. Substituting Eqs.(43a)-(43f) in Eq.(42), and omitting the same factor as that in (41) we have φ in the following form,

$$\begin{aligned} \varphi = & - \int_0^{\pi/2} d\theta \sec^2 \theta \left[\frac{k_1}{k_1-k_2} (I_{1,1} + I'_{1,1}) - \frac{k_2}{k_1-k_2} (I_{1,2} + I'_{1,2}) \right] \\ & + \int_{\theta_c}^{\pi/2} d\theta \sec^2 \theta \left[\frac{k_3}{k_3-k_4} (I_{2,1} + I'_{2,1}) - \frac{k_4}{k_3-k_4} (I_{2,2} + I'_{2,2}) \right] \\ & + \int_0^{\theta_c} d\theta \sec^2 \theta \left[\frac{k_3}{k_3-k_4} (I_{3,1} + I'_{3,1}) - \frac{k_4}{k_3-k_4} (I_{3,2} + I'_{3,2}) \right] \end{aligned} \quad (44)$$

In a similar manner we have φ_x in the following form:

$$\begin{aligned} \varphi_x = & - \int_0^{\pi/2} d\theta \sec^2 \theta \left[\frac{k_1}{k_1-k_2} (J_{1,1} + J'_{1,1}) - \frac{k_2}{k_1-k_2} (J_{1,2} + J'_{1,2}) \right] \\ & + \int_{\theta_c}^{\pi/2} d\theta \sec^2 \theta \left[\frac{k_3}{k_3-k_4} (J_{2,1} + J'_{2,1}) - \frac{k_4}{k_3-k_4} (J_{2,2} + J'_{2,2}) \right] \\ & + \int_0^{\theta_c} d\theta \sec^2 \theta \left[\frac{k_3}{k_3-k_4} (J_{3,1} + J'_{3,1}) - \frac{k_4}{k_3-k_4} (J_{3,2} + J'_{3,2}) \right] \end{aligned} \quad (45)$$

Substituting $(I_{i,j} + I'_{i,j})$ and $(J_{i,j} + J'_{i,j})$ (which are given in Appendices A, B, C) in the above equations (44) and (45), making use of Equation (40) and

omitting the static elevation and time factor, the elevation ζ is determined in non-dimensional form,

$$\begin{aligned}
 \frac{\rho g \zeta}{\Pi} = & - \frac{1}{4\pi^2 U^2} \left\{ \int_0^{\pi/2} d\theta \frac{\sec^3 \theta}{\sin \theta} \left\{ \frac{\sigma^2}{k_1 k_2} (I_1 - I_1') \right. \right. \\
 & + \sum_{\ell=1}^2 (-1)^{1+\ell} \frac{(U k_\ell \cos \theta - \sigma)^2}{k_\ell (k_1 - k_2)} [I_2(k_\ell) - I_2'(k_\ell)] \Big\} \\
 & + \int_{\theta_c}^{\pi/2} d\theta \frac{\sec^3 \theta}{\sin \theta} \left\{ \frac{\sigma^2}{k_3 k_4} (I_1^* - I_1'^*) \right. \\
 & + \sum_{\ell=3}^4 (-1)^{1+\ell} \frac{(U k_\ell \cos \theta + \sigma)^2}{k_\ell (k_3 - k_4)} [I_4(k_\ell) - I_4'(k_\ell)] \Big\} \\
 & + \int_0^{\theta_c} d\theta \frac{\sec^3 \theta}{\sin \theta} \left\{ \frac{\sigma^2}{k_3 k_4} (I_1^* - I_1'^*) \right. \\
 & \left. \left. + \sum_{\ell=3}^4 (-1)^{1+\ell} \frac{(U k_\ell \cos \theta + \sigma)^2}{k_\ell (k_3 - k_4)} [I_5(k_\ell) - I_5'(k_\ell)] \right\} \right\} \quad (46)
 \end{aligned}$$

where * indicates the complex conjugate, and

$$I_1 - I_1' = \sum_{m=1}^8 (-1)^m (\log |s_m| + i\pi^0), \quad s_m \geq 0 \quad (47)$$

$$I_2(k_\ell) - I_2'(k_\ell) = \sum_{m=1}^8 (-1)^{m+1} e^{i k_\ell s_m} \left\{ E_1[i k_\ell s_m] - i \frac{0}{2\pi} \right\}, \quad s_m \geq 0$$

$$\ell = 1, 2 \quad (48)$$

$$I_4(k_3) - I_4'(k_3) = \sum_{m=1}^8 (-1)^{m+1} e^{-i k_3 s_m} \left\{ E_1[-i k_3 s_m] - i \frac{2\pi}{0} \right\}, \quad s_m \geq 0 \quad (49)$$

$$I_4(k_4) - I_4'(k_4) = \sum_{m=1}^8 (-1)^{m+1} e^{-ik_4 s_m} \left\{ E_1[-ik_4 s_m] + \frac{0}{i2\pi} \right\}, s_m \geq 0 \quad (50)$$

$$I_5(k_3) - I_5'(k_3) = \begin{cases} \sum_{m=1}^8 (-1)^{m+1} e^{-ik_3 s_m} \left\{ E_1[-ik_3 s_m] - \frac{i2\pi}{0} \right\}, s_m \geq 0, \operatorname{Re}k_3 > 0 \\ \sum_{m=1}^8 (-1)^{m+1} e^{-ik_3 s_m} \left\{ E_1[-ik_3 s_m] - \frac{0}{0} \right\}, s_m \geq 0, \operatorname{Re}k_3 < 0 \end{cases} \quad (51)$$

$$I_5(k_4) - I_5'(k_4) = \begin{cases} \sum_{m=1}^8 (-1)^{m+1} e^{-ik_4 s_m} \left\{ E_1[-ik_4 s_m] + \frac{0}{i2\pi} \right\}, s_m \geq 0, \operatorname{Re}k_4 > 0 \\ \sum_{m=1}^8 (-1)^{m+1} e^{-ik_4 s_m} \left\{ E_1[-ik_4 s_m] + \frac{0}{0} \right\}, s_m \geq 0, \operatorname{Re}k_4 < 0 \end{cases} \quad (52)$$

s_m as well as the derivations of the above formulas are given in Appendices A, B, C and D.

The functions $(I_1 - I_1'), (I_2 - I_2')$, etc. in (47) to (52) contain sums of logarithmic functions. It might seem that each function has singularities at points (a, b) , $(-a, b)$, $(a, -b)$ and $(-a, -b)$ where a pair of s_m vanish (see Eq.A-5). But one can verify that the function has no singularities when all the terms are taken together or as one might also put it, any singularities in the individual terms are cancelled due to the alternating series. Thus, the solution is regular everywhere.

As a special case, consider the wave elevation due to a uniformly moving pressure distribution without oscillation. Then according to Eqs. (25b), (26b) and (26c) we have,

$$\begin{aligned} \tau &= 0, \quad k_1 = k_3 = 0 \\ k_2 &= k_4 = k_0 \sec^2 \theta \end{aligned} \quad (53)$$

Hence, Eq.(46) is reduced to

$$\frac{\rho g \zeta}{\Pi} = - \frac{1}{4\pi^2} \int_0^{\pi/2} \frac{\sec \theta}{\sin \theta} \{ I_2(k_2) - I_2'(k_2) + I_4(k_4) - I_4'(k_4) \} \quad (53a)$$

and further since $\{ I_2(k_2) - I_2'(k_2) \}$ and $\{ I_4(k_4) - I_4'(k_4) \}$ are complex conjugates of each other, the above is expressed in the form

$$\frac{\rho g \zeta}{\Pi} = - \frac{1}{2\pi^2} \int_0^{\pi/2} d\theta \frac{\sec \theta}{\sin \theta} \operatorname{Re} \{ I_2(k_0 \sec^2 \theta) - I_2'(k_0 \sec^2 \theta) \} \quad (53b)$$

The resultant elevation is the sum of the dynamic and static terms as shown in Eq.(40). The static pressure Π is discontinuous at $|x|=a$. The value of the discontinuity is defined as

$$\Pi(\pm a, y) = \frac{1}{2} [\Pi(\pm a + 0, y) + \Pi(\pm a - 0, y)] \quad (54)$$

Hence, the total non-dimensional elevation is obtained by adding the following to the dynamic term (46) or (53b),

$$\frac{\rho g \zeta}{\Pi}_{\text{static}} = \begin{cases} -\frac{1}{2} & |x|=a \\ -1 & |x|<a \end{cases} \quad (54a)$$

ESCAPE AREA AND VOLUME

The escape area A at the stern section and the volume V under the plenum area are obtained by integrating the wave elevation ζ of Eq.(46).

$$A = \int_{-b}^b \zeta dy$$

$$V = \int_{-a}^a \int_{-b}^b \zeta dy dx \quad (55)$$

Referring to Eq.(46), it is seen that the above integrations have to use the following component integrals:

For the Escape Area -

$$\int_{-b}^b (I_1 - I_1') dy = \frac{1}{i \sin \theta} (I_3 + I_3')_{-b}^b$$

$$\int_{-b}^b (I_2(k_\ell) - I_2'(k_\ell)) dy = \frac{1}{ik_\ell \sin \theta} \left\{ -(I_1 + I_1') + I_2(k_\ell) + I_2'(k_\ell) \right\}_{-b}^b$$

$$\int_{-b}^b (I_4(k_\ell) - I_4'(k_\ell)) dy = \frac{1}{-ik_\ell \sin \theta} \left\{ -(I_1^* + I_1'^*) + I_4(k_\ell) + I_4'(k_\ell) \right\}_{-b}^b \quad (56)$$

For the Volume -

$$\int_{-a}^a \int_{-b}^b (I_1 - I_1') dy dx = -\frac{1}{\cos \theta \sin \theta} (I_6 + I_6')_{-b, -a}^{b, a}$$

$$\int_{-a}^a \int_{-b}^b (I_2(k_\ell) - I_2'(k_\ell)) dy dx = \frac{1}{k_\ell^2 \sin \theta \cos \theta} \left\{ k_\ell (I_3 + I_3') + (I_1 + I_1') - (I_2(k_\ell) + I_2'(k_\ell)) \right\}_{-b, -a}^{b, a}$$

$$\int_{-a}^a \int_{-b}^b (I_4(k_\ell) - I_4'(k_\ell)) dy dx = \frac{1}{k_\ell^2 \sin \theta \cos \theta} \left\{ k_\ell (I_3^* + I_3'^*) + (I_1^* + I_1'^*) - (I_4(k_\ell) + I_4'(k_\ell)) \right\}_{-b, -a}^{b, a} \quad (57)$$

where

$$I_6 = \int_0^\infty dk \frac{e^{kz}}{k^3} (e^{iks_1} - e^{iks_2} + e^{iks_3} - e^{iks_4})$$

$$I_6' = \int_0^\infty dk \frac{e^{kz}}{k^3} (-e^{iks_5} + e^{iks_6} - e^{iks_7} + e^{iks_8}) \quad (58)$$

These are evaluated in Eq.(A-33) in Appendix A.

Using Eqs.(46), (56) and (57), and omitting the time factor $e^{i\sigma t}$, the non-dimensional escape area and volume are written in the following forms:

$$\alpha = \frac{\rho g A}{\pi L} = \frac{1}{4\pi^2 U^2 L} \left\{ \begin{aligned} & \int_0^{\pi/2} d\theta \frac{\sec^3 \theta}{\sin^2 \theta} \left\{ \frac{\sigma^2}{k_1 k_2} (l_3' + l_3') + \sum_{l=1}^2 (-1)^{1+l} \frac{(U k_l \cos \theta - \sigma)^2}{k_l^3 (k_1 - k_2)} \left[-(l_1 + l_1') + l_2(k_l) + l_2'(k_l) \right] \right\} \\ & - \int_{\theta_c}^{\pi/2} d\theta \frac{\sec^3 \theta}{\sin^2 \theta} \left\{ \frac{\sigma^2}{k_3 k_4} (l_3^* + l_3^*) + \sum_{l=3}^4 (-1)^{1+l} \frac{(U k_l \cos \theta + \sigma)^2}{k_l^3 (k_3 - k_4)} \left[-(l_1^* + l_1'^*) + l_4(k_l) + l_4'(k_l) \right] \right\} \\ & - \int_0^{\theta_c} d\theta \frac{\sec^3 \theta}{\sin^2 \theta} \left\{ \frac{\sigma^2}{k_3 k_4} (l_3^* + l_3^*) + \sum_{l=3}^4 (-1)^{1+l} \frac{(U k_l \cos \theta + \sigma)^2}{k_l^3 (k_3 - k_4)} \left[-(l_1^* + l_1'^*) + l_5(k_l) + l_5'(k_l) \right] \right\} \end{aligned} \right\} \quad (59)$$

$$v = \frac{\rho g V}{\pi L^2} = \frac{1}{4\pi^2 U^2 L^2} \left\{ \begin{aligned} & \int_0^{\pi/2} d\theta \frac{\sec^4 \theta}{\sin^2 \theta} \left\{ \frac{\sigma^2}{k_1 k_2} (l_6 + l_6') - \sum_{l=1}^2 (-1)^{1+l} \frac{(U k_l \cos \theta - \sigma)^2}{k_l^3 (k_1 - k_2)} \left[k_l (l_3 + l_3') + (l_1 + l_1') - (l_2(k_l) + l_2'(k_l)) \right] \right\} \\ & + \int_{\theta_c}^{\pi/2} d\theta \frac{\sec^4 \theta}{\sin^2 \theta} \left\{ \frac{\sigma^2}{k_3 k_4} (l_6^* + l_6^*) - \sum_{l=3}^4 (-1)^{1+l} \frac{(U k_l \cos \theta + \sigma)^2}{k_l^3 (k_3 - k_4)} \left[k_l (l_3^* + l_3'^*) + (l_1^* + l_1'^*) - (l_4(k_l) + l_4'(k_l)) \right] \right\} \\ & + \int_0^{\theta_c} d\theta \frac{\sec^4 \theta}{\sin^2 \theta} \left\{ \frac{\sigma^2}{k_3 k_4} (l_6^* + l_6^*) - \sum_{l=3}^4 (-1)^{1+l} \frac{(U k_l \cos \theta + \sigma)^2}{k_l^3 (k_3 - k_4)} \left[k_l (l_3^* + l_3'^*) + (l_1^* + l_1'^*) - (l_5(k_l) + l_5'(k_l)) \right] \right\} \end{aligned} \right\} \quad (60)$$

In the above Eqs.(59) and (60), the symbols for the integral limits have been omitted.

Since pairs of s_m (Eqs.A-5) vanish at the corner points such as $s_1=s_6=0$ at $x=a, y=b$, etc., the logarithmic functions and the exponential integrals in $l_1, l_1', l_2(k_\ell),$ etc., become evidently singular at the points. Examination shows, however, that the sums $\{-(l_1+l_1')+l_2(k_\ell)+l_2'(k_\ell)\},$ $\{-(l_1^*+l_1'^*)+l_4(k_\ell)+l_4'(k_\ell)\},$ etc., are all bounded at these corner points and each l_3, l_3', l_6, l_6' is bounded as well at these corner points. The regularity of the above expressions in Eqs.(59) and (60) are the expected results which derive from the integration of the regular function ζ in Eq.(46).

For the special case $\sigma \rightarrow 0,$ * the escape area at the stern and the volume under the plenum area are obtained from Eqs.(59) and (60) by using the conditions (53):

$$\alpha = \frac{\rho g A}{\pi L \sigma \rightarrow 0} = - \frac{1}{2\pi^2 L k_0} \int_0^{\pi/2} d\theta \frac{\cos\theta}{\sin^2\theta} \operatorname{Im} \left\{ -(l_1+l_1') + \left[l_2(k_0 \sec^2\theta) + l_2'(k_0 \sec^2\theta) \right] \right\}_{-b}^b \quad (61a)$$

and

$$v = \frac{\rho g V}{\pi L^2 \sigma \rightarrow 0} = - \frac{1}{2\pi^2 L^2 k_0^2} \int_0^{\pi/2} d\theta \frac{\cos\theta}{\sin^2\theta} \operatorname{Re} \left\{ k_0 \sec^2\theta (l_3+l_3') + (l_1+l_1') - \left[l_2(k_0 \sec^2\theta) + l_2'(k_0 \sec^2\theta) \right] \right\}_{-b,-a}^{b,a} \quad (61b)$$

The resultant escape area and the volume are obtained by adding the static terms to the dynamic terms, (59) to (61b).

Using Eq.(54), the static escape area at the stern and the static volume are given in non-dimensional form by

$$\alpha_{st} = \frac{\rho g A}{\pi L_{static}} = - \frac{b}{L}$$

and

$$v_{st} = \frac{\rho g V}{\pi L_{static}^2} = - \frac{4ab}{L^2} \quad (61c)$$

where a and b are half-length and beam of the rectangular pressure distribution and L is a nominal length of the SES or ACV.

*See footnote, p.24.

The asymptotic expression of α and v for the frequency $\sigma \rightarrow \infty^*$ are obtained from Eq.(59) and Eq.(60), respectively. Since $\theta \rightarrow \pi/2$ for $\sigma \rightarrow \infty$ in Eq.(29), the second integrals in Eqs.(59) and (60) vanish for $\sigma \rightarrow \infty$. Also, the terms contained in the summation symbols Σ should vanish for $\sigma \rightarrow \infty$ due to the expressions for the wave numbers as shown in Eq.(25). The terms with * in Eq.(59) and Eq.(60) are the complex conjugates of those which are independent of the frequency σ and the speed U .

In view of the above remarks, we have the asymptotic expression of the resultant α and v for $\sigma \rightarrow \infty$

$$\alpha_r = -\frac{1}{2\pi^2 L} \int_0^{\pi/2} d\theta \frac{\sec\theta}{\sin^2\theta} \operatorname{Im}(I_3 + I_3^*) - \frac{b}{L}$$

$$\alpha_i = 0 \quad (62a)$$

$$v_r = \frac{1}{2\pi^2 L^2} \int_0^{\pi/2} d\theta \frac{\sec^2\theta}{\sin^2\theta} \operatorname{Re}(I_6 + I_6^*) - \frac{4ab}{L^2}$$

$$v_i = 0 \quad (62b)$$

where the suffixes r and i indicate the real and imaginary components, respectively. In the above integrations, the symbols for the integral limits have been omitted.

From the expressions of α and v , it is seen that they are in phase with the pressure Π at the frequencies $\sigma \rightarrow 0$ and $\sigma \rightarrow \infty$.

* It should be noted that in the limiting cases when $\sigma \rightarrow 0$ or $\sigma \rightarrow \infty$, then σ and τ can be interchanged.

THE RELATIONSHIP BETWEEN BUBBLE PRESSURE AND HEAVE

The air pressure in the plenum of the SES (surface effect ship) is perturbed by the small vertical oscillatory motion heave $ze^{i\sigma t}$. The first order perturbed pressure $p_b e^{i\sigma t}$ which is dynamic and known as bubble pressure will be obtained by relating it to the first order heave $ze^{i\sigma t}$ in the following analysis.

Since the volume and pressure changes are assumed to occur rapidly, the state of air pressure and volume in the plenum is assumed to satisfy the adiabatic law,

$$pv^\gamma = \text{const.} \quad (63)$$

where γ is the ratio of specific heats which is 1.4 for air. The differentiation of the above with respect to time t gives

$$\frac{\partial p}{\partial t} + \gamma \frac{p}{v} \frac{\partial v}{\partial t} = 0 \quad (64)$$

Expanding p and v in the foregoing up to the first order, we have

$$\begin{aligned} p &= p^{(0)} + \epsilon p^{(1)} \\ v &= v^{(0)} + \epsilon v^{(1)} \end{aligned} \quad (65)$$

where $p^{(0)}$ and $v^{(0)}$ are the pressure and volume in the equilibrium stage $p^{(1)}$ and $v^{(1)}$ are the first order perturbed pressure and volume, respectively, and ϵ is a parameter.

Substituting Eq.(65) into (64) and collecting the first terms only, we then have

$$\frac{\partial p^{(1)}}{\partial t} = -\gamma \frac{p^{(0)}}{v^{(0)}} \frac{\partial v^{(1)}}{\partial t} \quad (66)$$

where

$$\begin{aligned} p^{(1)} &= p_b e^{i\sigma t} \\ v^{(1)} &= v_b e^{i\sigma t} = \text{the perturbed first order volume} \\ p^{(0)} &= p_o + p_a = \text{total pressure} \\ v^{(0)} &= v_o \end{aligned} \quad (67)$$

and

p_o = air pressure in equilibrium or ambient pressure

p_a = atmospheric pressure

v_o = the volume in equilibrium

Thus, Eq.(66) is written with omission of the time factor in the following form

$$i\sigma p_b = -\gamma \frac{p_o + p_a}{v_o} i\sigma v_b \quad (68)$$

where $i\sigma v_b$ is the variation of the volume flux which is positive in the direction outward normal to the plenum chamber as indicated in Figure 1c and is the sum of the flux normal across air-water interface, plenum ceiling, fans and seal apertures. The above relation and the normal volume flux have been used in References 3, 11, 12 which confirm that the use of (68) is identical to that of the method of momentum change in Reference 1. The normal volume flux¹¹ has been expressed by the surface integral of the normal velocity which is derived by the Green's function technique.

1. Over the Air-Water Interface

Equations (60), (61b) and (61c) give the volume due to the water wave elevation per unit pressure, distributed uniformly over the air-water interface. Hence, the contribution to the volume flux due to the bubble pressure is given by

$$i\sigma v_b = -i\sigma v \frac{L^2}{\rho_w g} p_b \quad (69)$$

where v is the non-dimensional volume due to wave elevation per unit uniform pressure over the rectangular patch and ρ_w is the water density. The minus sign indicates the sense of the flow direction.

2. Across the Plenum Ceiling

The variation of the volume flux normal outward to the plenum chamber across the ceiling, due to its heaving displacement z , is given by

$$i\sigma v_b = +i\sigma A_c z \quad (70)$$

where A_c is the cushion area or the area of ceiling. The + sign indicates the sense of the flow direction.

3. Across the Fan Aperture

The variation of the volume flux which flows into the plenum across the fan aperture is

$$i\partial v_b = -n \frac{\partial Q_f}{\partial p} p_b \quad (71)$$

where $\frac{\partial Q_f}{\partial p}$ is the discharge by fan per unit pressure per pair of fans. The minus sign in Eq.(71) indicates the sense of the flow direction and n is the number of pair of fans.

4. Across the Stern-Seal Aperture

The variation of the volume flux flowing outward from the plenum across the seal aperture in the plenum wall is estimated by applying the perturbation procedure to the nozzle discharge equation.

$$Q = k A \sqrt{\frac{2(p_1 - p_2)}{\rho_a}} \quad (72)$$

where k is the flow coefficient which varies between 0.6 and 0.8.* Hydrodynamic studies have shown that for an ideal fluid passing through a narrow slit or a circular opening $k \sim 0.611$ which has been experimentally verified.

A is the area of the nozzle throat or seal opening

p_1 is the pressure in the upstream or in the plenum

p_2 is the pressure at the nozzle or seal and identical to the atmospheric pressure p_a

ρ_a is the air density

Q is the discharge .

To evaluate the increase of volume flux from its equilibrium condition, we expand the terms Q , A and $p_1 - p_2$ up to the first order perturbed terms assuming that the terms are functions of ϵ . Namely, we have the following:

$$\begin{aligned} Q &= Q_0 + \epsilon Q^{(1)} \\ A_s &= A_0 + \epsilon A^{(1)} \\ p_1 - p_2 &= p_0 + \epsilon p^{(1)} \end{aligned} \quad (73)$$

where Q_0 , A_0 and p_0 are the zeroth order term, whereas $Q^{(1)}$, $A^{(1)}$ and $p^{(1)}$

*As the "nozzle" is formed by the water surface and the seal, the coefficient k will depend on Froude number and on Reynolds number for small opening areas, A , as measured at zero speed.³

are the first order terms. The first order terms are redesignated by

$$A^{(1)} = A_s e^{i\sigma t} ; Q^{(1)} = Q_s e^{i\sigma t} ; p^{(1)} = p_b e^{i\sigma t} . \quad (74)$$

Substituting (73) into (72) and making use of the following expansion

$$\sqrt{\frac{2(p_0 + \epsilon p^{(1)})}{\rho_a}} = \sqrt{\frac{2p_0}{\rho_a}} \left(1 + \frac{\epsilon p^{(1)}}{2p_0} \right) , \quad (75)$$

we have the expression for Q , from which the first order equation is obtained in the following form

$$Q_s = k \sqrt{\frac{2p_0}{\rho_a}} \left(\frac{A_0}{2p_0} p_b + A_s \right) \quad (76)$$

The variation A_s of the seal opening area A in (76) is due to heave z and bubble pressure p_b . Namely,

$$A_s = \frac{\partial A_s}{\partial z} z + \left(\frac{\partial A_s}{\partial p} - \alpha \frac{L}{\rho_w g} \right) p_b \quad (77)$$

where

$$\frac{\partial A_s}{\partial z} = \text{the rate of change of seal opening due to seal elasticity per unit heave}$$

$$\frac{\partial A_s}{\partial p} = \text{the rate of change of seal opening due to seal elasticity per unit pressure}$$

$$-\alpha \frac{L}{\rho_w g} = \text{the rate of change of opening due to the wave elevation per unit pressure, in way of the stern seal. } \alpha \text{ is the non-dimensional escape area which has been given in Eqs. (59), (61a), (61c), and (62a).}$$

Substituting (77) into (76), we have the following volume flux which flows outward in the normal direction to the plenum wall across the seal aperture:

$$i\sigma v_b = k \sqrt{\frac{2p_0}{\rho_a}} \left[\left(\frac{A_0}{2p_0} + \frac{\partial A_s}{\partial p} - \alpha \frac{L}{\rho_w g} \right) p_b + \frac{\partial A_s}{\partial z} z \right] . \quad (78)$$

Thus the itemization of the variation of volume fluxes has been completed.

The sum of the first order volume fluxes, Eqs.(69), (70), (71) and (78), is now substituted into Eq.(68). Solving for the unknown bubble pressure p_b , we have the non-dimensional expression in the following form

$$\frac{\frac{p_b}{p_o}}{\frac{z}{h}} = \frac{-\gamma \left(1 + \frac{p_a}{p_o}\right) \left(1 - \frac{i}{\sigma} \frac{k}{A_c} \frac{\partial A_s}{\partial z} \sqrt{\frac{2p_o}{\rho_a}}\right)}{1 - \gamma \left(1 + \frac{p_a}{p_o}\right) \frac{p_o}{v_o} \left[\frac{vL^2}{\rho_w g} + \frac{i}{\sigma} n \left| \frac{\partial Q_f}{\partial p} \right| + \frac{i}{\sigma} k \sqrt{\frac{2p_o}{\rho_a}} \left(\frac{A_o}{2p_o} + \frac{\partial A_s}{\partial p} - \alpha \frac{L}{\rho_w g} \right) \right]} \quad (79)$$

where the relation $\frac{\partial Q_f}{\partial p} = - \left| \frac{\partial Q_f}{\partial p} \right|$ and $v_o = A_c h$ have been used, while h indicates the bubble (or cushion) height.

The dynamic property of the stern seal $\frac{\partial A_s}{\partial z}$ and $\frac{\partial A_s}{\partial p}$ is unknown. At the present stage of investigation, we assume the seal is rigid. This assumption will evidently simplify the aero-hydrodynamic analysis. In addition to this, the analysis will be practically applied to the model test which uses a semi-rigid seal, e.g., in the case of the XR-5 SES model. Reference 3 reports the investigation of the seal stiffness on the aero-hydrodynamic bubble pressure of a SES model.

The above assumption reduces the expression of the bubble pressure to the following form,

$$\frac{\frac{p_b}{p_o}}{\frac{z}{h}} = \frac{-\gamma \left(1 + \frac{p_a}{p_o}\right)}{1 - \gamma \left(1 + \frac{p_a}{p_o}\right) \frac{p_o}{v_o} \left[\frac{vL^2}{\rho_w g} + \frac{i}{\sigma} \left\{ n \left| \frac{\partial Q_f}{\partial p} \right| + k \sqrt{\frac{2p_o}{\rho_a}} \left(\frac{A_o}{2p_o} - \alpha \frac{L}{\rho_w g} \right) \right\} \right]} \quad (80)$$

If the water wave induced volume v and area α are set equal to zero, the above relation will represent the bubble pressure due to heave of an air cushion vehicle above the ground.

Although Eq.(80) is derived by means of perturbation analysis keeping only the first-order term, two limiting values of the bubble pressure under extreme conditions can be obtained:

- a) When translation velocity U and frequency σ approach to zero with openings closed aft and no fans in operation (closed box), then

$$\lim_{\substack{U \rightarrow 0 \\ \sigma \rightarrow 0}} \frac{\frac{p_b}{p_o}}{\frac{z}{h}} \approx \rho_w g \quad (81b)$$

- b) When the heaving vehicle is in translatory motion, $U \neq 0$, with all the openings in effect, then when frequency $\sigma \rightarrow 0^*$

$$\lim_{\sigma \rightarrow 0} \frac{\frac{P_b}{P_o}}{\frac{z}{h}} \rightarrow 0 \quad \text{with } 90^\circ \text{ phase lag.} \quad (81b)$$

where the following information has been used, namely, for $\sigma \rightarrow 0$, according to (59) to (61):

- 1) α_r and v_r are negative real constant values
- 2) α_i and v_i are linearly proportional to σ

The above relation is also equally valid for the uncoupled aerodynamic analysis, namely, for $v = \alpha = 0$.

It is apparent that the asymptotic expression of the bubble pressure Eq.(80) for $\sigma \rightarrow \infty$ is dependent on the behavior of the wave-induced volume v for $\sigma \rightarrow \infty$ on the air-water interface. Since the asymptotic expression of v , Eq. (62b), is $v_r =$ a negative constant and $v_i = 0$, we have with water wave effects

$$\lim_{\sigma \rightarrow \infty} \frac{P_b}{P_o} \frac{z}{h} = \frac{-\gamma \left(1 + \frac{P_a}{P_o}\right)}{1 + \gamma \left(1 + \frac{P_a}{P_o}\right) \frac{P_o}{v_o} \frac{L^2}{\rho_w g} |v_r|_{\sigma \rightarrow \infty}}, \quad (82a)$$

whereas with no water wave effects,

$$\lim_{\sigma \rightarrow \infty} \frac{P_b}{P_o} \frac{z}{h} = -\gamma \left(1 + \frac{P_a}{P_o}\right) \quad (82b)$$

Both limiting values of pressure signatures show a 180-degree phase lag.

* It should be noted that in the limiting cases when $\sigma \rightarrow 0$ or $\sigma \rightarrow \infty$, then σ and τ can be interchanged.

ADDED MASS AND DAMPING COEFFICIENTS

The real and imaginary components of the bubble pressure Eq.(80) are given by

$$\left\{ \frac{p_b/p_o}{z/h} \right\}_r = \frac{-\gamma(1+p_a/p_o) \left[1 - \gamma(1 + p_a/p_o) \frac{p_o Q_r}{v_o} \right]}{\left[1 - \gamma(1+p_a/p_o) \frac{p_o Q_r}{v_o} \right]^2 + \left[\gamma(1+p_a/p_o) \frac{p_o Q_i}{v_o} \right]^2}$$

$$\left\{ \frac{p_b/p_o}{z/h} \right\}_i = \frac{-[\gamma(1+p_a/p_o)]^2 \frac{p_o Q_i}{v_o}}{\left[1 - \gamma(1+p_a/p_o) \frac{p_o Q_r}{v_o} \right]^2 + \left[\gamma(1+p_a/p_o) \frac{p_o Q_i}{v_o} \right]^2} \quad (83)$$

where

$$Q_r = v_r \frac{L^2}{\rho_w g} + \frac{k}{\sigma} \alpha_i \frac{L}{\rho_w g} \sqrt{\frac{2p_o}{\rho_a}}$$

$$Q_i = v_i \frac{L^2}{\rho_w g} + \frac{1}{\sigma} \left\{ n \left| \frac{\partial Q_f}{\partial p} \right| + k \sqrt{\frac{2p_o}{\rho_a}} \left(\frac{A_o}{2p_o} - \alpha_r \frac{L}{\rho_w g} \right) \right\} \quad (84)$$

The integration of the bubble pressure (83) over the cushion area yields the aero-hydrodynamic force due to heaving motion of a surface effect ship in translation on the calm water surface. The real and imaginary components of the force are designated as aero-hydrodynamic inertial and damping forces from which the added mass M'' and damping factor N are defined in the following form,

$$M'' = \frac{p_{b_r} A_c}{\sigma^2 z}$$

$$N = -\frac{p_{b_i} A_c}{\sigma z} \quad (85)$$

where the minus sign comes from the $\text{Re}(p_b A_c e^{i\sigma t})$.

The non-dimensional added mass and damping coefficients of Eqs.(85) can be defined in the following form,⁷

$$C_a = \frac{M''}{\frac{1}{2} \rho_w L^3} ; C_d = \frac{N}{\frac{1}{2} \rho_w UL^2} \quad (86)$$

The added mass M'' and damping factor N for $\sigma \rightarrow 0$ are derived by knowing the behavior of the α_r , α_i , v_r and v_i at $\sigma \rightarrow 0$;

$$\frac{\alpha_i}{\sigma} = \frac{d\alpha_i}{d\sigma} > 0$$

$$\frac{v_i}{\sigma} = \frac{dv_i}{d\sigma} > 0$$

$$v_r = -|v_r| ; \alpha_r = -|\alpha_r| \quad (87)$$

The results are given by

$$\begin{aligned} M''_{\sigma \rightarrow 0} &= \frac{E A_c^2}{D^2} \\ \sigma \rightarrow 0 N &= \frac{A_c^2}{D} \end{aligned} \quad (88)$$

where

$$\begin{aligned} D &= n \left| \frac{\partial Q_f}{\partial p} \right| + k \sqrt{\frac{2p_o}{\rho_a}} \left(\frac{A_o}{2p_o} + \left| \alpha_r \right|_{\sigma \rightarrow 0} \frac{L}{\rho_w g} \right) \\ E &= - \frac{v_o}{\gamma(p_a + p_o)} - \left| v_r \right|_{\sigma \rightarrow 0} \frac{L^2}{\rho_w g} + \frac{d\alpha_i}{d\sigma}_{\sigma \rightarrow 0} k \sqrt{\frac{2p_o}{\rho_a}} \frac{L}{\rho_w g} \end{aligned} \quad (89)$$

where D is always positive, whereas E may take positive or negative value. Thus the damping factor N is always positive and the added mass may be positive or negative (i.e., the motion of the vehicle and the added water mass are in opposite directions).⁴

Definite signs are obtained when the water wave effects are omitted.

Namely,

$$\begin{aligned} D &= n \left| \frac{\partial Q_f}{\partial p} \right| + k \sqrt{\frac{2p_o}{\rho_a}} \\ E &= - \frac{v_o}{\gamma(p_a + p_o)} \end{aligned} \quad (90)$$

From Eqs.(90) we have always the negative added mass and positive damping factor for the SES without water wave effects or ground effect machine at $\sigma \rightarrow 0$.

It is apparent from Eqs.(88), (89) and (90) that the added mass M'' and damping factor N at the vanishingly low frequency are proportional to the cushion area squared and dependent on the contributions by the fan, seal leakage, wave-induced area and volume and the cushion volume and ambient pressure which are chosen in the preliminary design stage.

SCALE EFFECT ON THE BUBBLE PRESSURE

Reference 12 presents the scale effect on the real component of the bubble pressure in the two-dimensional SES against the scale ratio $\lambda =$ ship length/model length. It shows that the scale effect is larger for the low frequency than for the high frequency.

A similar study can be carried out for the present three-dimensional SES model.

Since $p_o Q_r / v_o$ and $p_o Q_i / v_o$ in (83) are dimensionless, the scale effect on the magnitude of the pressure (or the components) can be estimated by scaling the ambient pressure p_o by λp_o . For the real component the ratio of the coefficient for ship and model is

$$\frac{\left(\frac{p_b/p_o}{z/h}\right)_{r_{\text{ship}}}}{\left(\frac{p_b/p_o}{z/h}\right)_{r_{\text{model}}}} = \frac{\gamma(1 + p_a/\lambda p_o) [1 - \gamma(1 + p_a/\lambda p_o) p_o Q_r / v_o]}{[1 - \gamma(1 + p_a/\lambda p_o) p_o Q_r / v_o]^2 + [\gamma(1 + p_a/\lambda p_o) p_o Q_i / v_o]^2} \Bigg/ \frac{\gamma(1 + p_a/p_o) [1 - \gamma(1 + p_a/p_o) p_o Q_r / v_o]}{[1 - \gamma(1 + p_a/p_o) p_o Q_r / v_o]^2 + [\gamma(1 + p_a/p_o) p_o Q_i / v_o]^2} \quad (91)$$

Similar expressions can be obtained for the imaginary component as well as for the resultant magnitude.

NUMERICAL CALCULATIONS AND DISCUSSION

Water Waves - Elevation, Escape Area and Volume

The model used in Reference 2 has been chosen to compare the analytical values of wave elevation, escape area at stern and volume on the air-water interface in the developments of that reference and the present study.

A series of calculations have been carried out for the elevation of the free surface along the wall $y=b$ at Froude number $F_n=0.5$ for different values of frequencies $\tau=0$, and $\tau=0.2375$ and $\tau=0.2750$ which bracket the critical frequency $\tau=0.25$. The results are shown in Figures 2a and 2b and compare very favorably with those of Doctors who defines $F_n = v/\sqrt{4ag}$. Figure 2c is a comparison of the values of wave elevation of the corner point $x/a=-1$ and $y/b=1$ in terms of frequency τ , evaluated by the present analysis and by that of Reference 2. In the low frequency regime the agreement is excellent, whereas outside that the discrepancy is quite substantial especially in the imaginary part of the elevation values.

Similar calculations were carried out for the escape area, α , at the stern and the volume, v , on the air-water interface for the entire frequency range of practical interest. A comparison of the results of both analytical solutions is shown in Figures 3a and 3b for the escape area coefficient, α , and volume coefficient, v , respectively, for a series of frequencies τ . The agreement is rather satisfactory up to $\tau=1.5$ except for the real value of the v coefficient. It is interesting to notice that the value of the escape area oscillates with τ , whereas the volume coefficient v behaves relatively monotonically. Sudden changes of the values of α and v are exhibited at the critical $\tau=0.25$ as should be expected. Furthermore, it is interesting to note that as $\tau \rightarrow 0$, the imaginary part of both quantities tends to zero whereas the real parts tend to finite negative values. These limiting values can be readily obtained from Equations (61a), (61b), and (62a), (62b). As the frequency approaches higher values, the imaginary parts of α and v diminish showing a trend to zero asymptote, whereas the real components tend to a negative non-zero asymptote. The non-zero values are less than the static values of $\alpha_r=-0.25$ and $v_r=-0.25$. It is apparent, therefore, that the dynamic values of α and v in Eqs.(62a) and (62b) are positive and their magnitudes are less than their corresponding static values (Eq.61c).

Similar calculations have been carried out for XR-5 SES model at $F_n = 0.72$, for which extensive experimental work is available.⁵⁻⁷ Figure 4 is a sketch of the model and Table 1 presents its principal particulars. The results for α and v are exhibited in Figures 5a and 5b versus the frequency τ . The trends of the results of both models are, in general, similar except that the oscillatory behavior of α has been reduced considerably in the second model.

Bubble Pressures

The values of bubble pressures in the plenum calculated from the expressions given by Eqs.(80), (81) and (82), for the XR-5 SES model at $F_n = 0.72$ are graphically exhibited in Figures 6a and 6b for a series of reduced frequencies τ .

Figure 6a shows the values of bubble pressure and phase shift angle versus τ in the presence or absence of water free surface effects. In the limit as $\tau \rightarrow 0$, the expression given by Eq.(81) shows the pressure amplitude reduces to zero with phase lag of 90 degrees. The pressure amplitude generally increases as τ increases tending to the asymptotic value given by Eqs.(82a) and (82b) for both cases, with and without the free surface wave effects.

Figure 6b gives the entire picture of bubble pressure versus τ ranging from zero to 600. It is seen that the amplitude reaches its asymptote, $\gamma(1 + p_a/p_0)$ at $\tau = 200$, whereas the phase angle may reach its asymptote at $\tau = 800$. It is to be noted, however, that the values of the bubble pressure in the uncoupled condition (i.e., without water wave effects) are, in general, much larger than those obtained under the coupled condition. In fact, the asymptotic value of the former is about thirty times larger than the latter.

Added Mass and Damping Coefficients

The heave added mass and damping coefficients C_a , C_d of the XR-5 SES model have been calculated and are shown in Figures 7a and 7b. The experimental values⁶ for the model are also compared with the theoretical values in Figure 7a. Both results show the same trend and the experimental damping coefficients agree better with the present theory when wave effects are taken into account. The asymptotic values of the coefficients obtained from Eq.(85)

and (88) as $\tau \rightarrow 0$ are the same for both coupled and uncoupled conditions. The imaginary part of the bubble pressure from which the damping factor N is determined is linearly proportional to the frequency τ (or σ) at low frequency for both coupled and uncoupled conditions (see Eq.85). The experiments⁴ also find this component linearly proportional to the frequency for an ACV model over the ground. The added mass coefficient is, in general, negative for the specific model except in a narrow region as indicated in Figure 7a.

The non-dimensional coefficients C_a and C_d diminish as τ increases. As τ approaches ∞ , the coefficients tend to vanish for both coupled and uncoupled conditions (see Figure 7b).

Scale Effect on the Bubble Pressure

The scale effect on the bubble pressure amplitude has been calculated for the XR-5 SES model at $F_n = 0.72$, and the results are shown in Figure 8. It is seen that the scale effect is increasing with increasing frequency at constant scale ratio λ and increases also with λ at constant frequency. The scale effect increases with both increasing frequency and scale ratio. For instance, the ship pressure at $\tau=4.5$ is underestimated by 14% when the model scale ratio $\lambda=10$, which corresponds to about a 133 long-ton ship.*

The previous work¹² on the scale effect is concerned with the real component of the pressure only. It shows that the scale effect is larger at low frequency, a trend which is opposite to the present result. However, it is to be noted that the analysis of Reference 12 deals with the two-dimensional theory and hence it is difficult to compare with the present three-dimensional analysis.

Heave Response

Since the theoretical heave added mass and damping coefficients are available, the heave response with pitch restrained has been calculated by utilizing test results⁶ for the restoring and exciting forces of the XR-5 SES model.

Figure 9a shows the mean line drawn among the experimental values of the non-dimensional heave exciting force⁶ versus the non-dimensional encounter frequency $\alpha\sqrt{L/g}$. The extrapolation has been made by assuming that the heave-exciting is identical to the restoring force at zero frequency. The

*These conclusions reached after the set of calculations performed for the XR-5 SES for given fan characteristics and discharge should be used with caution and cannot be generalized before extensive calculations are performed.

mean line has been cut-off at the frequency beyond which the data are unreliable.

The experimental added mass and damping coefficients have been obtained from the three test points indicated in Figures 18 and 19 of Reference 6. Using these values, three heave responses have been calculated. Figure 9b compares the semi-analytical and the experiment-based calculations. The semi-analytical response is higher than the experiment-based calculation results due to the fact that the theoretical damping coefficients are lower than the experimental values.

The theoretical calculations show a similar trend to that of the heave with pitch free (x symbols) which is obtained from Reference 7. The natural pitching frequency of the model is 5 rad/sec. It is seen in Figure 9b that the theoretical heave at the natural pitching frequency is about 50% of the heave with pitch free. This kind of characteristic heave response in coupled and uncoupled conditions for an SES model has been found by Fridsma^{8,9} at Davidson Laboratory.

Numerical Procedures

The computational work has been carried out at the Stevens Institute Computer Center on the PDP-10 high-speed digital computer. Program structure with Flow-Chart of the main subroutine VLLI, program listing and descriptions of input and output are given in Appendix E.

The exponential integral of complex argument, which is the basic element in all the analytical expressions, is discussed in detail in Appendix D with the view to utilizing high-speed digital computers.

Furthermore for convenience in the numerical integration of Eqs.(46) and (59) to (62), a transformation is introduced to simplify the structure of the singular behavior at θ_c (critical point, see Eq.29), and then the "Lagrange interpolation method" has been employed for the evaluation of the finite contribution of the high-order singularity.

SUMMARY AND CONCLUSIONS

A mathematical model has been developed for the evaluation of the added mass and damping coefficients of a heaving surface effect ship in uniform translation on a calm water surface.

The analysis furnishes the variation of bubble pressure in the plenum and its scale effect in terms of reduced frequency τ in the entire range of practical interest, and also provides information on the wave elevation of the free surface, the escape area at the stern and the volume on the air-water interface.

A program has been written in FORTRAN IV language and applied to the PDP-10 high-speed digital computer.

The following basic assumptions were made:

1. The deformation of the water surface participates in the generation of the bubble pressure in conjunction with the action of seals and fans.
2. The deformation of the free surface under the oscillatory rectangular pressure patch in uniform translation is used to display the way in which the motion of the water surface participates in the evaluation of the pressure variations in the plenum air.
3. In the dynamic analysis of the air flow phenomena, pressure and volume changes are assumed to occur sufficiently rapidly so that the adiabatic law governs the basic thermodynamic variations in the air cushion.
4. The bubble (or cushion) pressure is assumed to be spatially homogeneous.
5. The leakage of the air takes place only at fan and stern apertures.
6. The perturbed (or bubble) pressure and air volume have the same order of magnitudes as the heave displacement.

Expressions for the wave elevation, escape area and volume have been derived and their limiting values at $\tau \rightarrow 0$ and $\tau \rightarrow \infty$ have been studied.

The linear equations of bubble pressure and heave motion have been developed, applying perturbation procedure to the adiabatic law, and their asymptotic values at $\tau \rightarrow 0$ and $\tau \rightarrow \infty$ have been established.

A series of numerical calculations for the SES model have been carried out for the wave elevation, escape area, volume, bubble pressure, added mass, damping factor, the scale effect on the bubble pressure and the heave response with pitch restrained.

All the above results have been compared with available experimental data and their behavior as functions of the frequency discussed.

The following conclusions can be drawn from this investigation:

1. The assumption of a rigid-free surface is not valid. Considerable differences have been observed with and without the free surface waves.

2. The bubble pressure in the plenum has zero amplitude with 90° phase lag as $\tau \rightarrow 0$, whereas at $\tau \rightarrow \infty$ it reaches a constant value with 180° phase lag.

3. The added mass and damping factors as $\tau \rightarrow 0$ reach asymptotically finite values whereas as $\tau \rightarrow \infty$ they vanish.

4. The scale effect on the bubble pressure increases with increasing frequency and scale ratio. (More extensive calculations are needed before generalizing this.)

5. The present method can be applied to predict the heave response with restrained pitch motion utilizing experimental values of the restoring and exciting forces.

6. The added mass and damping factor compare favorably with the experimental data. Unfortunately a very limited number of experiments are at present available and before more experiments are conducted, no general conclusion as to the accuracy of the theoretical prediction can be drawn.

It is expected that the present method can be extended to calculate 1) the heave exciting force of a captive SES model uniformly running in head regular waves and 2) the heave restoring force acting on an SES model in uniform translation.

REFERENCES

1. Kaplan, Paul and Davis, Sydney, "A Simplified Representation of the Vertical Plane Dynamics of SES Craft," AIAA Paper No.74-314, Feb. 25-27, 1974.
2. Doctors, L.J., "The Hydrodynamic Influence on the Non-Linear Motion of an ACV over Waves," ONR 11th Symposium on Naval Hydrodynamics, MIT, June 1974.
3. Breslin, J.P. and Hires, R.I., "Theoretical and Experimental Study of Pneumo-Hydrodynamic Coupling in a Surface Effect Ship Model," Davidson Laboratory Report SIT-DL-76-9-1888, May 1976.
4. Van Den Brug, J.B. and Van Staveren, P., "An Experimental Study on the Dynamic Stability of a Ground Effect Machine Model in Heave, Pitch and Roll," Ministerie van Defensie (Marine), Hoofdafdeling Materieel Bureau, Scheepsbouw, Nederland, Report Nr.19074/6931/SB, March 1968.
5. Magnuson, Allen H. and Wolff, Kathryn, K., "Seakeeping Characteristics of the XR-5, a High Length-Beam Ratio Manned Surface Effect Testcraft; 1. XR-5 Model Response in Regular Head Waves," Naval Ship Research and Development Center, SPD-616-01, March 1975.
6. Fein, James A. and Murray, Lawrence, O., "Wave Excitation and Vertical Plane Oscillation Experiments on a High Length-to-Beam Ratio Surface Effect Ship," David W. Taylor Naval Ship Research and Development Center, SPD-697-01, July 1976.
7. Moran, David D., Fein, James, A. and Ricci, Joseph J., Jr., "Seakeeping Characteristics of a High Speed-To-Beam Ratio Surface Effect Ship," AIAA Paper No.76-862, AIAA/SNAME. Advanced Marine Vehicles Conference, Arlington, Virginia, September 20-22, 1976.
8. Fridsma, Gerard, "Tests on a Partial Length Sidewall SES Model in Regular and Irregular Waves," Stevens Institute of Technology, Davidson Laboratory Letter Report SIT-DL-72-1576, January 1972.
9. Fridsma, Gerard, "Tests in Waves of a Partial Length Sidewall SES with Length-to-Beam Ratio Two," Stevens Institute of Technology, Davidson Laboratory Letter Report SIT-DL-75-1847, October 1975.
10. Moran, D.C., "Cushion Pressure Properties of a High Length-to-Beam Ratio Surface Effect Ship," David Taylor NSRDC, Ship Performance Department, Report SPD-600-01, May 1975.
11. Tsakonas, S., Jacobs, W.R. and Ali, M.R., "Plenum Pressure of an Air-Cushion Supported Vehicle," Stevens Institute of Technology, Davidson Laboratory Report SIT-DL-76-1902, July 1976.

12. Breslin, J.P., "Aero-Hydronechanical Coupling in the Heaving, Translating Surface Effect Ship," presented at the 17th American Towing Tank Conference, June 1974.
13. Peters, A.S. and Stoker, J.J., "The Motion of a Ship as a Rigid Body in a Seaway," Institute of Mathematical Sciences, Report No. IMM-203, New York University, 1954.
14. Stoker, J.J., Water Waves. The Mathematical Theory with Applications, Interscience Publishers, Inc., New York, 1957.
15. Miles, J.W., "Transient Gravity Wave Response to an Oscillating Pressure," Journal of Fluid Mechanics, 13, 1962. pp.145-150.
16. IBM System/360 Scientific Subroutine Package, pp.368-370.
17. "Tables of the Exponential Integral for Complex Arguments," National Bureau of Standards, AMS.51, May 15, 1958.
18. Tsakonas, S., Jacobs, W.R. and Ali, M.R., "An Exact Linear Lifting-Surface Theory for a Marine Propeller in a Non-uniform Flow Field," Appendix D, Report SIT-DL-72-1509, February 1972.
19. Kim, C.H., "Über den Einfluss nichtlinearer Effekte auf hydrodynamische Kräfte bei erzwungenen Tauchbewegungen prismatischer Körper," Schiffstechnik 14 (1967) Nr.73.
20. Kim, C.H. and Tsakonas, S., "Waves Generated by a Uniformly Moving Oscillatory Surface Effect Ship," Davidson Laboratory Letter Report SIT-DL-76-1874, March 1976.

ACKNOWLEDGMENTS

The authors would like to thank Dr. L. J. Doctors and Dr. J. P. Breslin for their comments on the expression of the static elevation, and on the asymptotic behavior of the bubble pressures, respectively. Thanks is also extended to Mr. Ping Liao for his assistance in the refinement of the computer programs.

TABLE 1

PRINCIPAL CHARACTERISTICS OF XR-5 SES MODEL

Length overall, ft	LOA = 15.58
Length of bubble, ft	L = 13.83
Beam of bubble, ft	b = 2.12
Height of bubble, ft	h = 0.72
Test displacement, lb	$\Delta = 298$
Nozzle factor	k = 0.65
Fan flow rate per pair of fans, $\text{ft}^3/\text{lb-sec}$	$ \partial Q_f / \partial p = 0.03$
No. of pairs of fans	n = 2
Leak area at equilibrium	$A_l^{(0)} = 0.333$
Froude number	$F_n = 0.72$
Encounter frequency, rad/sec	$\omega_e = 3 \sim 22$
Natural pitching frequency, rad/sec	$\omega_x = 5$
Heave restoring force, lb/ft	B = 1350

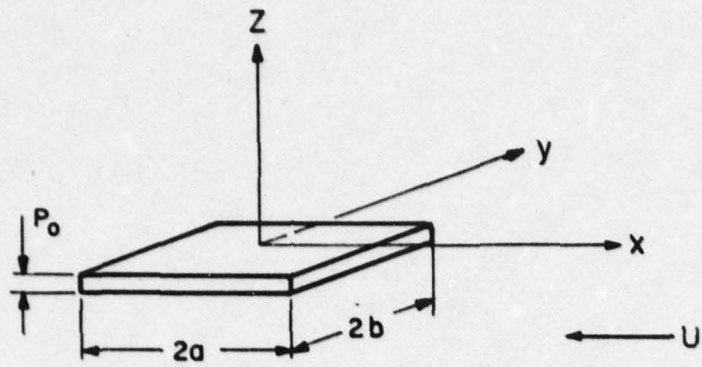


FIG. 1a. RECTANGULAR PRESSURE DISTRIBUTION

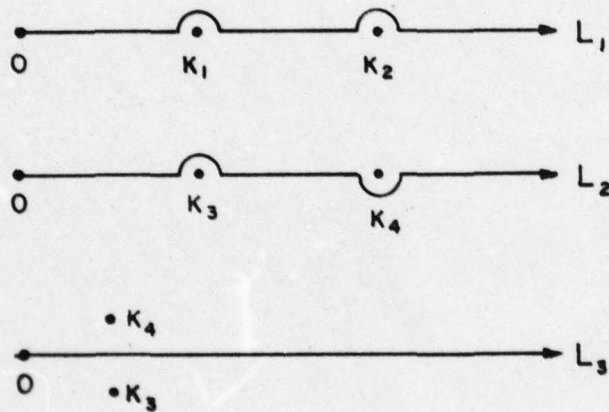


FIG. 1b. INTEGRATION PATHS

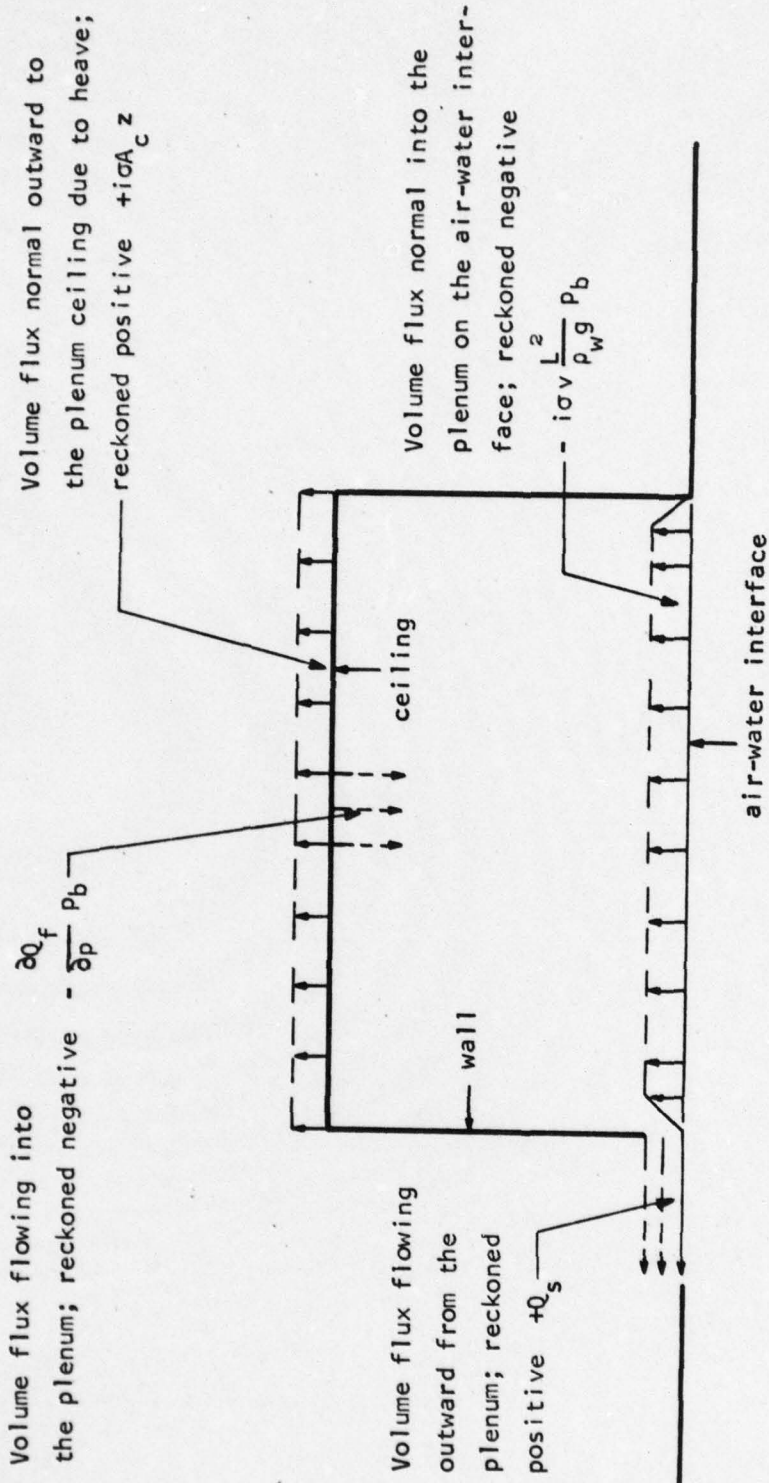


FIGURE 1c. SKETCH OF THE SENSES OF THE FLOW DIRECTION OF THE VOLUME FLUX NORMAL TO THE PLENUM WALL, CEILING AND AIR-WATER INTERFACE

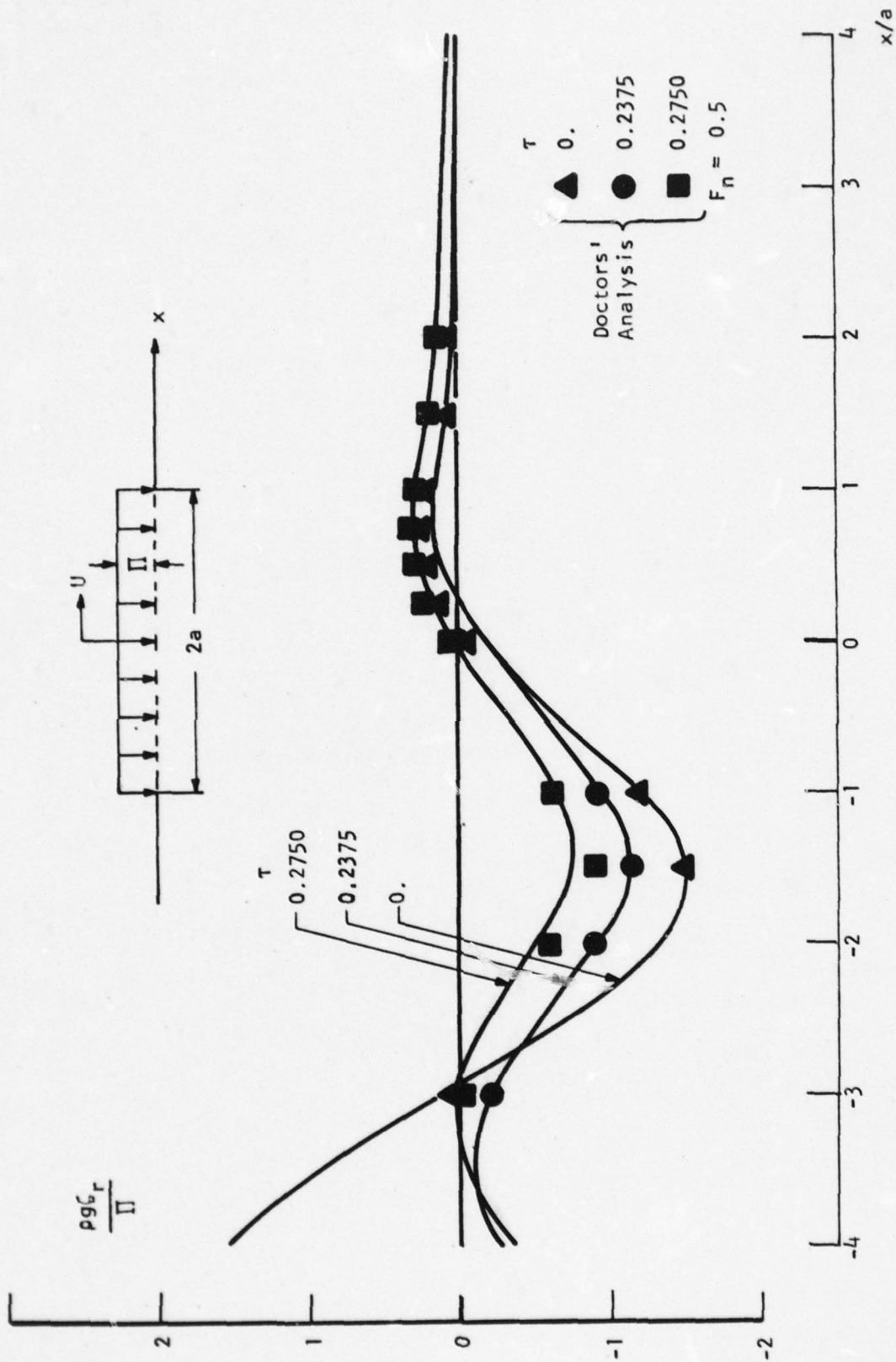


FIGURE 2a. ELEVATION ALONG THE LONGITUDINAL SECTION $y/b=1$

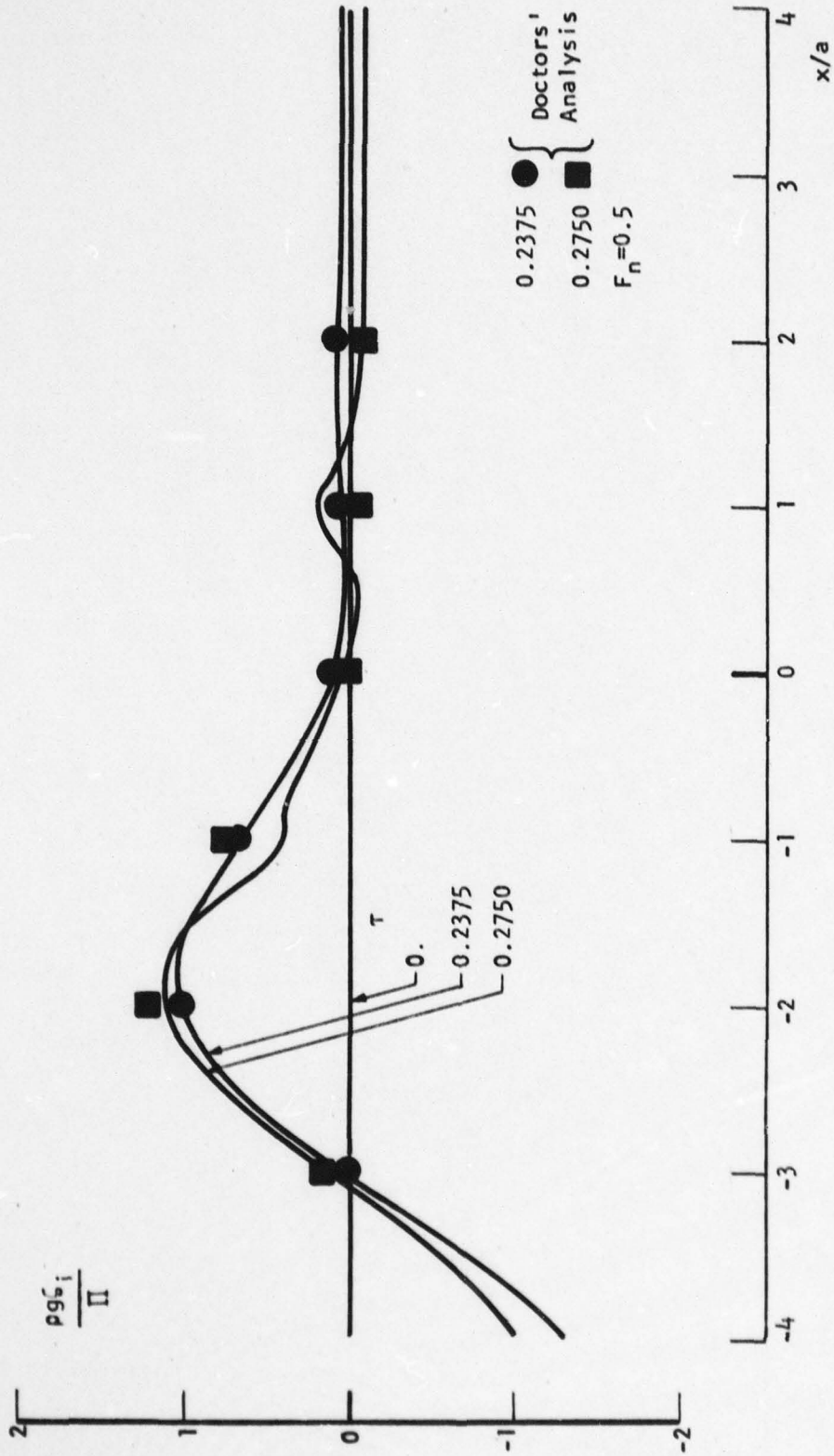
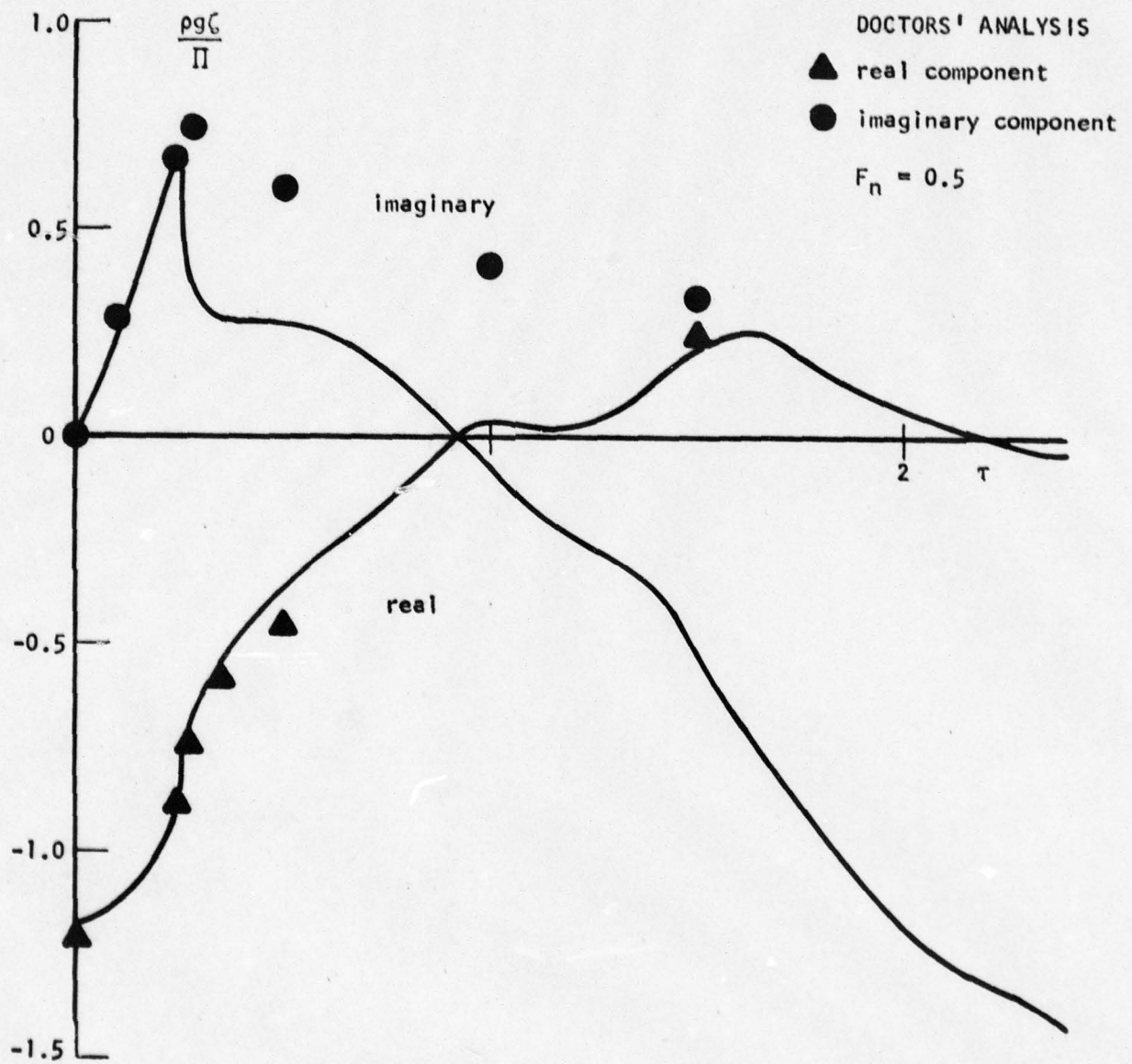


FIGURE 2b. ELEVATION ALONG THE LONGITUDINAL SECTION $y/b=1$

FIGURE 2c. ELEVATION VS. τ AT $x/a = -1$ AND $y/b = 1$

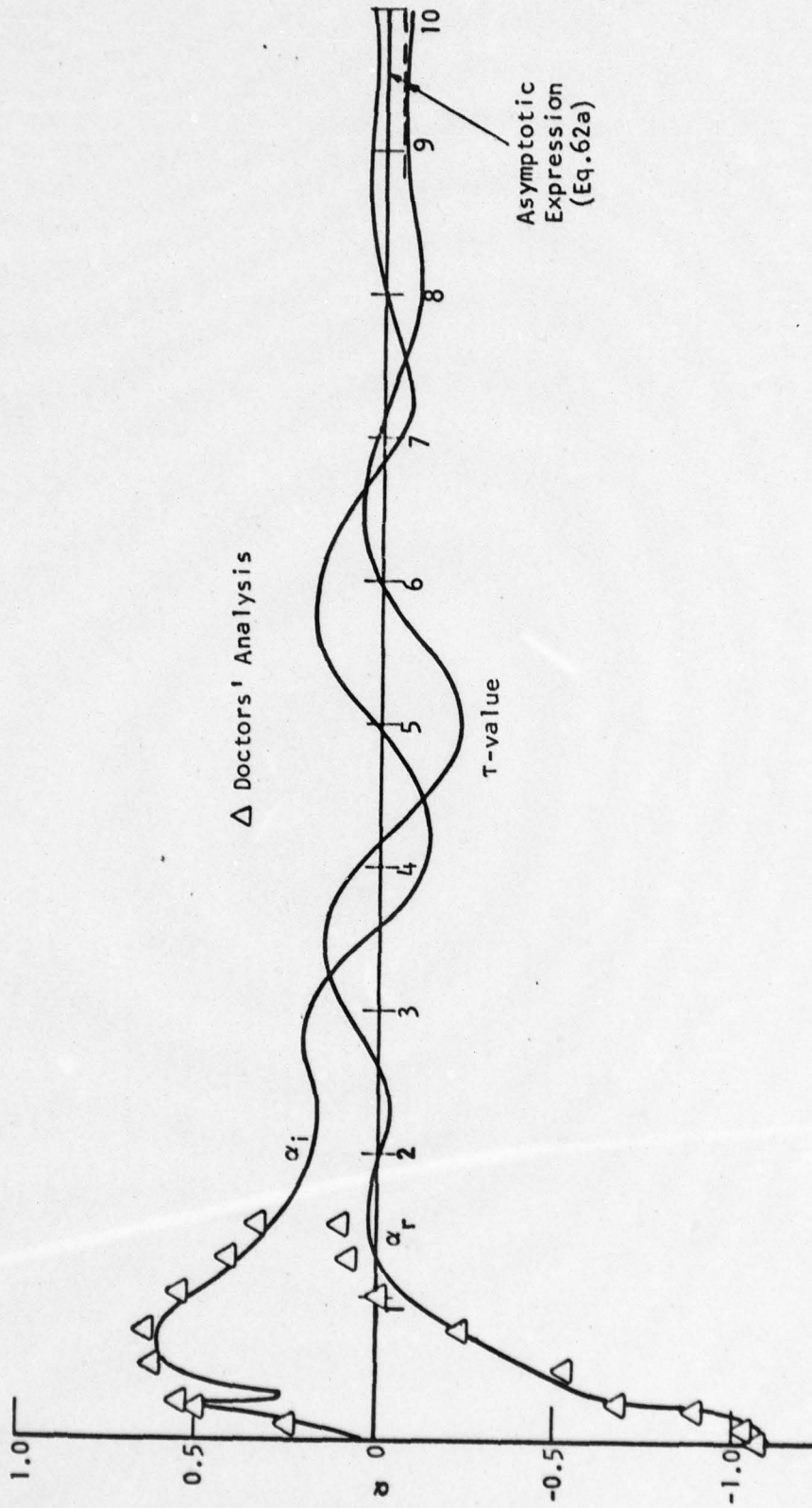


FIGURE 3a. ESCAPE AREA COEFFICIENT α AT STERN FOR THE MODEL IN REF.[2] VERSUS T FOR $F_n \approx 0.5$

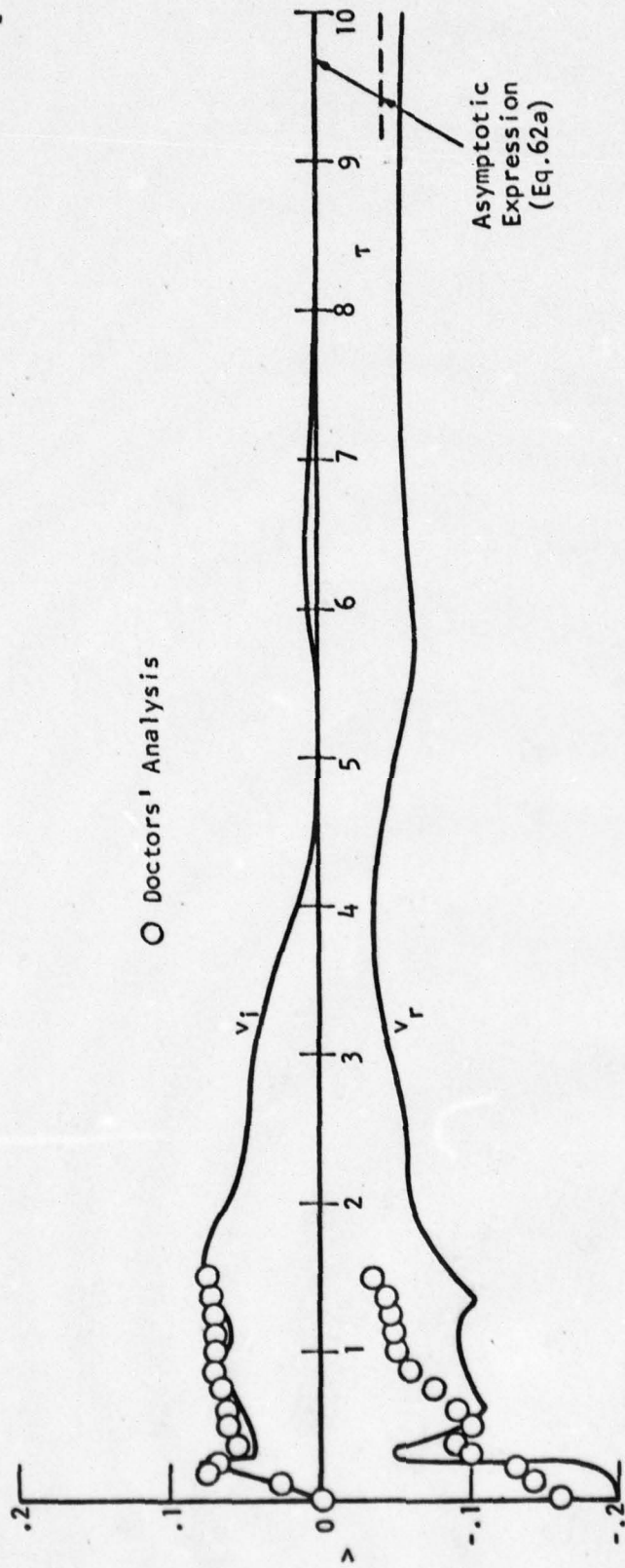


FIGURE 3b. VOLUME COEFFICIENT v VERSUS τ
FOR $F_n = 0.5$ FOR THE MODEL IN REF. [2]

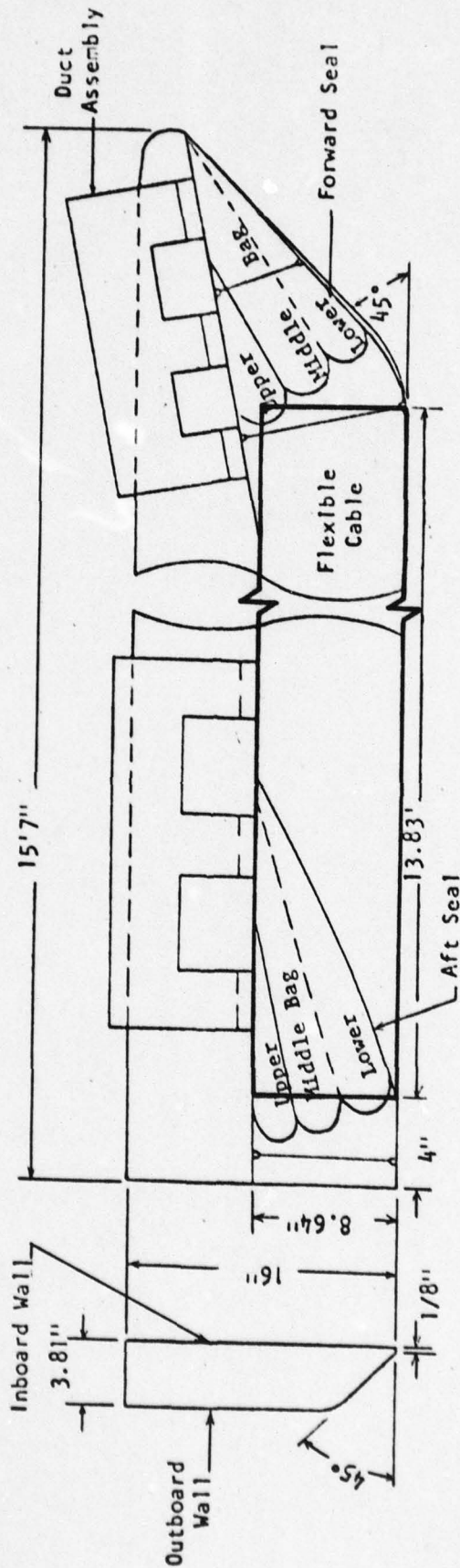


FIGURE 4. SKETCH OF SES MODEL INCLUDING BOW AND STERN SEAL CONFIGURATIONS AND MIDSTATION SIDEWALL SECTION

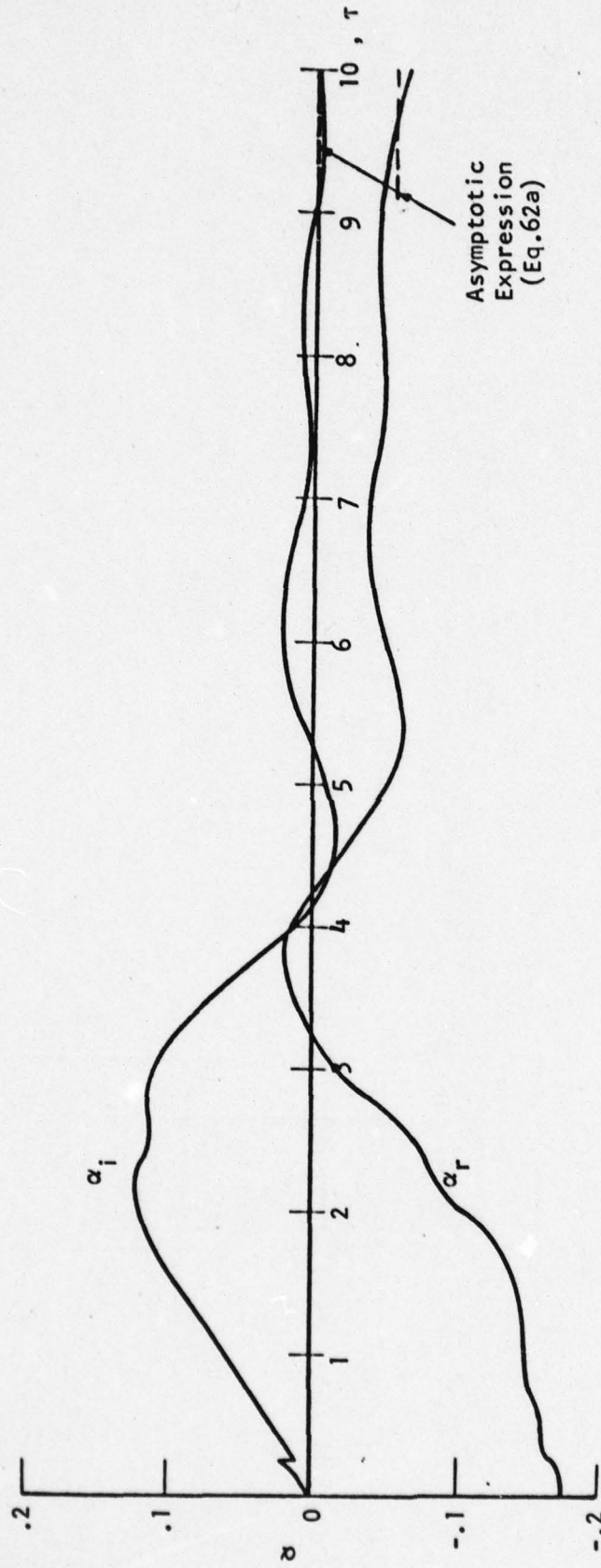


FIGURE 5a. ESCAPE AREA COEFFICIENT α AT STERN VERSUS τ
AT $F_n = 0.72$ FOR XR-5 SES MODEL

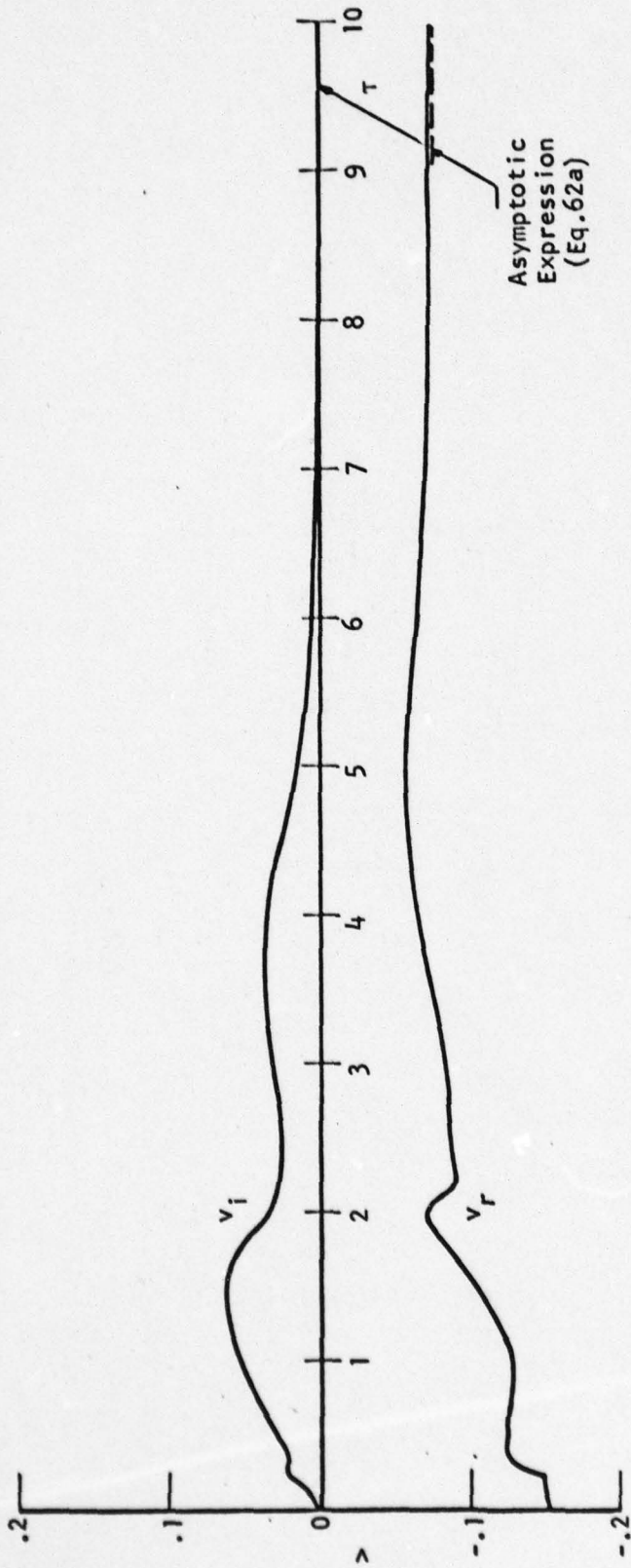


FIGURE 5b. VOLUME COEFFICIENT v VERSUS τ
AT $F_n = 0.72$ FOR XR-5 SES MODEL

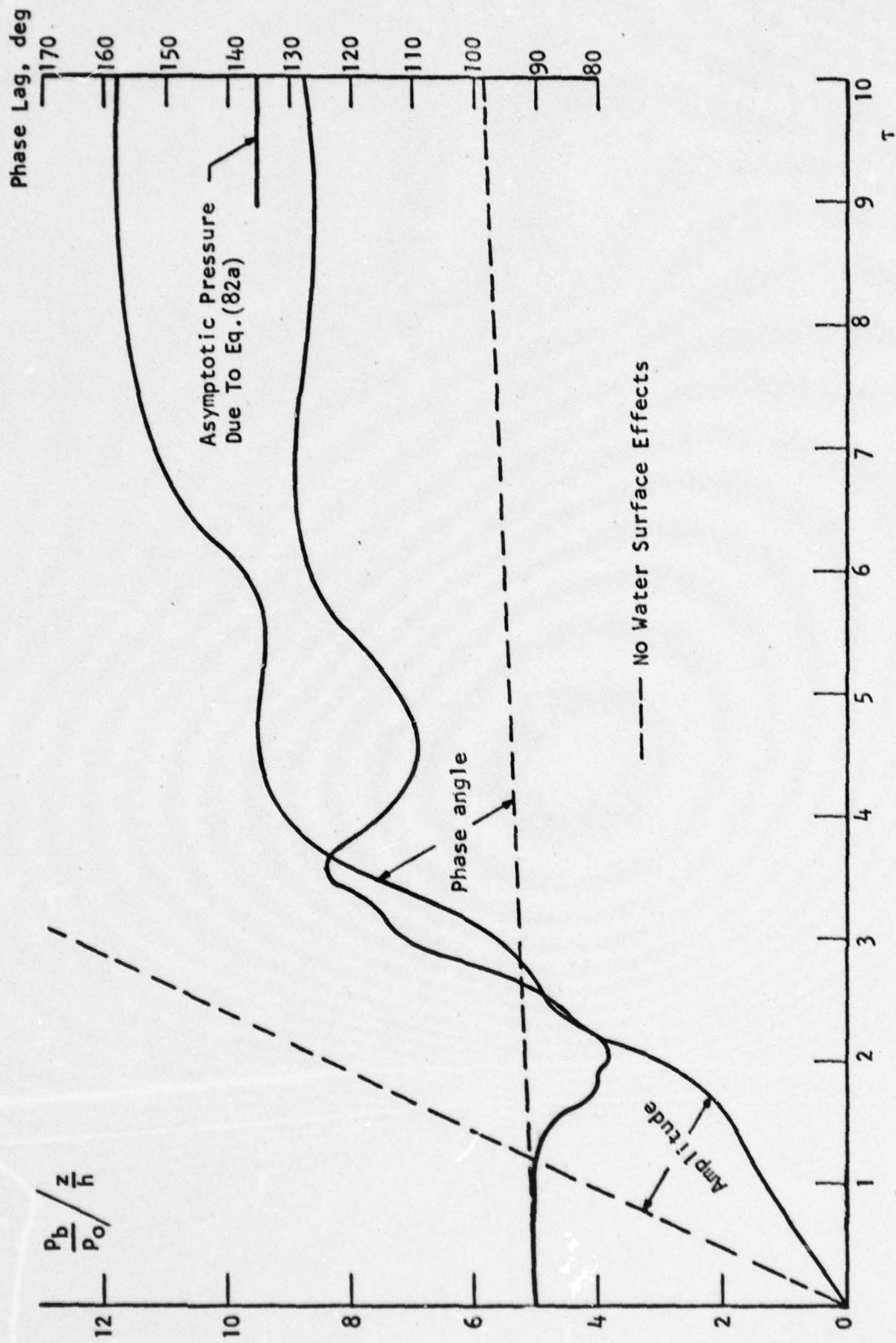


FIGURE 6a. BUBBLE PRESSURE COEFFICIENTS VERSUS τ AT $F_n = 0.72$ FOR XR-5 SES MODEL

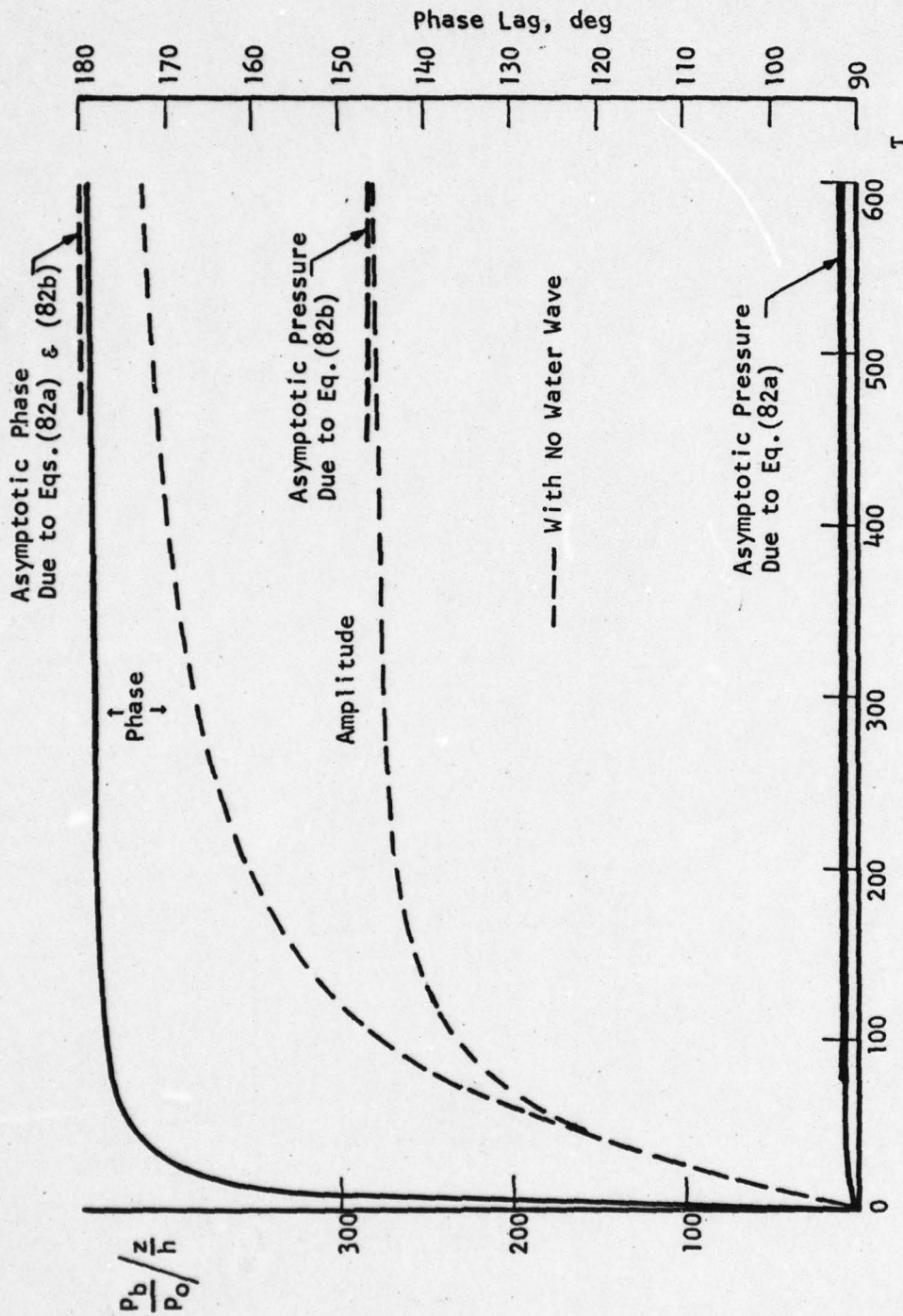


FIGURE 6b. BUBBLE PRESSURE IN THE HIGH FREQUENCY REGION

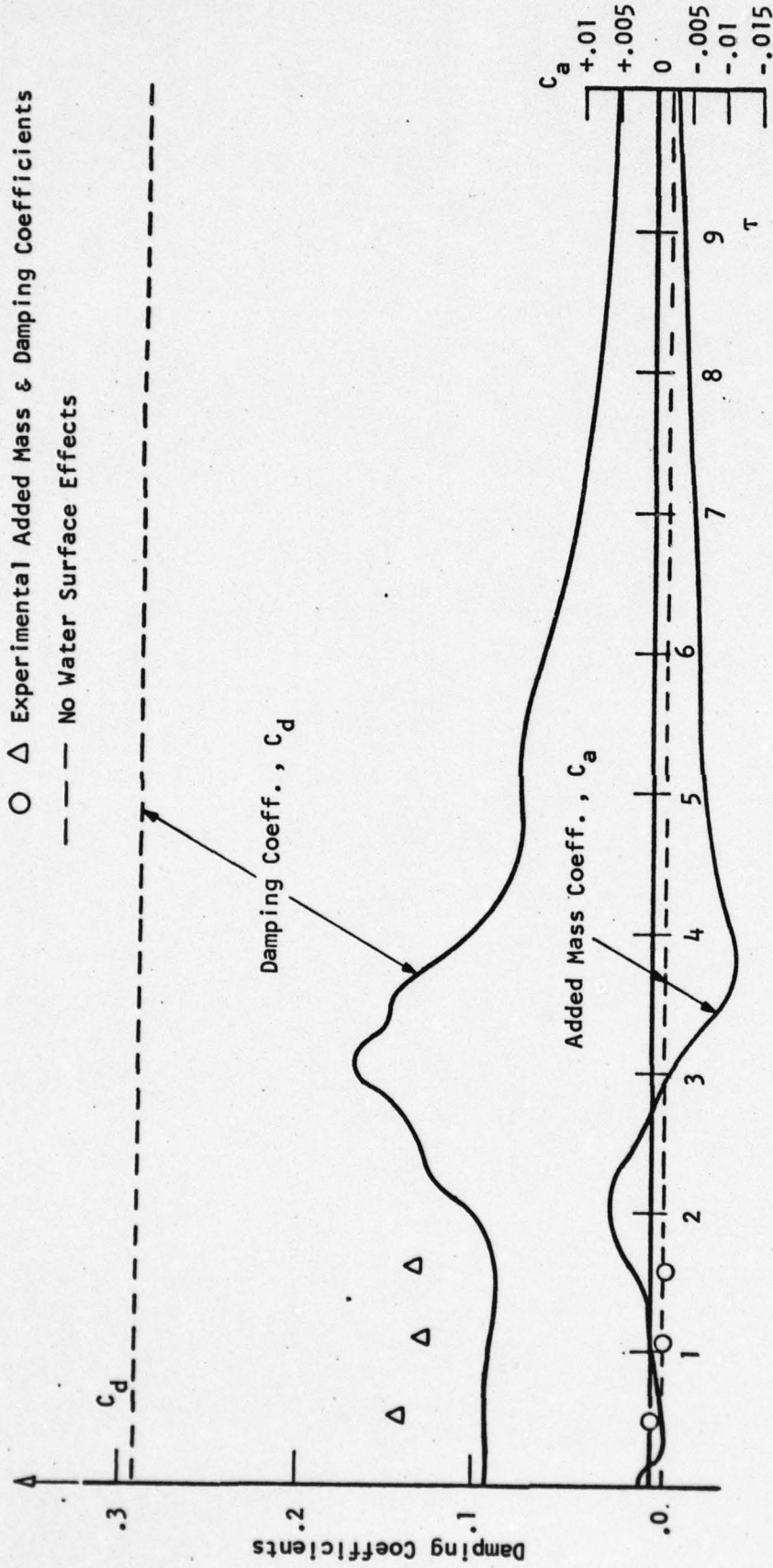


FIGURE 7a. ADDED MASS AND DAMPING COEFFICIENTS VERSUS τ
 AT $F_n = 0.72$ FOR XR-5 SES MODEL

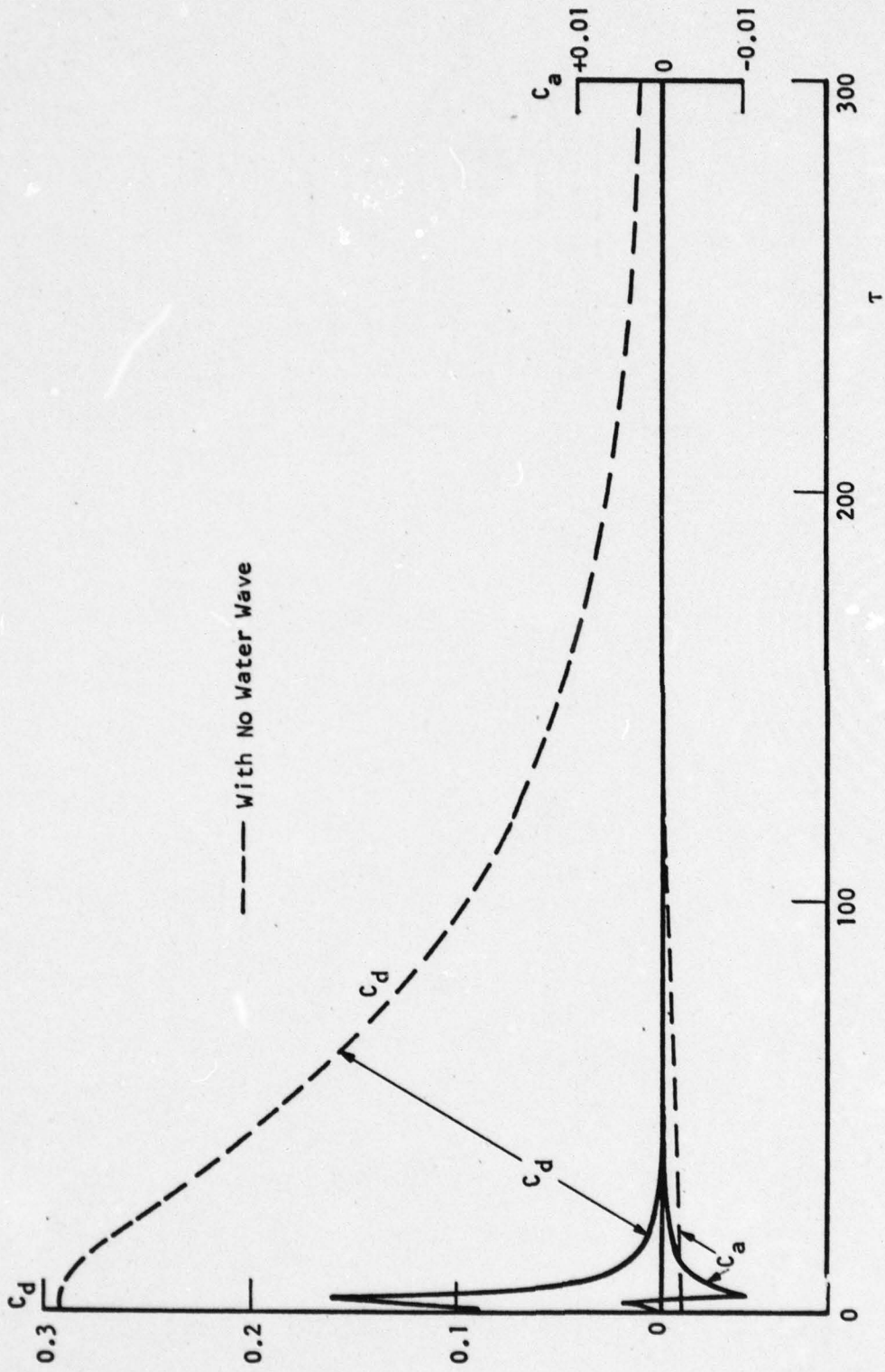


FIGURE 7b. ADDED MASS AND DAMPING COEFFICIENTS (c_a, c_d) IN THE HIGH FREQUENCY REGION

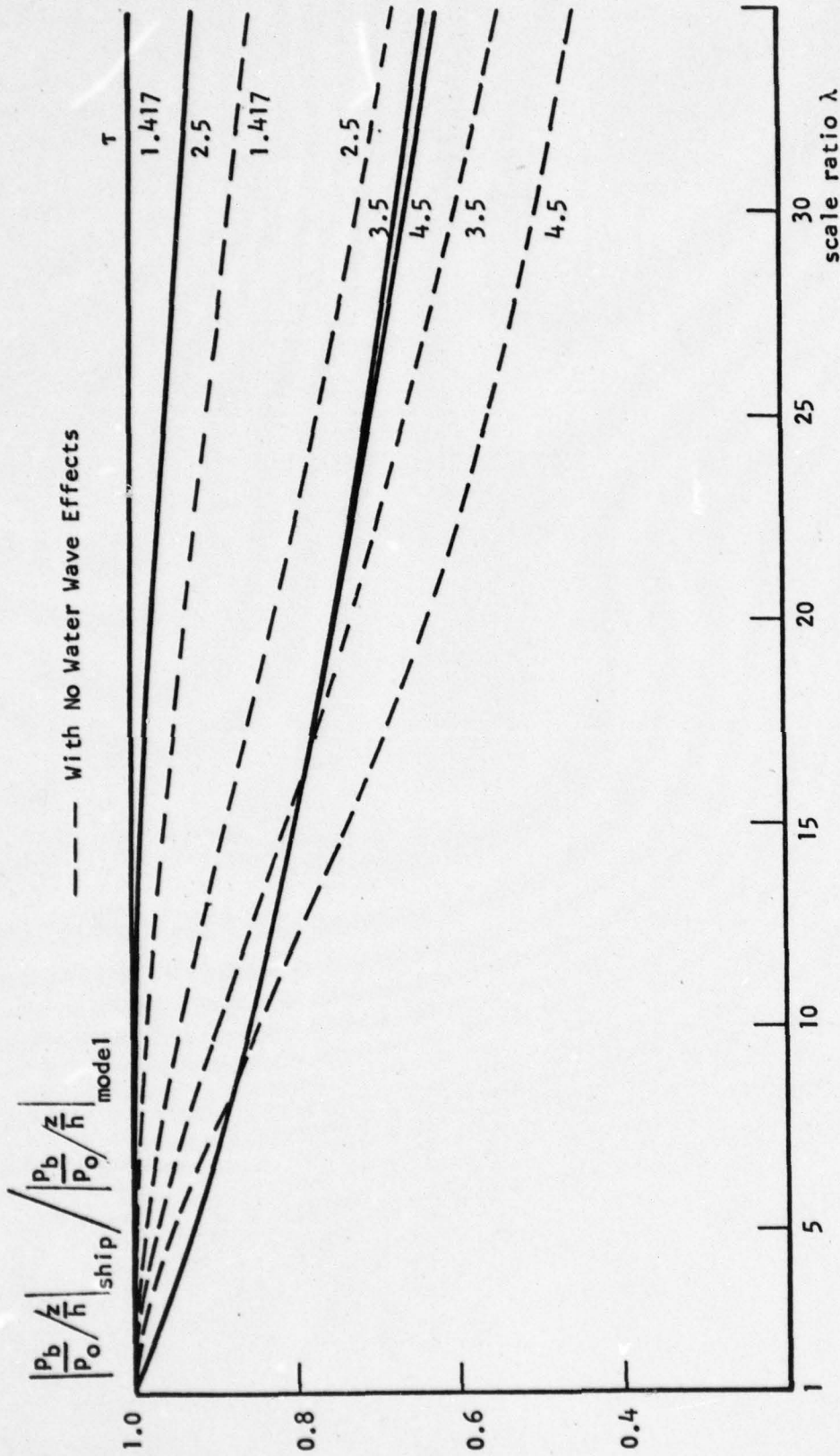


FIGURE 8. SCALE EFFECT ON THE BUBBLE PRESSURE VERSUS SCALE RATIO λ
 AT $F_n = 0.72$ FOR XR-5 SES MODEL

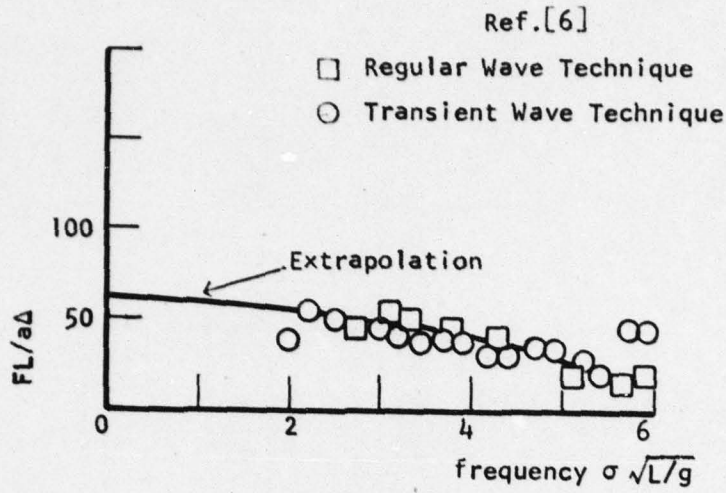


FIGURE 9a. HEAVE-EXCITING FORCE OF XR-5 SES MODEL AT $F_n = 0.72$

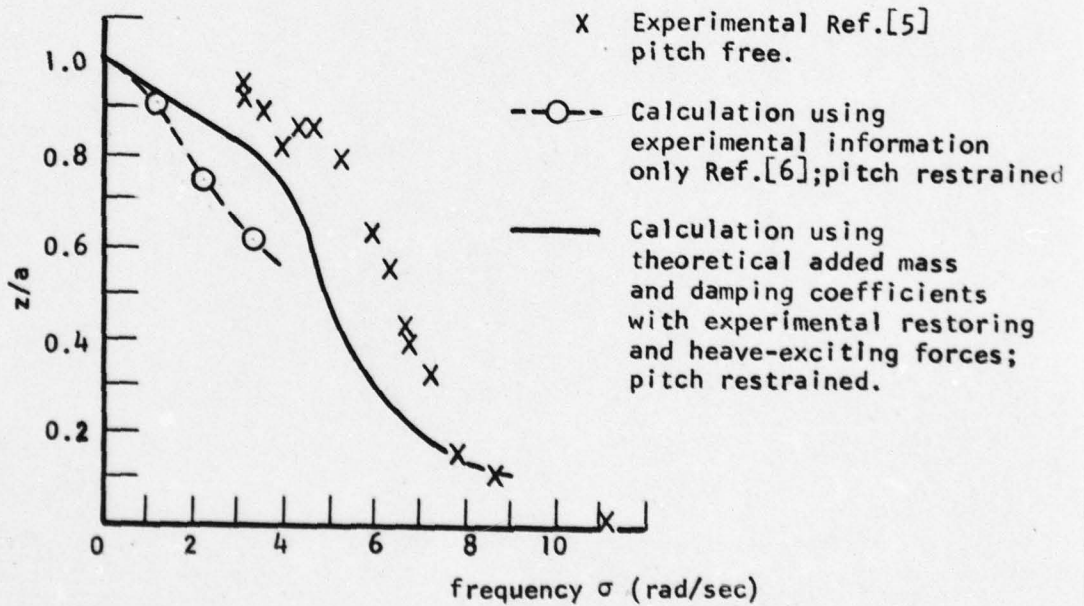


FIGURE 9b. HEAVE TO WAVE AMPLITUDE RATIO OF XR-5 SES MODEL AT $F_n = 0.72$

APPENDIX A

CALCULATION OF $I_{1,j}$, $I'_{1,j}$, $J_{1,j}$, $J'_{1,j}$ ($j=1,2$)

Integration of $I_{1,j}$ and $I'_{1,j}$ in Eqs.(43a) and (43b) with respect to ξ and η yields

$$I_{1,j} = -\frac{U}{\sin\theta} \int_0^{\infty} dk \frac{e^{kz} \left(e^{iks_1} - e^{iks_2} + e^{iks_3} - e^{iks_4} \right)}{k(k-k_j)} + \frac{\sigma}{\sin\theta \cos\theta} \int_0^{\infty} dk \frac{e^{kz} \left(\text{"} \right)}{k^2(k-k_j)} \quad (\text{A-1})$$

$$I'_{1,j} = \frac{U}{\sin\theta} \int_0^{\infty} dk \frac{e^{kz} \left(-e^{iks_5} + e^{iks_6} - e^{iks_7} + e^{iks_8} \right)}{k(k-k_j)} - \frac{\sigma}{\sin\theta \cos\theta} \int_0^{\infty} dk \frac{e^{kz} \left(\text{"} \right)}{k^2(k-k_j)} \quad (\text{A-2})$$

Differentiation of $I_{1,j}$ (A-1) and $I'_{1,j}$ (A-2) with respect to x yields

$$J_{1,j} = \frac{U \cos\theta}{i \sin\theta} \int_0^{\infty} dk \frac{e^{kz} \left(e^{iks_1} - e^{iks_2} + e^{iks_3} - e^{iks_4} \right)}{k-k_j} - \frac{\sigma}{i \sin\theta} \int_0^{\infty} dk \frac{e^{kz} \left(\text{"} \right)}{k(k-k_j)} \quad (\text{A-3})$$

$$J'_{1,j} = -\frac{U \cos\theta}{i \sin\theta} \int_0^{\infty} dk \frac{e^{kz} \left(-e^{iks_5} + e^{iks_6} - e^{iks_7} + e^{iks_8} \right)}{k-k_j} + \frac{\sigma}{i \sin\theta} \int_0^{\infty} dk \frac{e^{kz} \left(\text{"} \right)}{k(k-k_j)} \quad (\text{A-4})$$

where $j = 1, 2$ and

$$\begin{aligned}
 s_1 &= (x \cos \theta + y \sin \theta) - (a \cos \theta + b \sin \theta) \\
 s_2 &= (x \cos \theta + y \sin \theta) - (a \cos \theta - b \sin \theta) \\
 s_3 &= (x \cos \theta + y \sin \theta) + (a \cos \theta + b \sin \theta) \\
 s_4 &= (x \cos \theta + y \sin \theta) + (a \cos \theta - b \sin \theta) \\
 s_5 &= (x \cos \theta - y \sin \theta) - (a \cos \theta + b \sin \theta) \\
 s_6 &= (x \cos \theta - y \sin \theta) - (a \cos \theta - b \sin \theta) \\
 s_7 &= (x \cos \theta - y \sin \theta) + (a \cos \theta + b \sin \theta) \\
 s_8 &= (x \cos \theta - y \sin \theta) + (a \cos \theta - b \sin \theta)
 \end{aligned} \tag{A-5}$$

Since

$$\begin{aligned}
 \frac{1}{k(k-k_j)} &= -\frac{1}{k_j} \frac{1}{k} + \frac{1}{k_j} \frac{1}{k-k_j} \\
 \frac{1}{k^2(k-k_j)} &= -\frac{1}{k_j} \frac{1}{k^2} - \frac{1}{k_j^2} \frac{1}{k} + \frac{1}{k_j^2} \frac{1}{k-k_j}
 \end{aligned} \tag{A-6}$$

Equations (A-1) through (A-4) are expressed in the following forms,

$$\begin{aligned}
 I_{1,j} &= \left(\frac{U}{k_j \sin \theta} - \frac{\sigma}{k_j^2 \sin \theta \cos \theta} \right) (I_1 - I_2) - \frac{\sigma}{k_j \sin \theta \cos \theta} I_3 \\
 I'_{1,j} &= \left(-\frac{U}{k_j \sin \theta} + \frac{\sigma}{k_j^2 \sin \theta \cos \theta} \right) (I'_1 - I'_2) + \frac{\sigma}{k_j \sin \theta \cos \theta} I'_3 \\
 J_{1,j} &= \frac{\sigma}{ik_j \sin \theta} I_1 + \left(\frac{U \cos \theta}{i \sin \theta} - \frac{\sigma}{ik_j \sin \theta} \right) I_2 \\
 J'_{1,j} &= -\frac{\sigma}{ik_j \sin \theta} I'_1 + \left(-\frac{U \cos \theta}{i \sin \theta} + \frac{\sigma}{ik_j \sin \theta} \right) I'_2
 \end{aligned} \tag{A-7}$$

where $I_1 = \int_0^{\infty} dk \frac{e^{kz} \left(e^{iks_1} - e^{iks_2} + e^{iks_3} - e^{iks_4} \right)}{k}$

$$I_2 = \int_0^{\infty} dk \frac{e^{kz} \left(\begin{array}{c} \text{''} \\ \text{''} \end{array} \right)}{k-k_j}$$

(A-8)
[Cont'd]

$$I_3 = \int_0^{\infty} dk \frac{e^{kz} (e^{iks_1} - e^{iks_2} + e^{iks_3} - e^{iks_4})}{k^a} \quad (\text{A-8})$$

$$I_1' = \int_0^{\infty} dk \frac{e^{kz} (-e^{iks_5} + e^{iks_6} - e^{iks_7} + e^{iks_8})}{k}$$

$$I_2' = \int_0^{\infty} dk \frac{e^{kz} (\quad \quad \quad)}{k - k_j}$$

$$I_3' = \int_0^{\infty} dk \frac{e^{kz} (\quad \quad \quad)}{k^a} \quad (\text{A-9})$$

Integration of I_1, I_3, I_1', I_3'

To transform $kz + iks_1, kz + iks_2, \text{ etc.},$ we write

$$\zeta = x \cos\theta + y \sin\theta - iz$$

$$\zeta' = x \cos\theta - y \sin\theta - iz$$

$$\zeta_1 = a \cos\theta + b \sin\theta$$

$$\zeta_2 = a \cos\theta - b \sin\theta \quad (\text{A-10})$$

and we have

$$z + is_1 = i(\zeta - \zeta_1), \quad z + is_5 = i(\zeta' - \zeta_1)$$

$$z + is_2 = i(\zeta - \zeta_2), \quad z + is_6 = i(\zeta' - \zeta_2)$$

$$z + is_3 = i(\zeta + \zeta_1), \quad z + is_7 = i(\zeta' + \zeta_1)$$

$$z + is_4 = i(\zeta + \zeta_2), \quad z + is_8 = i(\zeta' + \zeta_2) \quad (\text{A-11})$$

Substituting the above in I_1, I_3, I_1', I_3' , we have

$$I_1(\zeta) = \int_0^{\infty} \frac{dk}{k} \left[e^{ik(\zeta - \zeta_1)} - e^{ik(\zeta - \zeta_2)} + e^{ik(\zeta + \zeta_1)} - e^{ik(\zeta + \zeta_2)} \right] \quad (\text{A-12})$$

$$I_3(\zeta) = \int_0^{\infty} \frac{dk}{k^a} \left[\quad \quad \quad \right] \quad (\text{A-13})$$

$$I_3 \Big|_{z=0} = -i[-(x \cos \theta + y \sin \theta) I_1 \Big|_{z=0} + \zeta_1 \{(\log |s_3| + \frac{0}{i\pi}) - (\log |s_1| + \frac{0}{i\pi})\} + \zeta_2 \{(\log |s_2| + \frac{0}{i\pi}) - (\log |s_4| + \frac{0}{i\pi})\}],$$

$$s_m \geq 0 \quad (\text{A-20b})$$

$$I_1' = -\left(\log \frac{\zeta_1 - \zeta_2}{\zeta_1 - \zeta_1} + \log \frac{\zeta_1 + \zeta_2}{\zeta_1 + \zeta_1}\right) \quad (\text{A-21a})$$

$$I_1' \Big|_{z=0} = (\log |s_5| + \frac{0}{i\pi}) + (\log |s_7| + \frac{0}{i\pi}) - (\log |s_6| + \frac{0}{i\pi}) - (\log |s_8| + \frac{0}{i\pi}), s_m \geq 0 \quad (\text{A-21b})$$

$$I_3' = -i(-\zeta_1 I_1' + \zeta_1 \log \frac{\zeta_1 - \zeta_1}{\zeta_1 + \zeta_1} + \zeta_2 \log \frac{\zeta_1 + \zeta_2}{\zeta_1 - \zeta_2}) \quad (\text{A-22a})$$

$$I_3' \Big|_{z=0} = -i[-(x \cos \theta - y \sin \theta) I_1' \Big|_{z=0} + \zeta_1 \{(\log |s_5| + \frac{0}{i\pi}) - (\log |s_7| + \frac{0}{i\pi})\} + \zeta_2 \{(\log |s_8| + \frac{0}{i\pi}) - (\log |s_6| + \frac{0}{i\pi})\}],$$

$$s_m \geq 0 \quad (\text{A-22b})$$

Integration of I_2 and I_2'

I_2 (A-8) and I_2' (A-9) are identical with each other in form; therefore it is necessary to consider the integral

$$G = \int_0^{\infty} \frac{e^{ik(s_1 - iz)}}{k - k_j} dk \quad (\text{A-23})$$

Transforming the above by translation

$$w = k - k_j \quad (\text{A-24})$$

and rotation

$$u = -iw(s_1 - iz) \quad (\text{A-25})$$

we have

$$G = e^{ik_j s_1 + k_j z} \int_{ik_j s_1 + k_j z}^{-i\infty(s_1 - iz)} \frac{e^{-u}}{u} du \quad (A-26)$$

The above is expressed by the exponential integral,¹⁷

$$G = e^{ik_j s_1 + k_j z} \left\{ E_1[ik_j s_1 + k_j z] - \frac{0}{i2\pi} \right\} \text{ for } s_1 \geq 0 \quad (A-27)$$

Hence for $z=0$,

$$I_2 = \sum_{m=1}^4 (-1)^{m+1} e^{ik_j s_m} \left\{ E_1[ik_j s_m] - \frac{0}{i2\pi} \right\} \text{ for } s_m \geq 0 \quad (A-28)$$

$$I_2' = -\sum_{m=5}^8 (-1)^{m+1} e^{ik_j s_m} \left\{ E_1[ik_j s_m] - \frac{0}{i2\pi} \right\} \text{ for } s_m < 0 \quad (A-29)$$

where $j = 1, 2$.

CALCULATION OF I_6 AND I_6'

We calculate the following integrals which are used for evaluation of the volume in Eq.(59):

$$I_6 = \int_0^{\infty} \frac{dk}{k^3} e^{kz} (e^{iks_1} - e^{iks_2} + e^{iks_3} - e^{iks_4})$$

$$I_6' = \int_0^{\infty} \frac{dk}{k^3} e^{kz} (-e^{iks_5} + e^{iks_6} - e^{iks_7} + e^{iks_8}) \quad (A-30)$$

The same procedure as that used previously in the Integration of I_1 , I_1' , I_3 and I_3' is used.

The I_6 and I_6' are similarly expressed in the following form:

$$I_6(\zeta) = \int_0^{\infty} \frac{dk}{k^3} \left[e^{ik(\zeta-\zeta_1)} - e^{ik(\zeta-\zeta_2)} + e^{ik(\zeta+\zeta_1)} - e^{ik(\zeta+\zeta_2)} \right]$$

$$I_6'(\zeta') = \int_0^{\infty} \frac{dk}{k^3} \left[-e^{ik(\zeta'-\zeta_1)} + e^{ik(\zeta'-\zeta_2)} - e^{ik(\zeta'+\zeta_1)} + e^{ik(\zeta'+\zeta_2)} \right] \quad (A-31)$$

For $\zeta_1 \rightarrow i\infty$, $I_6 \rightarrow 0$, and analytic in ζ and ζ' .

Differentiating $I_6(\zeta)$ and $I_6'(\zeta')$ three times with respect to ζ and ζ' , and integrating them with respect to k , we have

$$\frac{d^3 I_6}{d\zeta^3} = \frac{1}{\zeta - \zeta_1} - \frac{1}{\zeta - \zeta_2} + \frac{1}{\zeta + \zeta_1} - \frac{1}{\zeta + \zeta_2}$$

$$\frac{d^3 I_6'}{d\zeta'^3} = -\frac{1}{\zeta' - \zeta_1} + \frac{1}{\zeta' - \zeta_2} - \frac{1}{\zeta' + \zeta_1} + \frac{1}{\zeta' + \zeta_2} \quad (\text{A-32})$$

Integration of the above derivatives with respect to ζ and ζ' yields each time a pair of integration constants. The first two pairs of constants vanish, whereas the last pair results are $\frac{1}{2}(\zeta_1^2 - \zeta_2^2)$ and $-\frac{1}{2}(\zeta_1^2 - \zeta_2^2)$. Hence, the pure constant terms in $I_6(\zeta)$ and $I_6'(\zeta')$ disappear and the I_6 and I_6' are finally expressed in the following form:

$$\begin{aligned} I_6 \Big|_{z=0} = & -\frac{1}{2} (x \cos \theta + y \sin \theta)^2 I_1 \Big|_{z=0} - (x \cos \theta + y \sin \theta) \zeta_1 \left[(\log |s_1| + \frac{0}{i\pi}) - (\log |s_3| + \frac{0}{i\pi}) \right] \\ & + (x \cos \theta + y \sin \theta) \zeta_2 \left[(\log |s_2| + \frac{0}{i\pi}) - (\log |s_4| + \frac{0}{i\pi}) \right] \\ & + \frac{1}{2} \left[\zeta_1^2 \left\{ (\log |s_1| + \frac{0}{i\pi}) + (\log |s_3| + \frac{0}{i\pi}) \right\} - \right. \\ & \left. - \zeta_2^2 \left\{ (\log |s_2| + \frac{0}{i\pi}) + (\log |s_4| + \frac{0}{i\pi}) \right\} \right] \quad \text{for } s_m \geq 0 \end{aligned}$$

$$\begin{aligned} I_6' \Big|_{z=0} = & -\frac{1}{2} (x \cos \theta - y \sin \theta)^2 I_1' \Big|_{z=0} - (x \cos \theta - y \sin \theta) \zeta_1 \left[(\log |s_5| + \frac{0}{i\pi}) - (\log |s_7| + \frac{0}{i\pi}) \right] \\ & + (x \cos \theta - y \sin \theta) \zeta_2 \left[(\log |s_6| + \frac{0}{i\pi}) - (\log |s_8| + \frac{0}{i\pi}) \right] \\ & + \frac{1}{2} \left[\zeta_1^2 \left\{ (\log |s_5| + \frac{0}{i\pi}) + (\log |s_7| + \frac{0}{i\pi}) \right\} - \right. \\ & \left. - \zeta_2^2 \left\{ (\log |s_6| + \frac{0}{i\pi}) + (\log |s_8| + \frac{0}{i\pi}) \right\} \right] \quad \text{for } s_m \geq 0 \quad (\text{A-33}) \end{aligned}$$

APPENDIX B

CALCULATION OF $I_{2,l}$, $I'_{2,l}$, $J_{2,l}$, $J'_{2,l}$ ($l=1,2$; $j=3,4$)

Integrating $I_{2,l}$ and $I'_{2,l}$ with respect to ξ and η in (43c) and (43d), and making use of (A-5) and (A-6), we have

$$I_{2,l} = \left(\frac{U}{k_j \sin \theta} + \frac{\sigma}{k_j^2 \sin \theta \cos \theta} \right) (I_1^* - I_4) + \frac{\sigma}{k_j \sin \theta \cos \theta} I_3^* \quad (B-1)$$

$$I'_{2,l} = - \left(\frac{U}{k_j \sin \theta} + \frac{\sigma}{k_j^2 \sin \theta \cos \theta} \right) (I_1'^* - I_4') - \frac{\sigma}{k_j \sin \theta \cos \theta} I_3'^* \quad (B-2)$$

$$J_{2,l} = \frac{\sigma}{ik_j \sin \theta} I_1^* - \left(\frac{U \cos \theta}{i \sin \theta} + \frac{\sigma}{ik_j \sin \theta} \right) I_4 \quad (B-3)$$

$$J'_{2,l} = - \frac{\sigma}{ik_j \sin \theta} I_1'^* + \left(\frac{U \cos \theta}{i \sin \theta} + \frac{\sigma}{ik_j \sin \theta} \right) I_4' \quad (B-4)$$

where the * indicates the complex conjugate, and,

$$I_4 = \left\{ \begin{array}{l} \int_0^{\infty} dk \frac{e^{kz} \left(\begin{array}{c} \text{"} \\ k-k_3 \end{array} \right)}{\dots} \\ \int_0^{\infty} dk \frac{e^{kz} \left(\begin{array}{c} \text{"} \\ k-k_4 \end{array} \right)}{\dots} \end{array} \right. \quad (B-5)$$

$$I_4' = \left\{ \begin{array}{l} \int_0^{\infty} dk \frac{e^{kz} \left(\begin{array}{c} -iks_5 \\ -e \end{array} + \frac{-iks_6}{e} - \frac{-iks_7}{e} + \frac{-iks_8}{e} \right)}{k-k_3} \\ \int_0^{\infty} dk \frac{e^{kz} \left(\begin{array}{c} \text{"} \\ k-k_4 \end{array} \right)}{\dots} \end{array} \right. \quad (B-6)$$

Integration of I_4 and I_4'

It is apparent from (B-5) and (B-6) that an evaluation of two integrals is necessary:

$$G_1 = \int_0^{\infty} \frac{dk}{k-k_3} e^{-ik(s_1+iz)}$$

$$G_2 = \int_0^{\infty} \frac{dk}{k-k_4} e^{-ik(s_1+iz)} \quad (B-7)$$

Transforming G_1 and G_2 by translation,

$$w = k - k_j \quad (B-8)$$

and by rotation

$$u = iw(s_1+iz) \quad (B-9)$$

we have,

$$\left. \begin{array}{l} G_1 \\ G_2 \end{array} \right\} = e^{-ik_j s_1 + k_j z} \int_{-ik_j s_1 + k_j z}^{i\infty(s_1+iz)} \frac{e^{-u}}{u} du \quad (B-10)$$

Thus, by applying the formula for exponential integral¹⁷, we have

$$\begin{aligned} G_1 &= e^{-ik_3 s_1 + k_3 z} \{E_1[-ik_3 s_1 + k_3 z] - \frac{i2\pi}{0}\}, s_1 \geq 0 \\ G_2 &= e^{-ik_4 s_1 + k_4 z} \{E_1[-ik_4 s_1 + k_4 z] + \frac{0}{i2\pi}\}, s_1 \geq 0 \end{aligned} \quad (B-11)$$

Due to the above expressions (B-11), the I_4 and I_4' in (B-5) and (B-6) for $z=0$, are

$$I_4 = \begin{cases} \sum_{m=1}^4 (-1)^{m+1} e^{-ik_3 s_m} \{E_1[-ik_3 s_m] - \frac{i2\pi}{0}\}, s_m \geq 0 \\ \sum_{m=1}^4 (-1)^{m+1} e^{-ik_4 s_m} \{E_1[-ik_4 s_m] + \frac{0}{i2\pi}\}, s_m \geq 0 \end{cases} \quad (B-12)$$

$$I_4' = \begin{cases} -\sum_{m=5}^8 (-1)^{m+1} e^{-ik_3 s_m} \{E_1[-ik_3 s_m] - \frac{i2\pi}{0}\}, s_m \geq 0 \\ -\sum_{m=5}^8 (-1)^{m+1} e^{-ik_4 s_m} \{E_1[-ik_4 s_m] + \frac{0}{i2\pi}\}, s_m \geq 0 \end{cases} \quad (B-13)$$

APPENDIX C

CALCULATION OF INTEGRALS FOR COMPLEX k_3, k_4

We evaluate the integrals $I_5(k_\ell)$ and $I_5'(k_\ell)$ of the complex arguments in Eqs.(46 , (51) and (52).

Consider

$$G_3 = \int_0^{\infty} dk \frac{e^{-ik(s_1+iz)}}{k-k_j} \quad (C-1)$$

where $k_j = \text{complex}$, $k_3 = \text{complex conjugate of } k_4$ and $\text{Im}k_3 < 0$. And $\text{Re}k_j \geq 0$.

Translating and rotating by

$$w = k - k_j \quad \text{and} \quad u = iw(s_1+iz) \quad (C-2)$$

we have

$$G_3 = \int_{-ik_j s_1 + k_j z}^{i\infty(s_1+iz)} \frac{e^{-u}}{u} du \quad (C-3)$$

For k_3 , with $z=0$, we have the following relations:

If $s_1 > 0$,

$$\text{Re}(-ik_3 s_1) < 0$$

$$\text{Im}(-ik_3 s_1) \leq 0 \quad \text{for } \text{Re } k_3 \geq 0$$

If $s_1 < 0$,

$$\text{Re}(-ik_3 s_1) > 0$$

$$\text{Im}(-ik_3 s_1) \geq 0 \quad \text{for } \text{Re } k_3 \geq 0$$

For k_4 , with $z=0$, we have the following relations:

If $s_1 > 0$,

$$\operatorname{Re}(-ik_4 s_1) > 0$$

$$\operatorname{Im}(-ik_4 s_1) \leq 0 \quad \text{for } \operatorname{Re} k_4 \geq 0$$

If $s_1 < 0$,

$$\operatorname{Re}(-ik_4 s_1) < 0$$

$$\operatorname{Im}(-ik_4 s_1) \geq 0 \quad \text{for } \operatorname{Re} k_4 \geq 0$$

In addition to the above for both k_3 and k_4 with $z=0$,

$$\operatorname{Re}(is_1 \infty) = 0$$

$$\operatorname{Im}(is_1 \infty) \geq 0 \quad \text{for } s_1 \geq 0$$

Thus, applying formulas of exponential integrals,¹⁷ we have the following results for $z=0$,

For $\operatorname{Re} k_3 \geq 0$

$$G_3 = \begin{cases} e^{-ik_3 s_1} \{E_1[-ik_3 s_1] - \frac{i2\pi}{0}\}, & s_1 \geq 0 \\ e^{-ik_3 s_1} \{E_1[-ik_3 s_1] - \frac{0}{0}\}, & s_1 \leq 0 \end{cases} \quad (\text{C-4})$$

and for

$\operatorname{Re} k_4 \geq 0$

$$G_3 = \begin{cases} e^{-ik_4 s_1} \{E_1[-ik_4 s_1] + \frac{0}{i2\pi}\}, & s_1 \geq 0 \\ e^{-ik_4 s_1} \{E_1[-ik_4 s_1] + \frac{0}{0}\}, & s_1 \leq 0 \end{cases} \quad (\text{C-5})$$

Thus for $z=0$, the I_5 and I_5' are given:

$\operatorname{Re} k_3 \geq 0$

$$I_5 = \sum_{m=1}^4 (-1)^{m+1} e^{-ik_3 s_m} \{E_1[-ik_3 s_m] - \frac{i2\pi}{0}\} \quad s_m \geq 0 \quad (\text{Cont'd})$$

$$I_5 = \sum_{m=1}^4 (-1)^{m+1} e^{-ik_3 s_m} \{E_1[-ik_3 s_m] - \frac{0}{0}\}, s_m \geq 0$$

for $\text{Re}k_4 \geq 0$

$$I_5 = \begin{cases} \sum_{m=1}^4 (-1)^{m+1} e^{-ik_4 s_m} \{E_1[-ik_4 s_m] + \frac{0}{i2\pi}\}, s_m \geq 0 \\ \sum_{m=1}^4 (-1)^{m+1} e^{-ik_4 s_m} \{E_1[-ik_4 s_m] + \frac{0}{0}\}, s_m \geq 0 \end{cases} \quad (C-6)$$

for $\text{Re}k_3 \geq 0$

$$I_5 = \begin{cases} -\sum_{m=5}^8 (-1)^{m+1} e^{-ik_3 s_m} \{E_1[-ik_3 s_m] - \frac{i2\pi}{0}\}, s_m \geq 0 \\ -\sum_{m=5}^8 (-1)^{m+1} e^{-ik_3 s_m} \{E_1[-ik_3 s_m] - \frac{0}{0}\}, s_m \geq 0 \end{cases}$$

for $\text{Re}k_4 \geq 0$

$$I_5 = \begin{cases} -\sum_{m=5}^8 (-1)^{m+1} e^{-ik_4 s_m} \{E_1[-ik_4 s_m] + \frac{0}{i2\pi}\}, s_m \leq 0 \\ -\sum_{m=5}^8 (-1)^{m+1} e^{-ik_4 s_m} \{E_1[-ik_4 s_m] + \frac{0}{0}\}, s_m \geq 0 \end{cases} \quad (C-7)$$

APPENDIX D

EVALUATION OF EXPONENTIAL INTEGRAL OF COMPLEX ARGUMENT

To calculate the exponential integral of a complex argument $E_1[-ik_{\ell} s_m]$ as given in Eqs.(51) and (52), we put

$$z = -ik_{\ell} s_m \quad (D-1)$$

where k_{ℓ} represents a complex wave number k_3 or k_4 and the s_m has been given in Eq.(A-5), Appendix A.

The exponential integral is given by¹⁷

$$E_1[z] = -\gamma - \log z - \sum_{n=1}^{\infty} \frac{(-1)^n z^n}{n \cdot n!} \quad (|\arg z| < \pi) \quad (D-2)$$

Let the above z be given in polar coordinates

$$z = r e^{i\alpha} \quad (D-3)$$

$$\text{with } r = |-ik_{\ell} s_m|, \quad \alpha = \tan^{-1} \frac{\text{Im}(-ik_{\ell} s_m)}{\text{Re}(-ik_{\ell} s_m)} \quad (D-4)$$

Substituting z Eq.(D-3) into Eq.(D-2), we have

$$E_1[-ik_{\ell} s_m] = -C(r, \alpha) - iS(r, \alpha) \quad (D-5)$$

where

$$C(r, \alpha) = \gamma + \log r + \sum_{n=1}^{\infty} \frac{(-1)^n r^n \cos n\alpha}{n \cdot n!}$$

$$S(r, \alpha) = \alpha + \sum_{n=1}^{\infty} \frac{(-1)^n r^n \sin n\alpha}{n \cdot n!} \quad (D-6)$$

where $\gamma = 0.5772$.

Introducing a new variable β ,

$$\beta = \alpha + \pi \quad (D-7)$$

we have

$$z^n = (-1)^n [r^n \cos n\beta + i r^n \sin n\beta] \quad (D-8)$$

Hence, Eq.(D-5) is given by

$$E_1[-ik_{\ell} s_m] = -C(r, \beta) - iS(r, \beta) \quad (D-9)$$

where

$$C(r, \beta) = \gamma + \log r + \sum_{n=1}^{\infty} \frac{r^n \cos n\beta}{n \cdot n!}$$

$$S(r, \beta) = (\beta - \pi) + \sum_{n=1}^{\infty} \frac{r^n \sin n\beta}{n \cdot n!} \quad (D-10)$$

The exponential integral of a complex argument $-ik_{\ell} s_m$ ($k_{\ell} = k_{\ell r} + ik_{\ell i}$) in Eq.(D-1) approaches the exponential integral of a pure imaginary argument $-ik_{\ell i} s_m$ when $k_{\ell i} \rightarrow 0$ ($k_{\ell i} \geq 0$):

$$\lim_{k_{\ell i} \rightarrow 0} E_1[-ik_{\ell} s_m] = E_1[-ik_{\ell r} s_m] = -Ci(k_{\ell r} s_m) - i[Si(k_{\ell r} s_m) - \frac{\pi}{2}] \quad \text{for } k_{\ell r} > 0, s_m > 0 \quad (D-11)$$

where Ci and Si represent the cosine and sine integral, respectively.

Evaluation of the exponential integral of pure imaginary argument is carried out by making use of the standard subroutine "SICI"⁶ which has been given in the Scientific Subroutine Package. The program computes the sine and cosine integrals

$$Si(x) \quad \text{and} \quad Ci(x), \quad x > 0$$

and thus by making use of the above, we compute the exponential integral

$$E_1(ix) = -Ci(x) + i[Si(x) - \frac{\pi}{2}], \quad x > 0$$

and $E_1(-ix)$ with $x > 0$ by the complex conjugate of $E_1(ix)$.

Evaluation of Eqs. (51) and (52)

Since

$$e^{-ik_{\ell} s_m} = e^{k_{\ell i} s_m} e^{-ik_{\ell r} s_m} \quad (D-12)$$

we have

$$\begin{aligned} e^{-ik_{\ell} s_m} E_1[-ik_{\ell} s_m] &= -e^{k_{\ell i} s_m} \{ [\cos(k_{\ell r} s_m) C(r, \beta) + \sin(k_{\ell r} s_m) S(r, \beta)] \\ &\quad + i[-\sin(k_{\ell r} s_m) C(r, \beta) + \cos(k_{\ell r} s_m) S(r, \beta)] \} \end{aligned} \quad (D-13)$$

$$-i2\pi e^{-ik_3 s_m} = -2\pi e^{k_3 i s_m} [\sin(k_3 r s_m) + i \cos(k_3 r s_m)] \quad \text{for } k_3 r > 0, \quad s_m > 0 \quad (D-14)$$

and

$$i2\pi e^{-ik_4 s_m} = 2\pi e^{k_4 i s_m} [\sin(k_4 r s_m) + i \cos(k_4 r s_m)] \quad \text{for } k_4 r > 0, \quad s_m < 0 \quad (D-15)$$

Substituting Eqs. (D-13) to (D-15) in (51) and (52), one obtains the expressions for $I_5(k_{\ell}) - I_5'(k_{\ell})$.

$$\begin{aligned} e^{-ik_3 s_m} \{ E_1[-ik_3 s_m] - \frac{i2\pi}{0} \}, \quad s_m \geq 0, \quad \text{Re } k_3 > 0 \\ = -e^{k_3 i s_m} \{ \cos(k_3 r s_m) C(r, \beta) + \sin(k_3 r s_m) [S(r, \beta) + \frac{2\pi}{0}] \} \\ -ie^{k_3 i s_m} \{ -\sin(k_3 r s_m) C(r, \beta) + \cos(k_3 r s_m) [S(r, \beta) + \frac{2\pi}{0}] \} \end{aligned} \quad (D-16)$$

$$\begin{aligned} e^{-ik_4 s_m} \{ E_1[-ik_4 s_m] + \frac{i2\pi}{0} \}, \quad s_m \geq 0, \quad \text{Re } k_4 > 0 \\ = -e^{k_4 i s_m} \{ \cos(k_4 r s_m) C(r, \beta) + \sin(k_4 r s_m) [S(r, \beta) - \frac{0}{2\pi}] \} \\ -ie^{k_4 i s_m} \{ -\sin(k_4 r s_m) C(r, \beta) + \cos(k_4 r s_m) [S(r, \beta) - \frac{0}{2\pi}] \} \end{aligned} \quad (D-17)$$

Since Eq.(D-13) is formally identical to the complex conjugate of $(\psi_{0r} + i\psi_{0r})$ in the Appendix of Reference 19, and since the formula gives expressions for both small and large r for a rapid numerical calculation, the expression of the $\varphi_{0r} + i\psi_{0r}$ has been used.

For small r , Eq.(D-13) remains unchanged.

For large r , Eq.(D-13) takes the following form

$$e^{-ik_{\ell}^s m} E_1[-ik_{\ell}^s m] = - \sum_{n=1}^N (n-1)! \frac{\cos n \beta}{r^n} + i \sum_{n=1}^N (n-1)! \frac{\sin n \beta}{r^n} \quad (D-18)$$

where $N =$ truncation number.

Integration of Eqs. 46, 59 and 60

Integration with respect to θ in (46) (59) and (60) has been carried out numerically by employing the trapezoidal rule. For the singular behavior which appears in the neighborhood of $\theta = \frac{\pi}{2}$, a change of variable, adopted in Reference 2, has been employed for convenience.

$$\theta' = \frac{\sin \theta}{\cos^2 \theta}$$

which gives

$$\theta' \rightarrow 0 \quad \text{for } \theta \rightarrow 0$$

$$\theta' \rightarrow \infty \quad \text{for } \theta \rightarrow \frac{\pi}{2}$$

indicating the singular behavior has been shifted to $\theta' \rightarrow \infty$ at which the integrand tends to zero.

For the integration with respect to θ' , the upper limit has been truncated at 77 as being sufficient.

In the neighborhood of the critical point θ_c , however, when the τ values nearly satisfy the relation (29), singular behavior occurs also when $k_3 - k_4 \rightarrow 0$ as it is seen from Eq. (26b):

$$\frac{1}{k_3 - k_4} = - \frac{1}{k_0 \sec^2 \theta \sqrt{1 - 4\tau \cos \theta}}$$

$$(1 - 4\tau \cos \theta) \rightarrow 0 \text{ for } \theta \rightarrow \theta_c$$

In these cases the Lagrange interpolation method¹⁸ has been employed. The integration has been assumed to have the form

$$I = \int_{\theta_c - 2\delta}^{\theta_c + 2\delta} \frac{M(\theta)}{(\theta - \theta_c)^3} d\theta$$

where $\delta = 0.00033$ has been finally adopted and $M(\theta) = (\theta - \theta_c)^3$. [Integrand of Eq. (46) or (59) or (60)].

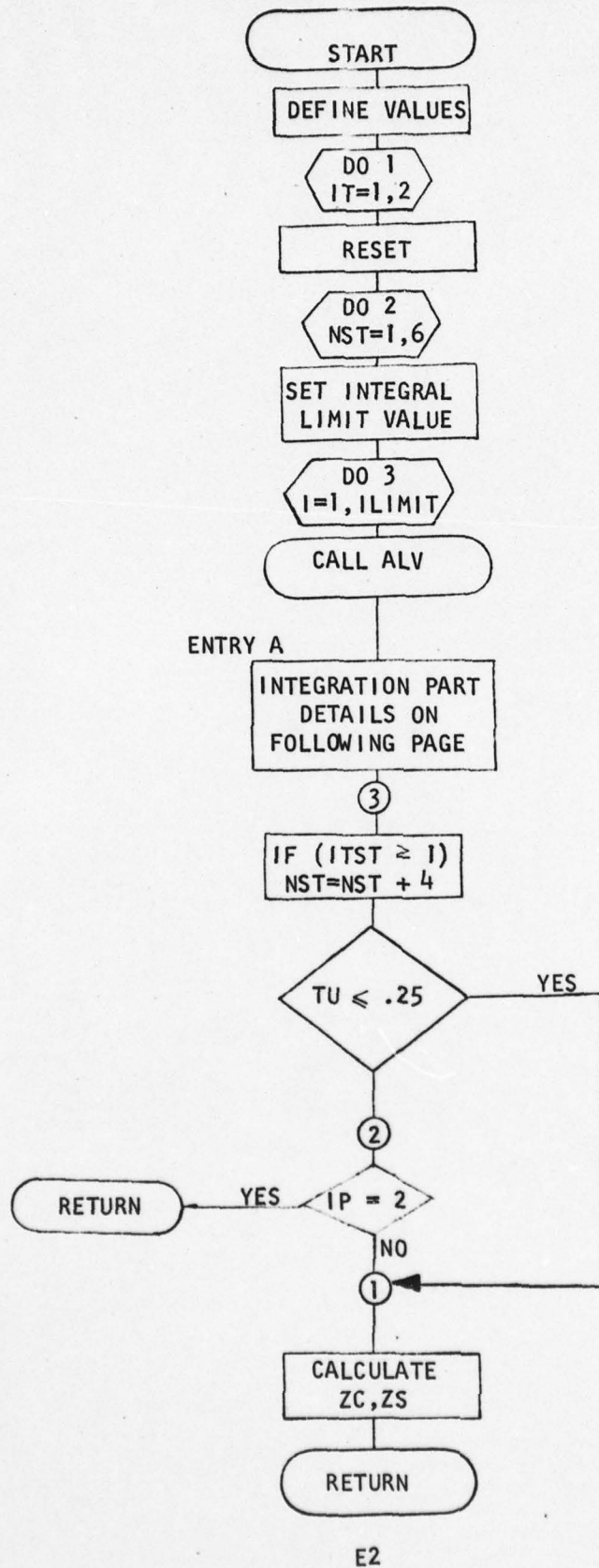
APPENDIX E
FLOW DIAGRAM AND PROGRAM SYSTEM

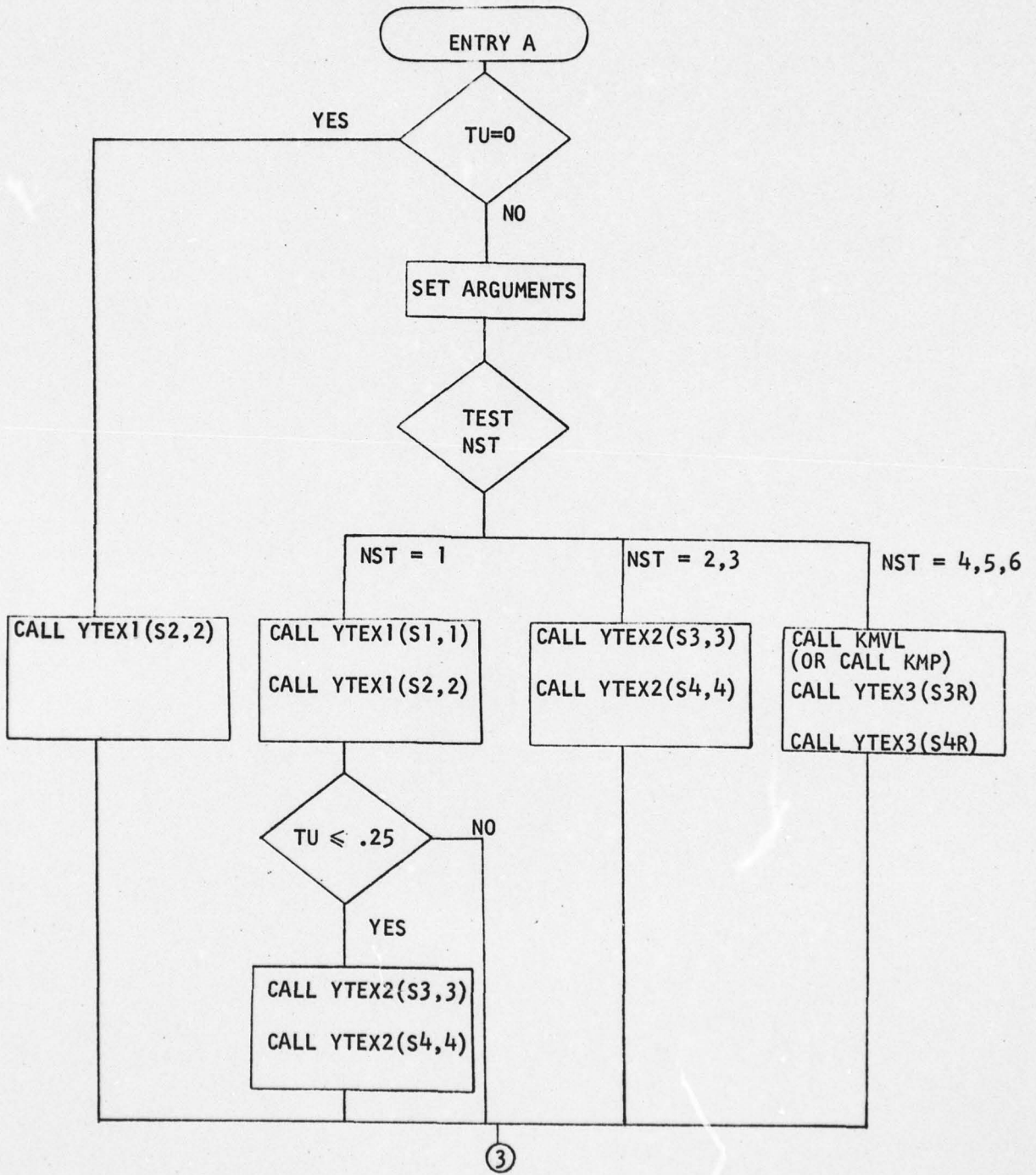
With the following input,

<u>IN PROGRAM</u>	<u>IN TEXT</u>	
TU	τ	= reduced frequency
FAN	$\left \frac{\partial Q_f}{\partial p} \right $	= fan discharge rate for a pair of fans
SK	k	= nozzle flow factor
ROW	ρ_w	= water density
SELA	A_o	= seal leakage at the equilibrium
BH	h	= cushion height
DS	Δ	= displacement
XNF	n	= number of pair of fans
SL	L	= nominal ship length
SB	B	= nominal ship beam
A	a	= half cushion length
B	b	= half cushion width
FN	F_n	= Froude number
one obtains the following results:		
RV	v_r	= real part of the volume coefficient
IV	v_i	= imaginary part of the volume coefficient
RA	α_r	= real part of the escape area coefficient
IA	α_i	= imaginary part of the escape area coefficient
AMP	$\left \frac{p_b}{p_o} / \frac{z}{h} \right $	= amplitude of the bubble pressure coefficient
PHA	phase lag	= phase lag of the bubble pressure
ADM	C_a	= added mass coefficient
DAM	C_d	= damping coefficient

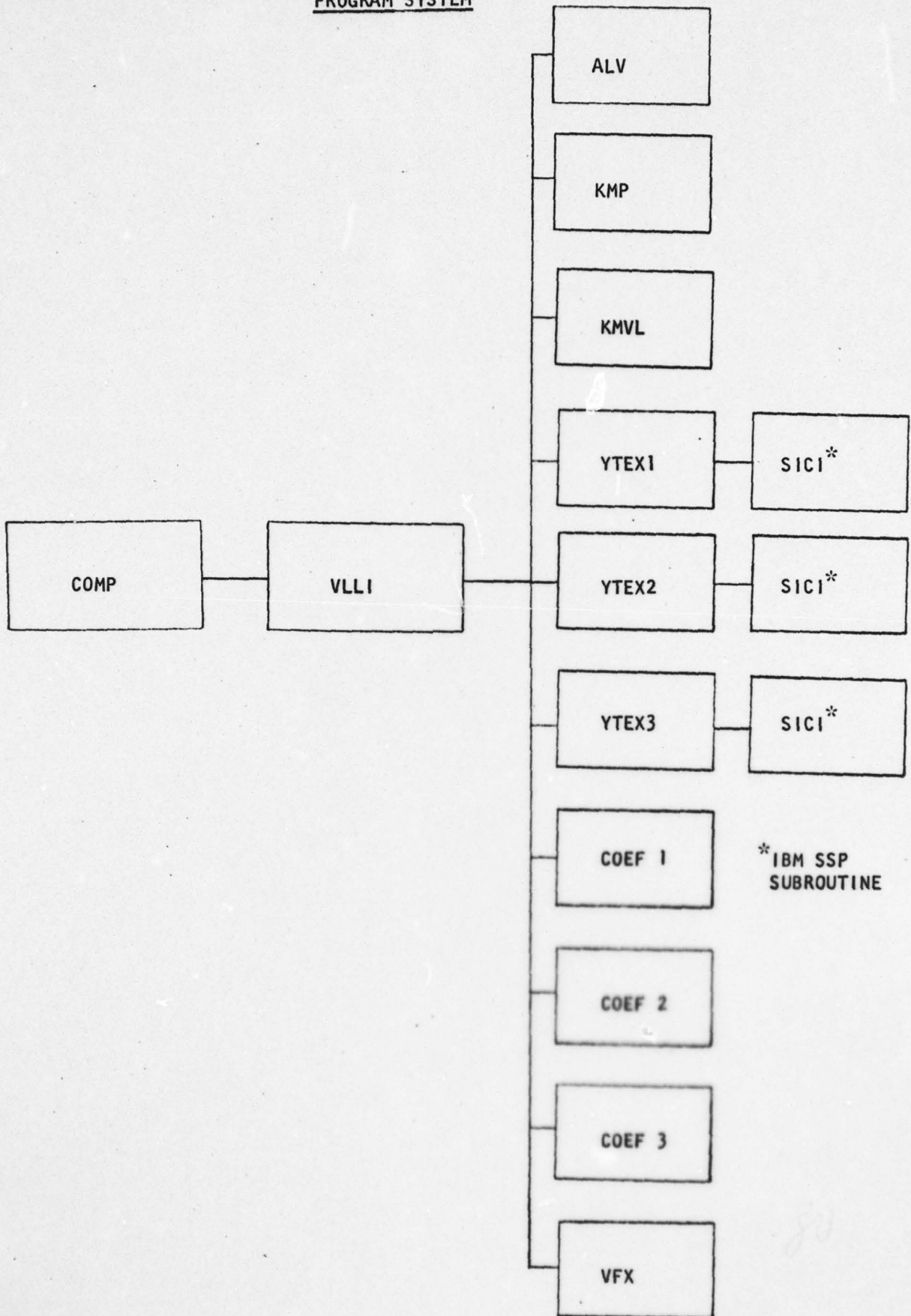
Appendix E includes three sections: Flow Diagram and Program System for Subroutine VLLI, INPUT-OUTPUT SAMPLE and PROGRAM LISTING.

FLOW DIAGRAM (SUBROUTINE VLL1)





PROGRAM SYSTEM



R-2040

APPENDIX E
(Cont'd)

INPUT OUTPUT SAMPLE

RUN ACVP

>> DEFINITIONS

RV = REAL PART VOLUME
IV = IMAGE PART VOLUME
RA = REAL PART ESCAPE AREA
IA = IMAGE PART ESCAPE AREA
AMP= BUBLE PRESSURE AMPLITUDE
PHA= BUBLE PRESSURE PHASE
ADM= ADDED MASS COEFFICIENT
DAM= DAMPING COEFFICIENT

>> INPUT FAN,SK,ROW,SELA,BH,DS,XNF
0.03 0.65 1.94 0.333 0.72 298. 2.

>> INPUT SL,SB,A,B,FN
13.83 2.12 6.915 1.06 0.72

>> INPUT TU, IF ANY. OTHERWISE KEY IN -1.
10.

TU =	10.00	RV =	-0.073	IV =	0.001
		RA =	-0.064	IA =	0.003
		AMP=	8.439	PHA=	-158.138
		ADM=	-.2813E-02	DAM=	.2177E-01

>> INPUT TU, IF ANY. OTHERWISE KEY IN -1.
-1.

END OF EXECUTION

R-2040

APPENDIX E
(Cont'd)

PROGRAM LISTING

```

00100 CCCC MAIN PROGRAM FOR COMPUTION OF VOLUM FLUX AND
00200 CCCC ESCAPE AREA OF ACV HEAVING IN UNIFORM STREAM
00300 CCCC IN ADDITION CALCULATE BUBLE PRESSURE, ADDED MASS
00400 CCCC AND DAMPING COEFFICIENTS
00500 CCCCCCCCCCCCCCCCCCCCCCCCCCCCCCCCCCCCCCCCCCCCCCCCCCCCCCCCCCCCC
00600 PROGRAM COMP
00700 COMMON /V1/SL,SB,A,B,FN,TU,EPSI,GAM,BTA
00800 COMMON /V2/BET,ZT1,ZT2,ZT3,ZT4
00900 COMMON /V3/ ALF1,ALF2,ALF3,ALF4,NST12,NST13,ILH
01000 COMMON /V4/NTS1,NTS2,NTS3,KT1,KT2,KT3,KT12,KT13
01100 COMMON /C1/ EPS(3),GAB(3)
01200 DATA EPS/.001,.0001,.0001/,GAB/.03325,.011,.011/
01300 DATA BTA,ZT1,ZT2,ZT3,ZT4/.05,.04,.06,.1,2./
01400 DATA ALF1,ALF2,NTS1,NTS2,NTS3,KT1/.033,.05,20,20,30,10/
01500 DATA GAMA,PA,ROA,G/1.4,2048.,0.00237,32.2/
01600 ALF3=ZT3
01700 ALF4=ZT4
01800 KT2=NTS2
01900 KT3=NTS3
02000 CCCC SL = NOMINAL SHIP LENGTH
02100 CCCC SB = NOMINAL SHIP BEAM
02200 CCCC A = HALF CUSHION LENGTH
02300 CCCC B = HALF CUSION WIDTH
02400 CCCC FN = FROUD NUMBER
02500 CCCC FAN = FAN DISCHARGE RATE FOR PAIR OF FANS
02600 CCCC XNF = NUMBER OF PAIR OF FANS
02700 CCCC SELA = SEAL LEAKAGE AT THE EQUILIBRIUM
02800 CCCC BH = BUBLE HEIGHT
02900 CCCC ROW = WATER DENSITY
03000 CCCC DS = DISPLACEMENT
03100 CCCCCCCCCCCCCCCCCCCCCCCCCCCCCCCCCCCCCCCCCCCCCCCCCCCCCCCCCCCC
03200 TYPE 600
03300 600 FORMAT(' >> DEFINITIONS'// RV = REAL PART VOLUME'
/
03400 1 ' IV = IMAGE PART VOLUME'//
03500 2 ' RA = REAL PART ESCAPE AREA'//
03600 3 ' IA = IMAGE PART ESCAPE AREA'//
03700 4 ' AMP= BUBLE PRESSURE AMPLITUDE'//
03800 5 ' PHA= BUBLE PRESSURE PHASE'//
03900 6 ' ADM= ADDED MASS COEFFICIENT'//
04000 7 ' DAM= DAMPING COEFICIENT'//)
04100 TYPE 300
04200 300 FORMAT(' >> INPUT FAN,SK,ROW,SELA,BH,DS,XNF')
04300 ACCEPT 100,FAN,SK,ROW,SELA,BH,DS,XNF
04400 TYPE 400
04500 400 FORMAT(' >> INPUT SL,SB,A,B,FN')
04600 ACCEPT 100,SL,SB,A,B,FN
04700 BL=2.*A
04800 BB=2.*B
04900 10 CONTINUE
05000 TYPE 500
05100 500 FORMAT(' >> INPUT TU, IF ANY. OTHERWISE KEY IN -1.')
05200 ACCEPT 100,TU
05300 IF(TU.LT.0.) CALL EXIT
05400 100 FORMAT(7F)

```

```

05500      VR=0.
05600      VI=0.
05700      CALL VLLI(VR,VI,1)
05800      AI=0.
05900      AR=0.
06000      CALL VLLI(AI,AR,2)
06100      IF(TU.EQ.0.) GOTO 20
06200      SP=FN*SQRT(BL*G)
06300      SIG=IU*G/SP
06400      SIG2=SIG*SIG
06500      FC=SK/SIG
06600      BL2=BL*BL
06700      CA=BL*BB
06800      VOL=CA*BH
06900      FO=DS/CA
07000      FOVO=FO/VOL
07100      FCTOR=FO/BH*CA
07200      COF=.5*ROW*BL2*BL
07300      COP=.5*ROW*SP*BL2
07400      C1=GAMA*(1.+FA/FO)
07500      C2=SQRT(2.*FO/ROA)
07600      C3=SQRT(2.*FO*ROA)
07700      C4=BL2/ROW/G
07800      C5=BL/ROW/G
07900      QR=VR*C4+FC*AI*C5*C2
08000      QI=VI*C4-FC*AR*C5*C2+FC*SELA/C3+XNF*FAN/SIG
08100      DLQR=FOVO*QR
08200      DLQI=FOVO*QI
08300      FB=(1.-C1*DLQR)**2+(C1*DLQI)**2
08400      FBR=-C1*(1.-C1*DLQR)/FB
08500      FBI=-C1*C1*DLQI/FB
08600      ADMC=FBR*FCTOR/SIG2/COF
08700      DAMC=-FBI*FCTOR/SIG/COP
08800      AMP=SQRT(FBR*FBR+FBI*FBI)
08900      PHAS=ATAN2(FBI,FBR)*57.29577
09000      TYPE 200,TU,VR,VI,AR,AI,AMP,PHAS,ADMC,DAMC
09100 200    FORMAT(2X,'TU = 'F8.2,' RV = 'F10.3,' IV = 'F10.3/
09200      1      15X,' RA = 'F10.3,' IA = 'F10.3/
09300      2      15X,' AMP= 'F10.3,' PHA= 'F10.3/
09400      3      15X,' ADM= 'E10.4,' DAM= 'E10.4/)
09500      GOTO 10
09600 20    AMP=0.
09700      PHAS=-90.
09800      TYPE 200,TU,VR,VI,AR,AI,AMP,PHAS
09900      GOTO 10
10000     END

```

```

00100  CCCC  SUBPROGRAM FOR COMPUTATION OF
00200  CCCC  VOLUME FLUX, IF IP = 1
00300  CCCC  ESCAPE AREA, IF IP = 2
00400  SUBROUTINE VLLI(ZC,ZS,IP)
00500  DIMENSION THR(3),THL(3),FRR(3),FIR(3),FRL(3),FIL(3)
00600  COMMON/MYTEX/ SM(8)
00700  DIMENSION ZCC(2),ZSS(2),FTR(3),FTI(3)
00800  COMMON/LOG/C1,C2,R1,R2
00900  COMMON /V1/SL,SB,A,B, FN, TU, EPSI, GAM, BTA
01000  COMMON /V2/BET, ZT1, ZT2, ZT3, ZT4
01100  COMMON /V3/ALF1,ALF2,ALF3,ALF4,NTS12,NTS13,ILM
01200  COMMON /V4/NTS1,NTS2,NTS3,KT1,KT2,KT3,KT12,KT13
01300  COMMON /CF1/ TV,S1,S2,S3,S4,SGC2,SGCO,NST,FDT,CN,SN,CSN
01400  COMMON /CF11/ SK05,TTM, TM
01500  COMMON /CF2/ EP(4),EI(4),EPD(4),EID(4),EPR(4,8),EPI(4,8)
01600  COMMON /C1/ EPSS(3),GAB(3)
01700  DATA X11,X44,X15/11.,144.,315./
01800  ZCC(1)=0.
01900  ZCC(2)=0.
02000  ZSS(2)=0.
02100  ZSS(1)=0.
02200  P=3.14159
02300  TP=2.*P
02400  P2=P*P
02500  SL2=SL*SL
02600  SB2SL=.5*SB/SL
02700  ABL2=4.*A*B/SL2
02800  G=32.2
02900  SLMN=77.
03000  BLF=0.000333
03100  EPSI=EPSS(IP)
03200  GAM=GAB(IP)
03300  BET=GAM
03400  LP=3
03500  LP1=LP+1
03600  X=-A
03700  Y=B-EPSI
03800  GAM3=3.*GAM
03900  KT12=KT1+KT2
04000  KT13=KT12+KT3
04100  RMA=SLMN-BET-ZT1*(KT1-1)-ZT2*KT2-ZT3*KT3
04200  MOD=RMA/ZT4
04300  RMB=MOD*ZT4
04400  DELTA=RMA-RMB
04500  KT14=KT13+MOD
04600  KT15=KT14+1
04700  NTS12=NTS1+NTS2
04800  NTS13=NTS12+NTS3
04900  IF(TU.LT..25) GO TO 127
05000  GC=1./(4.*TU)
05100  TCR=ACOS(GC)
05200  TVCR=SIN(TCR)/COS(TCR)**2
05300  EPS=LP*BLF
05400  RTA=SLMN-TVCR-EPS-ALF1*(NTS1-1)-ALF2*NTS2-ALF3*NTS3
05500  LO=RTA/ALF4

```

```

05600      RTB=LO*ALF4
05700      DELTB=RTA-RTB
05800      NTS14=NTS13+LO
05900      NTS15=NTS14+1
06000      RA=TVCR-EPS-GAM3
06100      LQM=RA/BTA
06200      RB=LQM*BTA
06300      DEL=RA-RB
06400      LQM1=LQM+1
06500      SMA=TVCR-BET-ZT1*(KT1-1)-ZT2*KT2-ZT3*KT3
06600      LOO=SMA/ZT4
06700      SMB=LOO*ZT4
06800      DELTC=SMA-SMB-.005
06900      LT14=KT13+LOO
07000      LT15=LT14+1
07100      ITST=2
07200      KT115=KT15
07300      IF(TVCR.GT.77.) ITST=1
07400      IF(TVCR.LE.66.) ITST=0
07500      IF(ITST.EQ.2) KT115=LT15
07600      127  CONTINUE
07700      SFC=1./(180.*BLF**2)
07800      SFCC=1./(180.*GAM**2)
07900      SP=FN*SQRT(G*SL)
08000      SIG=TU*G/SP
08100      SIG2=SIG**2
08200      SP2=SP**2
08300      FN2=FN**2
08400      SGC2=G/SP2
08500      FCT=4.*P2*SP2*SL2
08600      IF(IP.EQ.2) FCT=FCT/SL
08700      FCTR=FN**4/(2.*P2)
08800      IF(IP.EQ.2) FCTR=2.*P2*SL
08900      C   'IT' STANDS FOR CONTR REPET OF INTGR FOR X=-X;GIVES RSUL
T
09000      DO 1 IT=1,2
09100      CT3=0.
09200      CT4=0.
09300      SII=0.
09400      SIR=0.
09500      ZC1=0.
09600      ZS1=0.
09700      DO 2 NST=1,6
09800      IF(NST.EQ.1.OR.NST.EQ.6) GOTO 2216
09900      IF(ITST.GE.1) GOTO 2
10000      2216 CONTINUE
10100      IF(NST.EQ.1) TV=BET
10200      IF(NST.EQ.2) TV=BLF+TVCR
10300      IF(NST.EQ.3) TV=TVCR+EPS+BET
10400      IF(NST.EQ.4) TV=TVCR-EPS
10500      IF(NST.EQ.5) TV=GAM
10600      IF(NST.EQ.6) TV=TV+DEL-GAM
10700      IF(NST.EQ.6.AND.ITST.GE.1) TV=GAM
10800      IF(NST.EQ.2) THR(1)=TV
10900      IF(NST.EQ.4) THL(1)=TV
11000      IF(NST.EQ.1) ILM=KT15
11100

```

```

11200      IF(NST.EQ.2.OR.NST.EQ.4) ILM=3
11300      IF(NST.EQ.3) ILM=NTS15
11400      IF(NST.EQ.5) ILM=3
11500      IF(NST.EQ.6.AND.ITST.EQ.0) ILM=LQM1
11600      IF(NST.EQ.6.AND.ITST.GE.1) ILM=KT115
11700      DO 3 I=1,ILM
11800      IN=I+1
11900      CALL COEF1(TU)
12000      IF(IP.EQ.2) CSN=CSN/SGC2/CN
12100      IF(IP.EQ.2) SGC0=SGC0*CN
12200      FDTSG=FDT*SGC0
12300      122      CONTINUE
12400      S21=S2-S1
12500      S43=S4-S3
12600      R1=X*CN+Y*SN
12700      R2=X*CN-Y*SN
12800      C1=A*CN+B*SN
12900      C2=A*CN-B*SN
13000      SM(1)=R1-C1
13100      SM(2)=R1-C2
13200      SM(3)=R1+C1
13300      SM(4)=R1+C2
13400      SM(5)=R2-C1
13500      SM(6)=R2-C2
13600      SM(7)=R2+C1
13700      SM(8)=R2+C2
13800      CALL ALV(IP,Q1,Q2,Q3,Q4,Q5,Q6)
13900      IF(TU.EQ.0.) GO TO 100
14000      S1S=S1**2
14100      S2S=S2**2
14200      S3S=S3**2
14300      S4S=S4**2
14400      S1Q=S1S*S1
14500      S2Q=S2S*S2
14600      S3Q=S3S*S3
14700      S4Q=S4S*S4
14800      F3=SIG2/(S1*S2)
14900      FC33=F3
15000      F4=(SP*S1*CN-SIG)**2/(-S1Q*S21)
15100      F5=(SP*S2*CN-SIG)**2/(-S2Q*S21)
15200      F1=-SGC0*(SIG-SP*S1*CN)**2/(S1S*S21)
15300      F2=SGC0*(SIG-SP*S2*CN)**2/(S2S*S21)
15400      IF(TU.LE..25) GOTO 1231
15500      IF(NST.GE.4.OR.NST.EQ.1.OR.S43.LT..1E-7) GOTO 123
15600      1231      FC3=SIG2/(S3*S4)
15700      FC4=(SP*S3*CN+SIG)**2/(-S3Q*S43)
15800      FC5=(SP*S4*CN+SIG)**2/(-S4Q*S43)
15900      IF(IP.EQ.2) F3=SGC0*(SIG+SP*S3*CN)**2/(S3S*S43)
16000      IF(IP.EQ.2) F4=-SGC0*(SIG+SP*S4*CN)**2/(S4S*S43)
16100      IF(IP.EQ.2) FC4=-SIG2*SGC0/(S3*S4)
16200      123      CONTINUE
16300      IF(IP.EQ.2) FC3=SIG2*SGC0/(S1*S2)
16400      IF(NST.EQ.2.OR.NST.EQ.3) GOTO 19
16500      IF(NST.GE.4) GOTO 33
16600      CALL YTEX1(S1,1,EPR,EPI)
16700      CALL YTEX1(S2,2,EPR,EPI)
16800      IF(TU.LE..25) GOTO 66

```

AD-A070 886

STEVENS INST OF TECH HOBOKEN N J DAVIDSON LAB

F/G 13/10

ADDED MASS AND DAMPING OF THE HEAVING SURFACE EFFECT SHIP IN UN--ETC(U)

DEC 78 C H KIM, S TSAKONAS

N00014-77-C-0061

NL

UNCLASSIFIED

SIT-DL-78-9-2040

2 OF 2

AD
A070886



END
DATE
FILMED
8-79
DDC

```

16900      DELAC=DELTA
17000      CALL COEF2(1,2)
17100      IF(IP.EQ.2) GOTO 133
17200      CALL VFX(F3,F4,F5,Q1,Q2,Q3,Q4,Q5,Q6,1,2,YC1,YS1)
17300      GOTO 305
17400      133      CONTINUE
17500      YC1=F1*(EP(1)+EPD(1))+F2*(EP(2)+EPD(2))
17600      YS1=F1*(EI(1)+EID(1))+F2*(EI(2)+EID(2))
17700      YC1=YC1-(F1+F2)*Q1+FC3*Q3
17800      YS1=YS1-(F1+F2)*Q2+FC3*Q4
17900      YC1=YC1*FDT
18000      YS1=YS1*FDT
18100      GOTO 305
18200      19      CALL YTEX2(S3,3,EPR,EPI)
18300      CALL YTEX2(S4,4,EPR,EPI)
18400      CALL COEF2(3,4)
18500      IF(IP.EQ.2) GOTO 191
18600      CALL VFX(FC3,FC4,FC5,Q1,Q2,Q3,Q4,Q5,Q6,3,4,YC1,YS1)
18700      GOTO 192
18800      191      CONTINUE
18900      YC1=F3*(EP(3)+EPD(3))+F4*(EP(4)+EPD(4))
19000      YS1=F3*(EI(3)+EID(3))+F4*(EI(4)+EID(4))
19100      YC7=-(F3+F4)*Q1+FC4*Q3
19200      YS7=-(F3+F4)*Q2-FC4*Q4
19300      YC1=(YC1+YC7)*FDT
19400      YS1=(YS1+YS7)*FDT
19500      192      CONTINUE
19600      IF(NST.EQ.3) GOTO 506
19700      FRR(I)=YC1*(THR(I)-TVCR)**3
19800      FIR(I)=YS1*(THR(I)-TVCR)**3
19900      ALF=BLF
20000      GOTO 306
20100      506      CONTINUE
20200      DELAC=DELTA
20300      GOTO 305
20400      33      TM=-TM
20500      CTU=TM*.5
20600      S3R=SK05*TTM
20700      S4I=SK05*CTU
20800      S4R=S3R
20900      S3I=-S4I
21000      IF(IP.EQ.2) GOTO 335
21100      CALL KMVL(S4R,S4I,SIG,SP,CN,FD1,FD2,FD3,FD4R,FD4I)
21200      GOTO 336
21300      335      CALL KMP(S4R,S4I,SGCO,SIG,SP,CN,FK1,FK2,AC,BD)
21400      336      CONTINUE
21500      CALL YTEX3(S3R,S3I,3,EPR,EPI)
21600      CALL YTEX3(S4R,S4I,4,EPR,EPI)
21700      CALL COEF2(3,4)
21800      IF(IP.EQ.2) GOTO 337
21900      YC3=FD4R*(EP(3)+EPD(3)+EP(4)+EPD(4))-FD4I*(EI(3)
22000      1 +EID(3)-EI(4)-EID(4))
22100      YS3=FD4R*(EI(3)+EID(3)+EI(4)+EID(4))+FD4I*(EP(3)
22200      1 +EPD(3)-EP(4)-EPD(4))
22300      YC8=(FD1*Q1+FD2*Q3+FD3*Q5)
22400      YS8=(-FD1*Q2-FD2*Q4-FD3*Q6)
22500      YC1=(YC3+YC8)*FDTSG

```

```

22600      YS1=(YS3+YS8)*FDTSG
22700      GOTO 338
22800      337      YC3=AC*(EP(3)+EPD(3))-BD*(EI(3)+EID(3))+
22900      1          AC*(EP(4)+EPD(4))+BD*(EI(4)+EID(4))
23000      YS3=BD*(EP(3)+EPD(3))+AC*(EI(3)+EID(3))
23100      1          -BD*(EP(4)+EPD(4))+AC*(EI(4)+EID(4))
23200      YC8=-FK1*Q1+FK2*Q3
23300      YS8=FK1*Q2-FK2*Q4
23400      YC1=(YC3+YC8)*FDT
23500      YS1=(YS3+YS8)*FDT
23600      338      CONTINUE
23700      IF(NST.GE.5) GOTO 508
23800      FRL(I)=YC1*(THL(I)-TVCR)**3
23900      FIL(I)=YS1*(THL(I)-TVCR)**3
24000      ALF=BLF
24100      GOTO 306
24200      508      CONTINUE
24300      IF(ITST.GE.1) GO TO 125
24400      IF(NST.EQ.6) GOTO 136
24500      THR(I)=SIN(TV)**3
24600      FTR(I)=YC1*THR(I)
24700      FTI(I)=YS1*THR(I)
24800      ALF=GAM
24900      GOTO 306
25000      136      CONTINUE
25100      DELAC=BTA
25200      GOTO 305
25300      125      CONTINUE
25400      IF(ITST.EQ.1) DELAC=DELTA
25500      IF(ITST.EQ.2) DELAC=DELTC
25600      GOTO 305
25700      C          COMPUTATION OF V-FLX FOR TU<.25 IN BELOW
25800      66        CONTINUE
25900      CALL YTEX2(S3,3,EPR,EPI)
26000      CALL YTEX2(S4,4,EPR,EPI)
26100      CALL COEF2(1,4)
26200      DELAC=DELTA
26300      IF(IP.EQ.2) GOTO 665
26400      YC1=F4*(EP(1)+EPD(1))-F5*(EP(2)+EPD(2))
26500      YS1=F4*(EI(1)+EID(1))-F5*(EI(2)+EID(2))
26600      YC2=+FC4*(EP(3)+EPD(3))-FC5*(EP(4)+EPD(4))
26700      YS2=+FC4*(EI(3)+EID(3))-FC5*(EI(4)+EID(4))
26800      YC1=YC1+(-F4+F5)*Q1+(-F4*S1+F5*S2)*Q3+F3*Q5
26900      YS1=YS1+(-F4+F5)*Q2+(-F4*S1+F5*S2)*Q4+F3*Q6
27000      YC2=YC2+(-FC4+FC5)*Q1+(-FC4*S3+FC5*S4)*Q3+FC3*Q5
27100      YS2=YS2-(-FC4+FC5)*Q2-(-FC4*S3+FC5*S4)*Q4-FC3*Q6
27200      YC1=(YC1+YC2)*FDTSG
27300      YS1=(YS1+YS2)*FDTSG
27400      GOTO 305
27500      665      CONTINUE
27600      YC1=F1*(EP(1)+EPD(1))+F2*(EP(2)+EPD(2))
27700      YS1=F1*(EI(1)+EID(1))+F2*(EI(2)+EID(2))
27800      YC2=F3*(EP(3)+EPD(3))+F4*(EP(4)+EPD(4))
27900      YS2=F3*(EI(3)+EID(3))+F4*(EI(4)+EID(4))
28000      YC1=YC1-(F1+F2)*Q1+FC3*Q3
28100      YS1=YS1-(F1+F2)*Q2+FC3*Q4
28200      YC2=YC2-(F3+F4)*Q1+FC4*Q3

```

```

28300      YS2=YS2+(F3+F4)*Q2-FC4*Q4
28400      YC1=(YC1+YC2)*FDT
28500      YS1=(YS1+YS2)*FDT
28600      GOTO 305
28700      100      CONTINUE
28800      C      CAL OF VLL FOR TAU=0.
28900      CALL YTEX1(S2,2,EPR,EPI)
29000      CALL COEF2(2,2)
29100      YC1=CSN*FCTR*FCT*FDT*(EP(2)+EPD(2)-S2*Q3-Q1)
29200      IF(IP,EQ.2) YS1=CSN*FDT*(EI(2)+EID(2)-Q2)
29300      IF(IP,EQ.2) YC1=0.
29400      DELAC=DELTA
29500      305      CONTINUE
29600      IF(I,ER.1,OR,I,ER,ILM) YC1=0.5*YC1
29700      IF(I,ER.1,OR,I,ER,ILM) YS1=0.5*YS1
29800      IF(I,ER.1) ALF=BET
29900      IF(I,ER.1,AND,ITST,EQ.0,AND,NST,EQ.6) ALF=DEL
30000      ZC1=ZC1+YC1*ALF
30100      ZS1=ZS1+YS1*ALF
30200      NST1=NST
30300      ALF=ALFC(IN,NST1,DELAC,ITST)
30400      306      TV=TV+ALF
30500      IF(NST,EQ.2) THR(I+1)=TV
30600      IF(NST,EQ.4) THL(I+1)=TV
30700      3      CONTINUE
30800      991      FORMAT(2X,2E10.4)
30900      IF(TU,LE.0.25) GOTO 11
31000      IF(NST,EQ.5) CT3=SFC*(-X11*FTR(3)+X44*FTR(2)-X15*FTR(1))
31100      IF(NST,EQ.5) CT4=SFC*(-X11*FTI(3)+X44*FTI(2)-X15*FTI(1))
31200      IF(NST,NE.6) GOTO 2
31300      SIR1=X11*(FRL(1)-FRR(3))
31400      SIR2=-X44*(FRL(2)-FRR(2))
31500      SIR3=X15*(FRL(3)-FRR(1))
31600      SIR=SFC*(SIR1+SIR2+SIR3)
31700      SII1=X11*(FIL(1)-FIR(3))
31800      SII2=-X44*(FIL(2)-FIR(2))
31900      SII3=X15*(FIL(3)-FIR(1))
32000      SII=SFC*(SII1+SII2+SII3)
32100      2      CONTINUE
32200      11      ZC=(ZC1+SIR+CT3)/FCT
32300      ZS=(ZS1+SII+CT4)/FCT
32400      IF(TU,EQ.0.,AND,IP,EQ.2) ZS=ZS1/FCTR
32500      X=-X
32600      ZCC(IT)=ZC
32700      ZSS(IT)=ZS
32800      IF(IP,EQ.2) GOTO 99
32900      1      CONTINUE
33000      99      CONTINUE
33100      ZC=(ZCC(2)-ZCC(1))*2.-ABL2
33200      ZS=(ZSS(2)-ZSS(1))*2.
33300      IF(IP,EQ.2) ZS=ZS-SBSL
33400      IF(IP,EQ.2) ZC=-ZC-ABL2
33500      RETURN
33600      END

```

```

00100      SUBROUTINE KMP(S4R,S4I,SGCO,SIG,SP,CN,FK1,FK2,
00200      AC,BD)
00300      3      1      FORMAT(6E12,4)
00400      XX=2.*SP*SIG*CN
00500      SIG2=SIG**2
00600      S4R2=S4R**2
00700      S4I2=S4I**2
00800      XY2=S4R2+S4I2
00900      XF=2.*S4R
01000      XY4=XY2**2
01100      FK2=-SGCO*SIG2/XY2
01200      AA=(SP*S4R*CN+SIG)**2-(SP*S4I*CN)**2
01300      BB=2.*(SP*S4R*CN+SIG)*SP*S4I*CN
01400      DD=2.*S4I*(S4R2-S4I2)
01500      CC=4.*S4R*S4I2
01600      CCDD=CC**2+DD**2
01700      AC=(AA*CC-BB*DD)/CCDD*SGCO
01800      BD=- (BB*CC+AA*DD)/CCDD*SGCO
01900      FK1=2.*AC
02000      RETURN
02100      END
02200      SUBROUTINE ALV(IP,Q1,Q2,Q3,Q4,Q5,Q6)
02300      COMMON/MYTEX/ SM(8)
02400      DIMENSION ASM(8),AL(8),G1(8)
02500      COMMON/LOG/C1,C2,R1,R2
02600      C      Q1=RE(I1+I1D),Q2=IM(I1+I1D),Q3=RE(I3+I3D),Q4=IM(I3+I3D)
02700      C      Q5=RE(I9+I9D),Q6=IM(I9+I9D)
02800      PI=3.14159
02900      DO 1 M=1,8
03000      ASM(M)=ABS(SM(M))
03100      IF(ASM(M)) 3,3,4
03200      4      AL(M)=ALOG(ASM(M))
03300      GO TO 1
03400      3      CONTINUE
03500      1      CONTINUE
03600      AF1=-AL(1)+AL(2)-AL(3)+AL(4)
03700      AF2=AL(5)-AL(6)+AL(7)-AL(8)
03800      AF=AF1+AF2
03900      AP3=AL(3)-AL(1)
04000      AP4=AL(2)-AL(4)
04100      AP5=AL(5)-AL(7)
04200      AP6=AL(8)-AL(6)
04300      DO 31 K=1,8
04400      IF(SM(K).LT.0.) G1(K)=PI
04500      IF(SM(K).GE.0.) G1(K)=0.
04600      31      CONTINUE
04700      AQ1=G1(3)-G1(1)
04800      AQ2=G1(2)-G1(4)
04900      AQ3=G1(5)-G1(7)
05000      AQ4=G1(8)-G1(6)
05100      SII1=-G1(1)+G1(2)-G1(3)+G1(4)
05200      SII1D=G1(5)-G1(6)+G1(7)-G1(8)
05300      Q2=SII1+SII1D
05400      SII3=R1*AP1-C1*AP3-C2*AP4
05500      SII3D=R2*AP2-C1*AP5-C2*AP6

```

```

05600      Q4=SII3+SII3D
05700      Q1=AP
05800      SRI3=-R1*SII1+C1*AQ1+C2*AQ2
05900      SRI3D=-R2*SII1D+C1*AQ3+C2*AQ4
06000      Q3=SRI3+SRI3D
06100      IF(IP.EQ.2) RETURN
06200      SR9=-.5*R1**2*AP1-R1*C1*(AL(1)-AL(3))+R1*C2*(AL(2)-AL(4)
06300      1      )+0.5*C1**2*(AL(1)+AL(3))-0.5*C2**2*(AL(2)+AL(4))
06400      SI9=-.5*R1**2*SII1-R1*C1*(G1(1)-G1(3))-
06500      1      +R1*C2*(G1(2)-G1(4))+0.5*C1**2*(G1(1)+G1(3))-0.5*C2**2*
06600      2      (G1(2)+G1(4))
06700      SR9D=-0.5*R2**2*AP2+R2*C1*(AL(5)-AL(7))-R2*C2*(AL
06800      1      (6)-AL(8))-0.5*C1**2*(AL(5)+AL(7))+0.5*C2**2*(AL(6)+AL(8)
    ))
06900      SI9D=-.5*R2**2*SII1D+R2*C1*(G1(5)-G1(7))-R2*C2*(G1(6)
07000      1      -G1(8))-0.5*C1**2*(G1(5)+G1(7))+0.5*C2**2*(G1(6)+G1(8))
07100      Q5=SR9+SR9D
07200      Q6=SI9+SI9D
07300      RETURN
07400      END
07500      SUBROUTINE KMVL(S4R,S4I,SIG,SP,CN,A1,A2,A3,A4,A5)
07600      C      COMPUTES COEF OF KOMPLEX WAVE NUMBERS
07700      C      A1=FD1,A2=FD2,A3=FD3,A4=FD4R,A5=FD4I
07800      SIG2=SIG**2
07900      SP2=SP**2
08000      CN2=CN**2
08100      X=S4R
08200      Y=S4I
08300      X2=X**2
08400      X3=X2*X
08500      Y2=Y**2
08600      Y3=Y2*Y
08700      Y4=Y3*Y
08800      XY2=X2+Y2
08900      XY2P=XY2**2
09000      XY3P=XY2**3
09100      XZ=XY2*2.*X
09200      XY=3.*X2-Y2
09300      A=SP*SIG*CN
09400      B=SP2*CN2
09500      U=-6.*X2*Y2+2.*Y4
09600      V=2.*Y*X3-6.*X*Y3
09700      W=U**2+V**2
09800      G=(SP*X*CN+SG)**2-(SP*Y*CN)**2
09900      H=2.*(SP*X*CN+SIG)*SP*Y*CN
10000      A3=SIG2/XY2
10100      A4=(G*U+H*V)/W
10200      A5=(G*V-H*U)/W
10300      A2=-2.*(A4*X+A5*Y)
10400      A1=-2.*A4
10500      RETURN
10600      END
10700      SUBROUTINE YTEX1(SK,K,EPR,EPI)
10800      COMMON/MYTEX/ SM(8)
10900      DIMENSION EPR(4,8),EPI(4,8)

```

```

11000 12  FORMAT(/2X,' C,S,CI,SI'/)
11100 13  FORMAT(10E12.4)
11200 14  FORMAT(/2X,'SKM'/)
11300    P=3.14159
11400    TP=P*2.
11500    DO 6 M=1,8
11600    SKM=ABS(SK*SM(M))
11700    C=COS(SKM)
11800    S=SIN(SKM)
11900    CALL SICI(SI,CI,SKM)
12000    IF(SM(M)) 7,8,9
12100 7    EPR(K,M)=-C*CI-S*SI - TP*S
12200    EPI(K,M)=S*CI-C*SI - TP*C
12300    GO TO 6
12400 8    CONTINUE
12500    GO TO 6
12600 9    EPR(K,M)=-C*CI-S*SI
12700    EPI(K,M)=-S*CI+C*SI
12800 6    CONTINUE
12900 11   FORMAT(/3X,'SINGULAR'/)
13000    RETURN
13100    END
13200    SUBROUTINE YTEX2(SK,K,EPR,EPI)
13300    COMMON/NYTEX/ SM(8)
13400    DIMENSION EPR(4,8),EPI(4,8)
13500 12   FORMAT(/2X,'C,S,CI,SI'/)
13600 13   FORMAT(10E12.4)
13700 14   FORMAT(/2X,'SKM'/)
13800    P=3.14159
13900    TP=2.*P
14000    DO 6 M=1,8
14100    SKM=ABS(SK*SM(M))
14200    C=COS(SKM)
14300    S=SIN(SKM)
14400    CALL SICI(SI,CI,SKM)
14500    IF(SM(M)) 7,8,9
14600 7    EPR(K,M)=-C*CI-S*SI
14700    EPI(K,M)=-S*CI+C*SI
14800    IF(K.EQ.4) GO TO 19
14900    GO TO 6
15000 8    CONTINUE
15100    GO TO 6
15200 19   EPR(K,M)=EPR(K,M)-S*TP
15300    EPI(K,M)=EPI(K,M)+C*TP
15400    GO TO 6
15500 9    EPR(K,M)=-C*CI-S*SI
15600    EPI(K,M)=S*CI-C*SI
15700    IF(K.EQ.3) GO TO 18
15800    GO TO 6
15900 18   EPR(K,M)=EPR(K,M)-TP*S
16000    EPI(K,M)=EPI(K,M)-TP*C
16100 6    CONTINUE
16200 11   FORMAT(/2X,'SINGL'/)
16300    RETURN
16400    END

```

```

16500      SUBROUTINE YTEX3(SR,SI,K,EPR,EPI)
16600      DIMENSION EPR(4,8),EPI(4,8)
16700      COMMON/XYTEX/ SM(8)
16800      2    FORMAT(1X,10G10.4)
16900      P=3.14159
17000      TP=P*2.
17100      IT=0
17200      IF(K.EQ.4.AND.SR.GT.0.) IT=3
17300      IF(K.EQ.3.AND.SR.GT.0.) IT=1
17400      DO 60 M=1,8
17500      IF(SM(M).EQ.0.) GO TO 60
17600      X=-SR*SM(M)
17700      XY=-X
17800      Y=SI*SM(M)
17900      X2=X**2
18000      Y2=Y**2
18100      AX=ABS(X)
18200      BA=(X2+Y2)**0.5
18300      C=COS(AX)
18400      S=SIN(AX)
18500      IF(Y.GE.80.) Y=80.
18600      IF(Y.LE.-80.) Y=-80.
18700      E=EXP(Y)
18800      BB=BA
18900      AT=ATAN2(X,Y)
19000      BC=AT+P
19100      IF(SR.EQ.0.) BC=P
19200      BE=0.
19300      BD=0.
19400      IF(BA-6.) 28,30,30
19500      28  MM=1
19600      25  BD=BD+BB*COS(FLOAT(MM)*BC)
19700      BE=BE+BB*SIN(FLOAT(MM)*BC)
19800      BB=BB*BA*FLOAT(MM)/FLOAT((MM+1)**2)
19900      MM=MM+1
20000      IF(BB.GT.0.1E-5*BA) GO TO 25
20100      BD=(0.577+ALOG(BA)+BD)
20200      BE=(BE+AT)
20300      GO TO 26
20400      30  DO 31 MM=1,5
20500      BD=BD+COS(FLOAT(MM)*BC)/BB
20600      BE=BE+SIN(FLOAT(MM)*BC)/BB
20700      BB=BA*BB/FLOAT(MM)
20800      31  CONTINUE
20900      26  CONTINUE
21000      IF(SR.EQ.0.) GO TO 69
21100      GAS=TP*E*S
21200      GAC=TP*E*C
21300      IF(BA-6.) 70,77,77
21400      IF(BA-6.) 70, 77, 77
21500      70  GA=E*(C*(-BD)+SIGN(S,XY)*(-BE))
21600      GB=E*(-SIGN(S,XY)*(-BD)+C*(-BE))
21700      IF(K.EQ.3.AND.SR.GT.0..AND.SM(M).GT.0.) GA=GA-GAS
21800      IF(K.EQ.3.AND.SR.GT.0..AND.SM(M).GT.0.) GB=GB-GAC
21900      IF(K.EQ.4.AND.SR.GT.0..AND.SM(M).LT.0.) GA=GA-GAS

```

```
22000      IF(K.EQ.4.AND.SR.GT.0..AND.SM(M).LT.0.) GB=GB+GAC
22100      GO TO 80
22200      77      IF(IT.EQ.1.AND.SM(M).GT.0.) GO TO 92
22300      IF(IT.EQ.3.AND.SM(M).LT.0.) GO TO 93
22400      GO TO 94
22500      92      GA=-BD-E*TP*S
22600      GB=BE-E*TP*C
22700      GO TO 80
22800      93      GA=-BD-E*TP*S
22900      GB=BE+E*TP*C
23000      GO TO 80
23100      94      GA=-BD
23200      GB=BE
23300      GO TO 80
23400      69      CONTINUE
23500      GA=-E*BD
23600      GB=0.
23700      80      EPR(K,M)=GA
23800      EPI(K,M)=GB
23900      60      CONTINUE
24000      99      FORMAT(/2X,'SINFULAR'/)
24100      RETURN
24200      END
```